

**Aus dem Institut für Virologie
des Fachbereichs Veterinärmedizin
der Freien Universität Berlin**

Identification of ZDHHC enzymes catalyzing acylation of influenza virus Hemagglutinin

**Inaugural-Dissertation
zur Erlangung des Grades eines
Doctor of Philosophy (PhD)
an der
Freien Universität Berlin**

**vorgelegt von
Mohamed Rasheed Abdelalim Mohamed Gadalla
Tierarzt aus Kairo /Ägypten**

**Berlin 2020
Journal-Nr.: 4189**

Aus dem Institut für Virologie
des Fachbereichs Veterinärmedizin
der Freien Universität Berlin

**Identification of ZDHHC enzymes catalyzing acylation of influenza
virus Hemagglutinin**

Inaugural-Dissertation
zur Erlangung des Grades eines
Doctor of Philosophy (PhD)
an der Freien Universität Berlin

vorgelegt von

Mohamed Rasheed Abdelalim Mohamed Gadalla

Tierarzt

aus Kairo /Ägypten

Berlin 2020

Journal-Nr.: 4189

Gedruckt mit Genehmigung des Fachbereichs Veterinärmedizin
der Freien Universität Berlin

Dekan: Univ.-Prof. Dr. Jürgen Zentek
Erster Gutachter: PD Dr. Michael Veit
Zweiter Gutachter: Univ.-Prof. Dr. Klaus Osterrieder
Dritter Gutachter: Univ.-Prof. Dr. Hafez Mohamed Hafez

Deskriptoren (nach CAB-Thesaurus):

Man, Cell lines, Cell Culture, Respiratory system, Influenza viruses, Hemagglutinins, Matrix protein, CRISPR-Cas9, Transmembrane proteins, Fatty acids, Stearic acid, Palmitate, Polymerase chain reaction, SDS-PAGE, Western Blotting, MALDI-TOF

Tag der Promotion: 25.02.2020

Bibliografische Information der *Deutschen Nationalbibliothek*

Die Deutsche Nationalbibliothek verzeichnet diese Publikation in der Deutschen Nationalbibliografie; detaillierte bibliografische Daten sind im Internet über <<https://dnb.de>> abrufbar.

ISBN: 978-3-96729-040-0

Zugl.: Berlin, Freie Univ., Diss., 2020

Dissertation, Freie Universität Berlin

D188

Dieses Werk ist urheberrechtlich geschützt.

Alle Rechte, auch die der Übersetzung, des Nachdruckes und der Vervielfältigung des Buches, oder Teilen daraus, vorbehalten. Kein Teil des Werkes darf ohne schriftliche Genehmigung des Verlages in irgendeiner Form reproduziert oder unter Verwendung elektronischer Systeme verarbeitet, vervielfältigt oder verbreitet werden.

Die Wiedergabe von Gebrauchsnamen, Warenbezeichnungen, usw. in diesem Werk berechtigt auch ohne besondere Kennzeichnung nicht zu der Annahme, dass solche Namen im Sinne der Warenzeichen- und Markenschutz-Gesetzgebung als frei zu betrachten wären und daher von jedermann benutzt werden dürfen.

This document is protected by copyright law.

No part of this document may be reproduced in any form by any means without prior written authorization of the publisher.

alle Rechte vorbehalten | all rights reserved

© Mensch und Buch Verlag 2020

Choriner Str. 85 - 10119 Berlin

verlag@menschundbuch.de – www.menschundbuch.de

Dedication

To my Great Parents

To my wonderful wife ♥ Asmaa ♥

To my Little Kids ♥ Ziad & Layan ♥

To my Brother (Ahmed)

To my Beloved Sisters (Heba & Dina)

Table of contents

Table of contents	I
Abbreviations	V
List of Figures	VII
List of Tables	VIII
1. Introduction	1
1.1. Influenza A virus	1
1.1.1. Virus taxonomy and nomenclature	1
1.1.2 Virus structure and genome organization	2
1.1.3. Replication cycle	3
1.1.4 Hemagglutinin glycoprotein (HA).....	7
1.1.4.1. Structure and function of HA.....	7
1.1.4.2. Intracellular transport and processing	9
1.2. Acylation/Palmitoylation of proteins	10
1.2.1. S-acylated proteins of viruses pathogenic for human.....	10
1.2.1.1. S-acylated proteins of Influenza viruses	12
1.2.1.2. S-acylation of proteins from other viruses.....	14
1.3. Enzymology of S-acylation	17
1.3.1. Crystal structures of ZDHHC enzymes.....	20
1.3.2. Lipid- and protein substrate specificities of ZDHHC proteins	21
1.3.3. Acylprotein thioesterases and other enzymes that deacylate proteins	22
1.4. Methods to study s-acylation of proteins	23
I. Radioactive labeling.....	23
II. Acyl biotin exchange (ABE) and Acyl-resin assisted capture (Acyl-RAC).....	23
III. Click Chemistry based methods (Radioactive free labeling)	24
1.4.1. Methods to identify ZDHHC substrate pairs	25
2. Aim of the study	26
3. Materials and Methods	27
3.1. Materials	27
3.1.1. Chemicals, consumables and equipment.....	27
3.1.1.1. Chemicals	27
3.1.1.2. Consumables	29
3.1.1.3. Equipment.....	30
3.1.1.4. Software	31
3.1.1.5. Enzymes and markers.....	32
3.1.1.6. Kits	33

3.1.2. Primers.....	33
3.1.2.1. Primers used for generation of HA acylation mutant by reverse genetics.....	33
3.1.2.2. Primers used for expression profiling of Human ZDHHCs.....	34
3.1.2.3. Guide RNA sequences and screening primers used for generation of CRISPR/Cas9 Knockout cell lines	35
3.1.2.4. Sequencing Primers used for validation of gRNA cloning in CRISPR vectors..	36
3.1.3. Antibodies.....	36
3.1.4. Prepared solutions and Buffers.....	37
3.2. Methods	39
3.2.1. Molecular biology methods	39
3.2.1.1. Preparation of chemically competent E. coli.....	39
3.2.1.2. Transformation of competent bacterial cells	39
3.2.1.3. Plasmid purification	39
3.2.1.4. Quick Change Site directed mutagenesis.....	40
3.2.1.5. Screening and Sequencing Polymerase chain reaction (PCR)	42
3.2.1.6. Agarose gel electrophoresis	42
3.2.1.7. DNA extraction or clean up from agarose gel	42
3.2.1.8. CRISPR/Cas9 technology	43
3.2.1.8.1. CRISPR/Guide RNA annealing and vector cloning	45
3.2.1.9. Quantitative Real-time PCR (qPCR).....	46
3.2.1.10. siRNA transfection and Knockdown.....	47
3.2.2. Cell culture and micro scopy	48
3.2.2.1. Cultivation and maintenance of mammalian cells.....	48
3.2.2.2. Freezing and thawing of cells.....	48
3.2.2.3. Transfection.....	48
3.2.2.4. Isolation of single cell clones and generation of knockout cell lines	48
3.2.2.5. Confocal fluorescence microscopy	51
3.2.3. Virological Methods	52
3.2.3.1. Generation of influenza acylation mutants with reverse genetics system	52
3.2.3.2. Virus infection and propagation	53
3.2.3.3. Plaque assay and virus growth kinetics	53
3.2.3.4. Ultracentrifugation and virus purification	54
3.2.4. Biochemical Methods	54
3.2.4.1. Determination of protein concentration	54
3.2.4.2. SDS polyacrylamide gel electrophoresis (SDS-PAGE)	54
3.2.4.3. Western blotting	55
3.2.4.4. S-acylation analysis assays	55

3.2.4.4.1. Acyl-Resin assisted capture (Acyl-RAC).....	55
3.2.4.4.2. Radioactive metabolic labelling and fluorography	56
3.2.4.4.3. Click chemistry and In-Gel fluorescence	57
4. Results	58
4.1. Expression of ZDHHC proteins in different tissues of the human respiratory tract and corresponding cell lines.....	58
4.1.1. Expression level of ZDHHCs in different human cell lines.....	59
4.1.2. Effect of influenza infection on ZDHHC expression profile	61
4.1.3. Influenza virus NS-1 significantly upregulate ZDHHC22 expression	62
4.2. Knockout of ZDHHC22 in A549 cells using CRISPR/Cas9	63
4.2.1. Effect of ZDHHC22 knockout on acylation pattern and growth kinetics of influenza A virus.....	64
4.2.2. MALDI-TOF mass spectrometric analysis of virus particles produced by ZDHHC22 KO cells.....	66
4.2.3. Identification ZDHHC22 acyltransferase potential substrates by LC-MS/MS	68
4.3. SiRNA screening for ZDHHC modifying influenza virus HA protein	71
4.4. Validation of ZDHHC proteins knockout in HAP1 cells	73
4.4.1. Knockout of ZDHHC2, 8, 15 or 20 in HAP1 cells reduces acylation of HA of influenza A virus.....	74
4.4.2. HAs of both phylogenetic groups and the viral proton channel M2 are acylated by a similar set of ZDHHC proteins.....	76
4.4.3. ZDHHC 2, 8, 15 and 20 have no effect on acylation of Flu B HA and HEF of Flu C	78
4.5. Co-localization of ZDHHC2, 8, 15 and 20 with HA in a human lung cell line.....	79
4.6. Knockout of ZDHHC 2, 8, 15 and 20 in influenza susceptible A549 cells using CRISPR/Cas9.....	81
4.6.1. Effect of ZDHHC 2,8,15 and 20 on acylation of HA and virus replication.....	82
4.6.2. Generation of double ZDHHC knockout A549 cell lines (Δ 2/15 and Δ 2/20).....	83
5. Discussion	85
5.1. Influenza virus significantly upregulate ZDHHC22 upon infection but not involved in acylation of viral proteins	85
5.2. ZDHHC2, 8, 15 and 20 are involved in acylation of HA and M2 of influenza A virus	86
5.3. Fatty acid specificities of ZDHHCs involved in acylation of HA	89
5.4. Protein substrate recognition of ZDHHCs involved in acylation of HA and M2...91	91
6. Summary	95
7. Zusammenfassung.....	96
8. References	98
9. Publications	115

10. Acknowledgements	115
11. Selbständigkeitserklärung	117

Abbreviations

ABHD17	α/β -hydrolase domain-containing proteins
APT	Acylprotein thioesterase
cDNA	Complementary deoxyribonucleic acid
CT	Cytoplasmic tail
DMEM	Dulbecco's Minimal Essential Medium
DNA	Deoxyribonucleic acid
ds	Double strand
FP	Fusion Peptide
FPV-I	Fowl Plague Virus I
GFP	Green fluorescent protein
HIV	Human Immunodeficiency Virus
HRP	Horse radish peroxidase
IAV	Influenza A virus
Kbp	Kilo base pair
kDa	Kilodalton
M1/2	Matrix protein 1 and 2
MDCK	Madin-Derby Canine kidney cells
MOI	Multiplicity of infection
NA	Neuraminidase
NP	Nucleoprotein
ON	Overnight
ORF	Open reading frame.
PA	Polymerase Acidic Protein
PM	Plasma Membrane
PB1	Polymerase Basic Protein 1
PB2	Polymerase Basic Protein 2
PBS	Phosphate buffered saline
PCR	Polymerase chain reaction
PFU	Plaque-forming units
qRT-PCR	Real Time quantitative reverse transcription PCR
RT	Room temperature

SDS	Sodium dodecyl sulfate
TM	Transmembrane
Chikv	Chikungunya virus
CRD	Cysteine Rich Domain
EM	Electron Microscopy
HBV	Hepatitis B virus
HCMV	Human cytomegalovirus
HCV	Hepatitis C virus
HEF	Hemagglutinin Esterase Fusion
HRSV	Human Respiratory Syncytial virus
HSV-1	Human herpes simplex virus 1
IFITM	Interferon induced transmembrane
MERS	Middle East Respiratory Syndrome
MHV	Mouse Hepatitis virus
NDV	Newcastle disease virus
SARS	Severe Acute Respiratory Syndrome
SFV	Semilki Forest virus
SRE	sterol-regulatory elements
SREBP	Sterol regulatory element binding protein
STING	stimulator of interferon genes
SCC	Single cell clone
VSV	Vesicular Stomatitis virus

List of Figures

Figure 1. Classification and susceptible species of Orthomyxoviridae family members.....	1
Figure 2. Schematic diagram of influenza A virus particle and viral ribonucleoprotein complex (vRNP).....	3
Figure 3. Replication cycle of influenza A virus.....	5
Figure 4. Structure of influenza virus hemagglutinin (HA).....	8
Figure 5. Membrane topology of s-acylated viral proteins.....	12
Figure 6. S-acylation pattern of HA glycoprotein in different influenza subtypes.....	13
Figure 7. Dynamic protein S-palmitoylation.....	18
Figure 8. Crystal structure of ZDHHC20 and ZDHHC15 acyltransferases.....	21
Figure 9. Methods used for studying S-acylation of proteins.....	24
Figure 10. Schematic overview of Quick-change site directed mutagenesis protocol.....	40
Figure 11. Schematic overview of CRISPR/Cas9 system and plasmids used for generation of knockout cell lines.....	44
Figure 12. Schematic overview of ZDHHC siRNA knockdown procedures.....	47
Figure 13. Plate setup for limited dilution method used for isolation of single cell clones.....	49
Figure 14. Experimental procedures for Isolation of single cell clones by cell culture cloning cylinders.....	51
Figure 15. Principle of acyl-resin assisted capture (acyl-RAC) method for enrichment of acylated proteins.....	56
Figure 16. Expression of ZDHHCs in human lung tissues.....	59
Figure 17. Expression profile of ZDHHC enzyme family members by quantitative real-time PCR (qPCR) for the cell lines used in this study.....	60
Figure 18. IAV significantly upregulate ZDHHC22 in A549 and Calu-3 human lung cells.....	61
Figure 19. Influenza NS1 significantly induce upregulation of ZDHHC22.....	62
Figure 20. Workflow of CRISPR/Cas9 mediated Knockout of ZDHHC22 in A549 cells.....	64
Figure 21. Effect of ZDHHC22 Knockout on palmitoylation of influenza virus HA and M2 proteins.....	65
Figure 22. Multistep growth cycle of FPV-I (A) and WSN (B) influenza viruses in wild type and ZDHHC22 Knockout cells.....	66
Figure 23. MALDI-TOF MS analysis of hemagglutinin from WSN and FPV-I viruses grown in wild type or Δ ZDHHC22 A549 cells.....	67
Figure 24. siRNAs against ZDHHC2 and 8 block acylation of HA in transfected Hela cells.....	71
Figure 25. siRNAs against ZDHHC2, 8, 15 and 20 block acylation of HA as demonstrated by 3H-palmitate labelling.....	72

Figure 26. Expression of relevant ZDHHCs in CRISPR/Cas9 knockout relative to wild type HAP1 cells.....	73
Figure 27. Genotyping of CRISPR/Cas9 induced mutations in ZDHHCs knockout HAP1 cells by PCR and Sanger sequencing..	74
Figure 28. HAP1 cells deficient in ZDHHC2, 8, 15 and 20 show compromised acylation of HA.....	75
Figure 29. HAP1 cells deficient in ZDHHC2, 8, 15 and 20 show compromised acylation of a group 1 HA.....	76
Figure 30. HAP1 cells deficient in ZDHHC2, 8, 15 and 20 show compromised acylation of M2.....	77
Figure 31. HAP1 cells deficient in ZDHHC2, 8, 15 and 20 exhibit no effect on acylation of HEF from Flu C and HA from Flu B..	79
Figure 32. ZDHHCs 2, 8, 15 and 20 co-localize with HA at membranes of the exocytic pathway in human lung cells.....	80
Figure 33. Validation of ZDHHC2, 8, 15 and 20 knockout in A549 cells by PCR, qPCR and Sanger sequencing..	82
Figure 34. Effect of ZDHHC 2, 8, 15 and 20 knockout on acylation of hemagglutinin and virus growth kinetics in A549 cells.	83
Figure 35. Generation of double knockout A549 cells and its effect on acylation of HA and virus replication..	84
Figure 36. Structure of human ZDHHC20 and a model for ZDHHC8.	91
Figure 37. Structure of the viral substrate proteins HA and M2..	93

List of Tables

Table 1. Collective summary of influenza virus genomic RNA and its encoded proteins	6
Table 2. Structural characteristics, interaction domains and intracellular localization of human ZDHHC S-acyltransferases	19
Table 3. Expression of ZDHHC proteins in tissue of the human respiratory tract and in A549 cells.....	58
Table 4. Possible ZDHHC22 palmitoyltransferase substrates identified from two biological replicates.....	69
Table 5. Possible ZDHHC22 palmitoyltransferase substrates identified from a single MS measurment.	70
Table 6: Amino acids near the acylation sites of viral substrate proteins.....	92

1. Introduction

1.1. Influenza A virus

1.1.1. Virus taxonomy and nomenclature

Influenza A virus (IAV) belongs to the family *Orthomyxoviridae* that contain pathogens of humans and animals. Members of the family orthomyxoviridae have segmented; single-stranded negative-sense RNA (ssRNA(-)) genomes. Based on the final report from the international committee on viral taxonomy (ICTV), the family *Orthomyxoviridae* is classified into seven different genera, Influenza virus A, Influenza virus B, Influenza virus C, Influenza virus D, Isavirus, Thogotovirus, and Quarantivirus. This classification is based on serologic reactions of the viral nucleoprotein (NP) and matrix protein 1 (M1) by an immunoprecipitation test (i.e., agar gel immunodiffusion test [AGID]) [1]. The genus Influenza B has only one virus species (Influenza B virus), mainly infects humans, but seals, and ferrets are also susceptible. This virus is less genetically diverse than influenza A due to a lower mutation rate. Likewise, Influenza C is even more antigenically stable and causes only mild infections in humans and pigs. Influenza D, the most recent genus of the family *Orthomyxoviridae* include a single virus associated with respiratory disease in cattle and pigs [2]. The Isavirus group includes the important fish pathogen infectious anemia virus [3], the Thogotoviruses are tick-borne arboviruses that have been isolated from both humans and livestock [4], and the Quarantiviruses are tick-associated viruses that have been detected in humans and birds [5] (Fig.1).

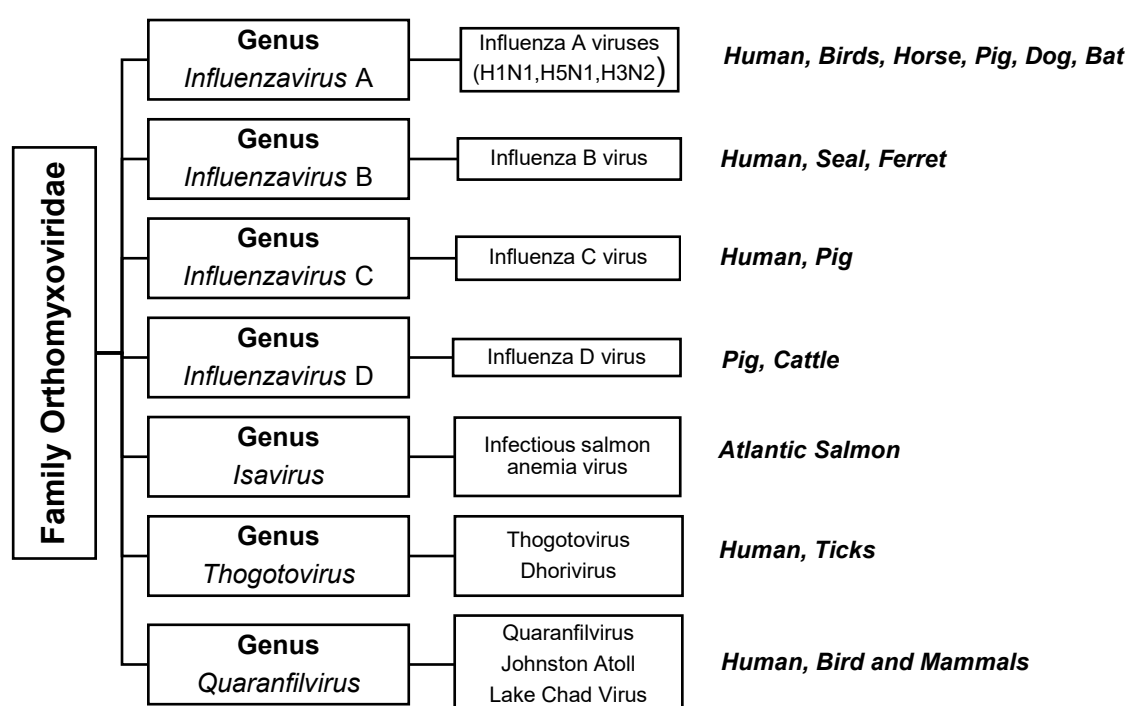


Figure 1. Classification and susceptible species of Orthomyxoviridae family members

Influenza virus A is further classified into subtypes on the basis of antigenicity or sequence analysis of the envelope glycoproteins hemagglutinin (HA) and Neuraminidase (NA) [6]. Until now, there are 18 different hemagglutinin subtypes (H1-H18) and 11 different neuraminidase subtypes (N1-N11). Almost all these subtypes have been detected and isolated from avian species, except for H17N10 and H18N11 subtypes, that have been only found in bats [7]. Since 1980, the nomenclature for subtyping of HA and NA has been standardized for all type A influenza viruses from birds, pigs, horses, and humans. The nomenclature system follows the pattern H(x) N(y) including the host from which the virus was isolated (omitted if human), geographical location, strain number, isolation year and, in the case of the influenza A viruses, the hemagglutinin (H) and neuraminidase (N) subtypes [8,9]. Therefore, for example, the isolate of an H5N1 virus from ducks in Germany, which isolated in 2006 is named (A/tufted duck/Bavaria/27/2006(H5N1)) or the virus isolated from human is called influenza A/Panama/2007/1999 (Pan H3N2).

1.1.2 Virus structure and genome organization

Influenza virions are pleomorphic with either a spherical or filamentous morphology (20 µm in length), or a mixture of both and ranges between 80-120 nm in diameter. Influenza virus particles directly isolated from clinical samples are mainly filamentous whereas highly passaged ones or lab-adapted strains have exclusively spherical morphology [10,11]. The genome of influenza A viruses consists of eight unique segments of single-stranded negative sense RNA (~13kb) encoding at least 14 proteins (HA, NA, NP, PB1, PB2, PA, M1, M2, NS1, NS2)[12]. Several other viral proteins have been recently described with strain-specific or as yet of unknown functions: PB1-F2 [13,14], PB1-N40 [15], PA-X [16], PA-N155 and PA-N182 [17], M42 [18] and NS3 [19]. Influenza type C and D viruses only possess seven gene segments, where the genes encoding HA and NA are replaced by single gene segment that encodes the hemagglutinin–esterase fusion protein [1,2].

Influenza virus particles are enveloped with a lipid membrane that is derived from the host cellular membrane during budding. The viral envelope harbor 3 viral membrane proteins, the two glycoproteins, HA and NA with a molar ratio of 1:4, and small amounts of M2. HA forms a homotrimer and play a major role in the virus replication cycle and infectivity by being responsible for receptor binding and membrane fusion [20]. While homotetrameric NA is responsible for enzymatic cleavage of sialic acids receptors on the surface of host cell and release of infectious virus particles [21]. M2 protein forms a homotetrameric proton channel with only few copies inserted into the viral membrane however; it is highly expressed in the infected cells and critically involved in pH-dependent uncoating of the viral genome. The ion channel activity of M2 allows acidification of the interior of the incoming viral particle. The acidification of the viral particle is essential for viral replication, because it allows incoming vRNPs to dissociate from M1 proteins for nuclear import and initiation of virus replication

[22,23]. The inner side of the lipid membrane is lined with a layer of M1 protein, one of the most abundant viral proteins, which polymerize underneath the lipid envelope and structurally supports the virion morphology [24,25]. Each of the 8 vRNA segments of influenza genome is associated with NP protein and heterotrimeric RNA-dependent RNA polymerase complex (PB1, PB2 and PA) via its 3' and 5' terminal sequences to form what is called the viral ribonucleoprotein complex (vRNP) [26,27] (Fig.2).

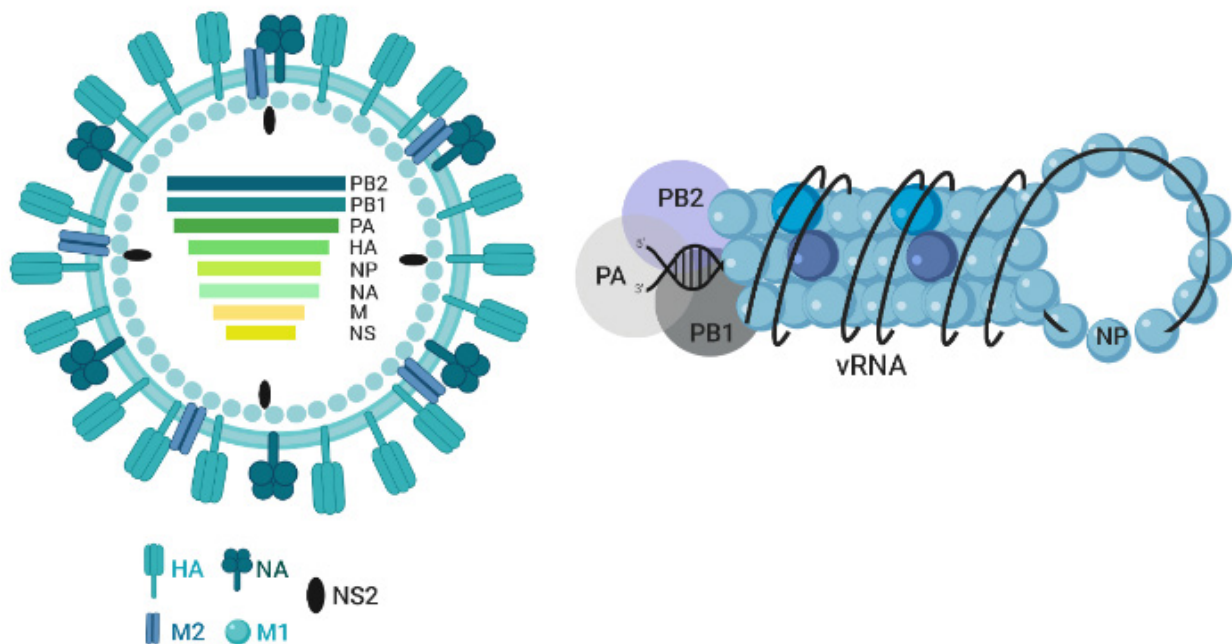


Figure 2. Schematic diagram of influenza A virus particle and viral ribonucleoprotein complex (vRNP). Influenza viruses are enveloped with Hemagglutinin (HA), neuraminidase (NA) and proton ion channel protein M2 embedded in the viral membrane. Matrix (M1) protein forms a shell beneath the lipid membrane. Internally, the virus contains eight segments of viral ribonucleoproteins (vRNPs). Each vRNP has rod shaped structure and consists of single stranded negative sense viral RNA wrapped around Nucleoprotein along with heterotrimeric polymerase complex (PB1, PB2 and PA).

1.1.3. Replication cycle

As a unique exception of RNA viruses, Influenza and Bornaviruses replicate in the nucleus of host cell. Influenza virus replication is initiated by the binding of HA via its receptor binding site (RBS) to sialic-acid (SA) containing receptors (SA). The SA receptor determinant are usually bound to the penultimate galactose (Gal) by either α 2,3- or α 2,6-linkage [28]. α 2,6-linked sialic acid receptors are most abundant in the lung and the upper respiratory tract, the primary site for influenza replication in human, whereas α 2,3 linked receptors are predominantly expressed in the digestive tract of avian species. This suggests that the type of sialic acid species is a major determinant of host range for influenza A viruses [29]. The virus is then internalized into the host cell via endocytosis, which can occur either in a clathrin dependent manner, using dynamin and Epsin-I protein as a co-factor for clathrin

recruitment [30] or by macropinocytosis [31]. The latter mechanism has been shown to be the main entry route of long, filamentous influenza particles which do not fit into clathrin-coated vesicles [32]. Once the virus has entered the cell, virions are transported inside the vesicles to the late endosome in the perinuclear region [33] (Fig.3). Acidification of the internal endosomal environment (pH ~5.0–5.5) during maturation leads to large conformational changes in HA with exposure of the fusion peptide, which insert into the endosomal membrane and mediates fusion of both viral and endosomal membranes [20]. In addition, the low pH activates the ion channel activity of M2 [34] enabling proton influx leading to viral core acidification, which triggers detachment of M1 from vRNPs allowing its release into the cytoplasm via fusion pore [35]. Afterwards, the vRNP utilizes their surface exposed nuclear localization signal (NLS) to activate importin α/β nuclear import pathway, which in turn directs vRNP to host nucleoplasm via nuclear pore [36,37]. In the nucleus, transcription and replication of influenza virus RNA is carried out by viral polymerase complex in a 2-step mechanism: Transcription of negative sense viral RNA (–vRNA) to mRNA for protein synthesis and the second step include the synthesis of complementary RNA (cRNA) which serve as a template for transcription of new vRNA. For initiation of mRNA synthesis, transcription should be primed by “cap snatching”, a mechanism orchestrated by viral polymerase complex where PB2 binds to 5' caps of nascent host mRNA and via its endonucleolytic activity, PA cleaves 10-13 nucleotides downstream of the cap structure [38], then PB1 starts mRNA synthesis from vRNA [39]. Elongation of viral transcription is terminated by 5-7 uridine residues just before the 5' end of vRNA template. This uridine stretch serves as a template for “polyadenylation” required for translation by cellular ribosomes in the cytoplasm [40]. The viral proteins are subdivided into early and late proteins according to timing of synthesis during replication cycle [41]. The core proteins NP, PA, PB1, PB2 as well as NS1 are synthesized first, followed by M1, NEP and the viral surface proteins. Viral envelope peplomers (HA and NA) along with M2 are synthesized at ribosomes associated with rough endoplasmic reticulum (ER) where they gain access to the secretory pathway to be inserted into cellular plasma membrane.

Although both transcription and replication of influenza genome is catalyzed by viral polymerase complex however, they are 2 mechanistically distinct processes. Replication and synthesis of new viral genome occur in a primer independent manner where the newly synthesized vRNA are neither capped nor polyadenylated. The switch between mRNA and cRNA transcription is regulated by virus encoded small RNA (svRNA) [42,43], Short (18-30 nucleotides in length) non-coding RNAs which corresponds to 5' end of vRNA and highly expressed in both mammalian and avian influenza infected cells. Synthesis of svRNA is thought to be promoted by nuclear export protein (NEP). They involved in vRNA synthesis from cRNA in a segment specific manner through binding to *Trans* acting viral polymerase

via RNA binding channel in PA subunit [42-44]. The cRNAs are produced by a process that depends on binding of free rNTPs (Mainly GTP and ATP) to vRNAs at its 3' end. This complementation locks vRNAs into active site of viral polymerase (PB1) and results in formation of A-G dinucleotide from which synthesis of cRNA is initiated [45]. The new synthesized cRNA associates with NP molecules and viral polymerase complex to form new cRNP and assemble with other proteins into progeny virions.

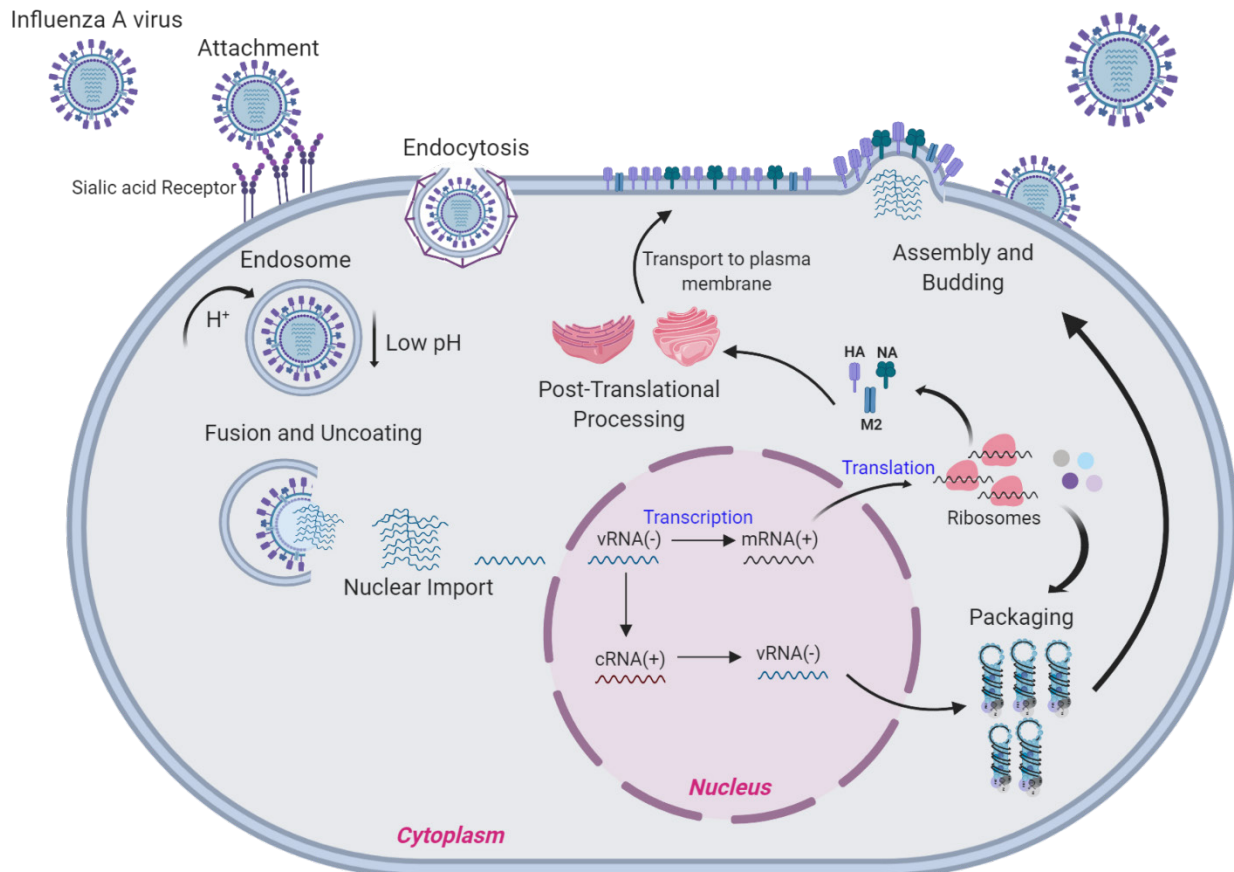


Figure 3. Replication cycle of influenza A virus. Replication of influenza A virus starts with binding of viral hemagglutinin to sialic acid receptors ($\alpha 2,6$ or $\alpha 2,6$) displayed on host cell surface followed by entry via receptor mediated endocytosis. Acidification of the endosomal environment leads to fusion of endosomal and viral membrane and release of the viral genome. Viral genes are then transported to the nucleus, where the genome replication starts. Viral encoded *RDRP* polymerase use the negative sense vRNAs as template for transcription of mRNAs and synthesis of complementary positive sense cRNAs to be used as a template for synthesis of new vRNAs. The mRNAs are delivered to the cytoplasm for translation of proteins; PB1, PB2, PA and NP are transported back to the nucleus to initiate assembly of viral genome whereas NEP and M1 are required for the export of newly assembled vRNPs into the cytosol. After synthesis, the viral envelope proteins HA, NA and M2 are post-translationally modified and transported to the plasma membrane through secretory pathway. HA and NA aggregate and form clusters on the plasma membrane and initiate the assembly by recruiting other viral proteins. Progeny vRNPs are exported to the cytoplasm and Viral assembly takes place at plasma membrane then progeny viruses are released from the cell by sialidase activity of viral NA.

Segment Number	Length (nt)	Viral encoded proteins					
		Name	Length A.As.	M.W. kDa	Carbohydrates Side chain	copy no. per virion	Main function(s)
1	2341	PB2	759	87	-	30-60	<ul style="list-style-type: none"> Part of RNA polymerase complex. Host-cell capped mRNA recognition and binding.
		PB2-S1	508	55	-	NA	<ul style="list-style-type: none"> Inhibit the RIG-I-dependent interferon signaling pathway Interfere with viral polymerase activity by competing to PB1 binding
2	2341	PB1	757	96	-	30-60	<ul style="list-style-type: none"> Component of RNA transcriptase complex. RNA dependent RNA polymerase activity and capped mRNA endonuclease activity.
		PB1-F2	87	10.5	-	2650	<ul style="list-style-type: none"> Induction of apoptosis /Modulation of host interferon response.
		PB1-N40	718	80	-	NA	<ul style="list-style-type: none"> Maintains the balance between PB1 and PB1-F2
3	2233	PA	716	85	-	30-60	<ul style="list-style-type: none"> Component of RNA transcriptase complex. Essential for viral replication and transcription by binding to PB1 and PB2 forming heterotrimeric complex.
		PA-X	252	29	-	NA	<ul style="list-style-type: none"> Suppression of host antiviral response and enhance viral virulence.
		PA-N155	562	62	-	NA	<ul style="list-style-type: none"> Promotes viral replication and pathogenesis
		PA-N182	535	60	-	NA	
4	1778	HA	566	63	+	500	<ul style="list-style-type: none"> Surface trimer glycoprotein and has major antigenic determinant sites. Responsible for receptor binding and membrane fusion.
5	1565	NP	498	56	-	1000	<ul style="list-style-type: none"> Associated with RNA segments to form ribonucleoprotein (vRNP) and protect it from nucleases. Trafficking of vRNP between cytoplasm and nucleus.
6	1413	NA	454	60	+	100	<ul style="list-style-type: none"> Has Sialidase activity required for cleavage of terminal sialic acid to allow release of viral particles.
7	1027	M1	252	28	-	3000	<ul style="list-style-type: none"> Virus assembly and morphogenesis, involved in RNP transport out of nucleus.
		M2	97	15	-	20-60	<ul style="list-style-type: none"> Ion channel activity and involved in uncoating of viral membrane.
8	890	NS1	230	26	-	NA	<ul style="list-style-type: none"> Inhibit mRNA transport from nucleus and antagonize host interferon response.
		NS2/NEP	121	14	-	130-200	<ul style="list-style-type: none"> Nuclear export of vRNP /Regulate vRNA transcription.

Table 1. Collective summary of influenza virus genomic RNA and its encoded proteins

1.1.4 Hemagglutinin glycoprotein (HA)

1.1.4.1. Structure and function of HA

Hemagglutinin is encoded by segment 4 of the influenza A virus genome. It is a type I membrane protein displayed on the viral envelope as a homotrimer. Each HA molecule is consisting of the N-terminal signal peptide which is cleaved at the endoplasmic reticulum (ER), a large ectodomain, a membrane anchor domain (TMD) (25-27 amino acids) and a short cytoplasmic tail (CT) (10-11 Aa). Based on their sequence homology, influenza A HAs are divided into two groups: group 1 HA (H1, H2, H5, H6, H8, H9, H11, H12, H13, H16, and H17) and group 2 HA (H3, H4, H7, H10, H14, and H15) [46]. HA is synthesized as a single precursor polypeptide (HA0), which is post-translationally cleaved into two disulfide-linked subunits (Fig.4A), HA1 and HA2. The HA1 polypeptide encompasses the membrane distal globular head that harbors RBS. The HA2 polypeptide includes the stalk region and the CD helix that forms the trimeric coiled-coil and the A-helix [20,47,48]. The cleavage of HA0 is a prerequisite for viral infectivity [49]. Pathogenicity and virulence of influenza viruses is directly related to the cleavability of HA. In low pathogenic influenza viruses, HA is characterized by having one or 2 nonconsecutive basic amino acids at the cleavage site that can be cleaved by trypsin and trypsin-like proteases. As a consequence, replication of low pathogenic viruses is limited to epithelial cells that express trypsin-like proteases [50]. In avian hosts, the replication is limited to the respiratory and gastrointestinal tract, while in humans only cells of the respiratory tract can be infected. In contrast, HA of highly pathogenic viruses ones (H5 and H7) have multiple basic amino acids (R-X-K/RR) at the cleavage site that can be intracellularly processed by proteases like furin and PC6 [51,52]. These furin and furin like proteases are ubiquitously expressed in most tissues. Thus, the tissue tropism of influenza viruses mainly depends on the availability and expression of proteases responsible for the cleavage of viral HAs which leading to variations in virus pathogenicity [53].

The three-dimensional structure of influenza HA molecule was first revealed for the ectodomain of human H3N2 virus (A/Hongkong/1/68(H3N2)). It showed that HA consists of two structurally distinct regions, a globular head and a fibrous stalk (Fig.4b). The globular head contains HA1 molecule forming an 8 stranded antiparallel β -sheet representing the RBS, which is surrounded by highly variable antigenic loop structures. The fibrous stalk region, more proximal to the viral membrane is made of amino acid residues from both HA1 and HA2. The trimeric structure is mostly supported and stabilized by the fibrous stem regions with a rather weak association of the globular head. The cleavage site between HA1 and HA2 is positioned at the middle of the stalk domain. In HA0, the cleavage site makes a projecting surface loop at the center of the stalk. A cavity is found next to the cleavage site that is incompletely filled by the carboxy terminus of HA1. Once cleavage happens, the carboxy terminus of HA1 show up on the trimer surface, representing a key rearrangement

and conformational change after cleavage of the HA₀. The fusion peptide represented by hydrophobic amino terminus of the HA2 fill the cavity by hiding in the trimeric 3D structure [48,54].

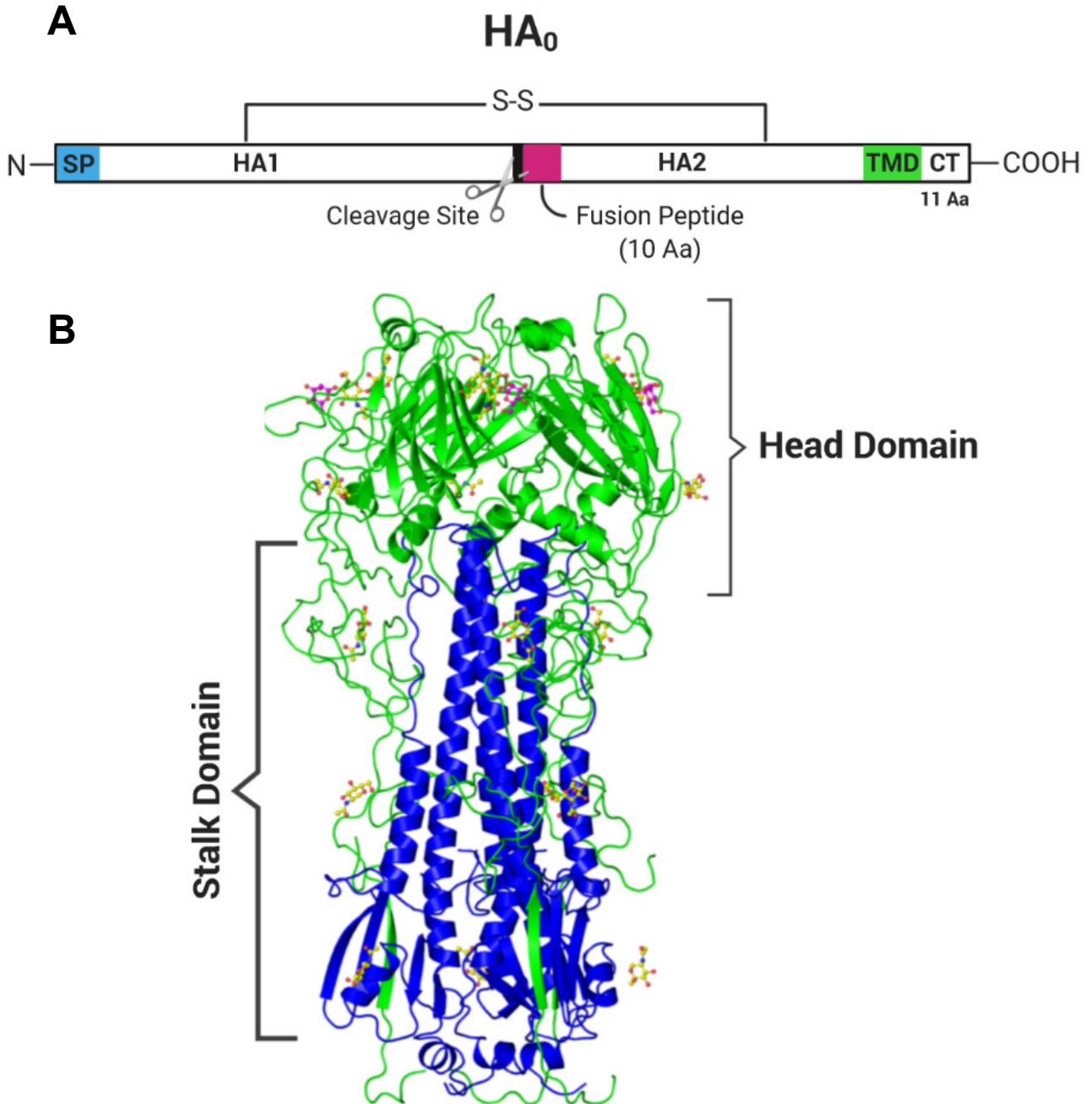


Figure 4. Structure of influenza virus hemagglutinin (HA). (A) Structural arrangement of HA₀ protein, it consists of 2 disulfide linked subunits (HA1 and HA2) with a signal peptide at the amino terminus, HA2 has the fusion peptide, a membrane spanning domain (TMD) and a short cytoplasmic tail of 10-11 amino acids. (B) 3D structure of head and stalk regions of influenza virus HA trimer (PDB: 2HMG).

1.1.4.2. Intracellular transport and processing

Hemagglutinin is synthesized as a precursor HA0 in the ER, where it transiently interacts with the GRP78-BiP protein [55] and calnexin [56] before acquiring high mannose-oligosaccharide chains and making trimers, a prerequisite for its transport out of the ER [55]. Interaction of HA via its N-linked glycans with ER-resident chaperone proteins like GRP78-BiP, calnexin and calreticulin is essential for proper oligomerization and folding of HA. Disulfide bridges formed between thiol groups of cysteine residues play an important role in intracellular synthesis and processing of HA. Cysteine residues located at HA's ectodomain are crucial for both efficient folding and stabilization of the folded protein [57]. Formation of disulfide bond occurs co and post-translationally in the ER. Misfolded HA will be degraded while properly folded monomers assemble into trimers and are transported to cis-Golgi [58]. In the Golgi apparatus, the HA-bound oligosaccharides are processed further to more complex ones. HA is hydrophobically modified during its intracellular transport between the late endoplasmic reticulum and the early Golgi by addition of long chain fatty acids to conserved cysteines in a process known as „acylation “. Acylation of influenza virus proteins and its effect on virus replication will be discussed in detail in the next section.

In polarized cells, the final step of HA maturation is transport to the apical cell surface [59]. Transport of viral HA across apical membrane is mediated by “proteolipid MAL”, a non-glycosylated integral membrane protein and a major component of the apical transport pathway. Signals responsible for apical transport are located in the transmembrane and/or cytoplasmic regions of HA [60]. Mutation of the sorting signal in the HA cytoplasmic tail from apical to basolateral directs more than 50% of the mutant HAs to the basolateral membrane, but the mutant viruses budded mainly from the apical membrane, highlighting that factors other than the HA sorting signal might play a role in apical budding [61].

Interaction of HA with lipid rafts was first described by *Scheiffele et al* [62]. Lipid rafts are sphingomyelin and cholesterol enriched microdomains in the plasma membrane. They are biochemically defined as “detergent resistant membranes” (DRM) that resist solubilization by nonionic detergents such as Triton X-100 on ice and float to a low buoyant density upon density gradient centrifugation, but they are sensitive to cholesterol extraction and inhibitors of sphingolipid synthesis [63]. Lipid rafts are assumed to provide platforms for the assembly and budding of viruses, most likely by increasing the local concentration of viral structural proteins. HA binds and interacts with rafts through its transmembrane region; however, cytoplasmic tail HA deficient mutants showed impaired raft association as well [64]. Wild-type HA forms clusters at the surface of infected cells; in contrast to raft association mutant which was randomly distributed over plasma membrane. 'Non-raft' virus mutant was characterized by abrogated budding and fusion activity [65].

1.2. Acylation/Palmitoylation of proteins

Protein S-acylation is an often reversible, dynamic post-translational lipid modification that involves attachment of fatty acids to the thiol side chain of cysteine residues via a labile thioester linkage [66,67]. This modification is also known as “S-palmitoylation“, because palmitate is the most common fatty acid attached to S-acylated proteins. However, other saturated (e.g., myristic and stearic) and unsaturated (e.g., oleic and arachidonic) lipid moieties can be also added, but to a lesser extent [68]. In general, it is important for targeting proteins to membranes or membrane domains and modulates a wide range of protein properties, including protein conformation, stability and function including protein interactions. In contrast to other lipid modifications, such as N-myristoylation and isoprenylation, palmitoylation requires no specific consensus motif. However, palmitoylated cysteine are frequently located between the transmembrane and cytoplasmic regions of the substrate, often in the vicinity of basic or hydrophobic amino acids [69]. This process is mediated by an enzyme family characterized by having a conserved “DHHC” motif, These DHHC-proteins are present in all eukaryotes, but not in the bacteria [70,71] However, intracellular bacteria hijack and utilize the acylation machinery of the host to target injected effector proteins to membranes [72]. One of the unique features of S-acylation relative to other lipid modifications is its enzymatic reversibility, which implies a fundamental important role in trafficking and localization of cellular proteins through S-acylation and de-acylation cycles [69].

S-acylation was first described by Schmidt and Schlesinger in 1979, who identified binding of the fatty acid palmitate to the glycoprotein (G) of vesicular stomatitis virus [73] and since then hundreds of palmitoylated proteins have been reported. Historically, studying palmitoylation and its potential regulatory mechanisms on protein functions was relatively difficult due to technical challenges associated with the identification of protein substrates, such as low sensitivity of detection methods, lack of defined consensus sequence for fatty acid attachment and shortage of information about the enzymes involved in the acylation process. However, due to recent technological advances in studying lipid modifications, many more palmitoylated have been identified, more sensitive and quantitative methods have been developed and the first crystal structure of palmitoyl-acyltransferase was resolved leading to great improvement in the available knowledge and understanding of mechanisms and dynamics of protein S-acylation.

1.2.1. S-acylated proteins of viruses pathogenic for human

Viruses do not encode for palmitoylation enzymes, but many viral proteins are palmitoylated by the host cell machinery and play a crucial role in different aspects of their life cycle from viral entry to viral budding [74]. Palmitoylated viral proteins are classified based on their membrane topology into two main groups, transmembrane and peripheral membrane

proteins (Fig.5). The best example for the first group is viral spike glycoproteins, which mostly belong to type I transmembrane proteins. These proteins are composed of an N-terminal cleavable signal peptide, an extra-viral ectodomain, a transmembrane region and a cytoplasmic tail [74]. Palmitoylated type I transmembrane spike proteins are mainly involved in receptor binding and virus entry, such as hemagglutinin (HA) of influenza viruses, S-protein of coronavirus (CoVs), glycoprotein G of vesicular stomatitis virus (VSV), E1 and E2 of toga viruses (Semilki forest virus and Sindbis virus) and Fusion protein (F) of several members of paramyxoviridae (e.g. Measles virus).

A key role of S-acylation for efficient transport of viral spike proteins (and other cargo) through the Golgi was recently proposed. Palmitoylation occurring at the *cis*-Golgi catalyzed by mainly ZDHHC 3 and 7 acts as a biophysical switch that causes self-sorting of transmembrane proteins to the curved rims of Golgi cisternae [75,76]. However, significant delay in transport of deacylated HA along the secretory pathway was not observed in previous reports [77,78]. In contrast, transport was strongly retarded if a cholesterol-binding site located at the outer part of HA's transmembrane region was mutated [79,80]. Furthermore, several viral proteins are acylated, but are never transported to the plasma membrane since they bud from internal membranes. Thus, the proposed model is attractive, but may not be applicable for every S-acylated viral glycoprotein.

Another category of palmitoylated viral proteins are called "Viroporins", which are small hydrophobic proteins encoded by a wide variety of pathogenic viruses, such as hepatitis C virus (HCV), HIV-1, influenza, coronaviruses, poliovirus and togaviruses. They are abundantly expressed and oligomerize in infected cells forming hydrophilic pores in the cell membrane to facilitate assembly and budding of viral particles. The viroporins have either type III membrane topology (one membrane-spanning domain and long cytoplasmic tail) or a hairpin like topology (2 TM domains connected by a loop). The third group are peripheral membrane proteins that lack a hydrophobic amino acid sequence required for membrane insertion. Instead, s-acylation promotes stable membrane anchoring [69]. Examples of viral peripheral membrane proteins that are palmitoylated are UL11 and UL51 of herpesvirus, F13l protein of vaccinia virus, the core protein of HCV and non-structural protein nsP1 of sindbis and semilki forest virus (SFV).

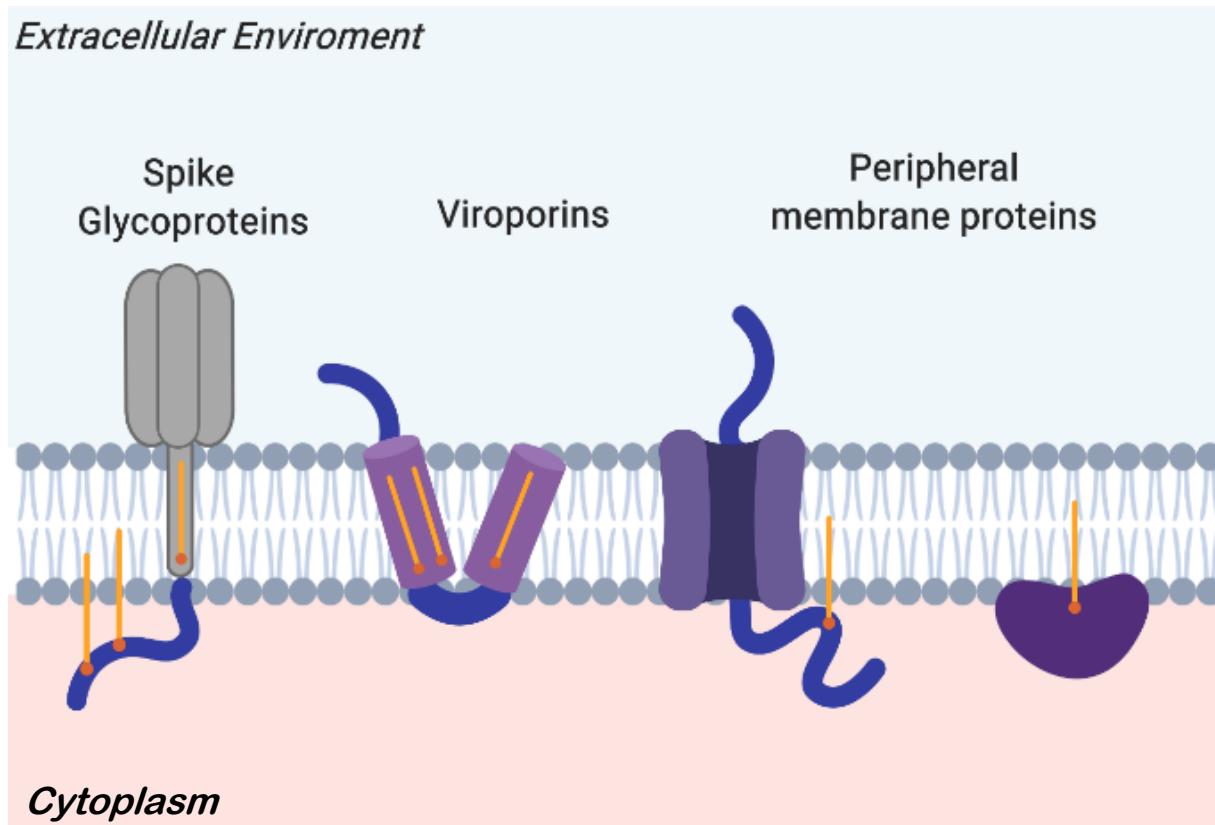


Figure 5. Membrane topology of s-acylated viral proteins. Three major categories of viral proteins, (1) Transmembrane glycoproteins like influenza HA which consists of large ectodomain, Transmembrane region and short cytoplasmic tail. (2) Viroporins are small hydrophobic proteins embedded in the plasma membrane of infected cells. (3) Peripheral membrane proteins, which lacks the hydrophobic sequence, required for membrane binding. Fatty acids bound to cysteine residues are shown in orange.

1.2.1.1. S-acylated proteins of Influenza viruses

Among the different proteins of influenza viruses, only HA and M2 are known to be acylated. Influenza A and B viruses have HA as major viral displayed glycoprotein responsible for receptor binding and membrane fusion while Influenza C virus has a single glycoprotein doing both functions of HA and NA in flu A and B viruses called Hemagglutinin esterase fusion protein (HEF). Virus particles contain also minor amounts of the M2 proton channel, which is palmitoylated at a cysteine positioned in an amphiphilic helix near the TMR [78,81,82]. HA and HEF as well as M2 are S-acylated with different fatty acids at cytoplasmic and transmembrane cysteine residues [78,81-85]. Hemagglutinin of Influenza B virus have 2 cysteines in the cytoplasmic tail which are mainly bound to palmitic acid (97%), while HEF of Influenza C virus is predominantly modified with stearic acid (88%) at a single cysteine at the end of the transmembrane region (TMR) (Fig.6). HAs of Influenza A virus contain a mixture of palmitate and stearate, but MS analysis revealed that stearate is exclusively attached to the cysteine positioned at the end of the transmembrane region, whereas the two cytoplasmic cysteines are always acylated with palmitate, attachment of stearate was always

less than 5% [86,87]. The percentage of stearate in all HA variants varies from 35% (i.e. each TMR cysteine is modified with stearate) to 12% (showing that only one of three TMR cysteines in the trimeric HA spike is stearylated). However, the main signal for stearate attachment is the location of an acylation site relative to the transmembrane span since shifting the TMR cysteine to a cytoplasmic location virtually eliminated attachment of stearate [88].

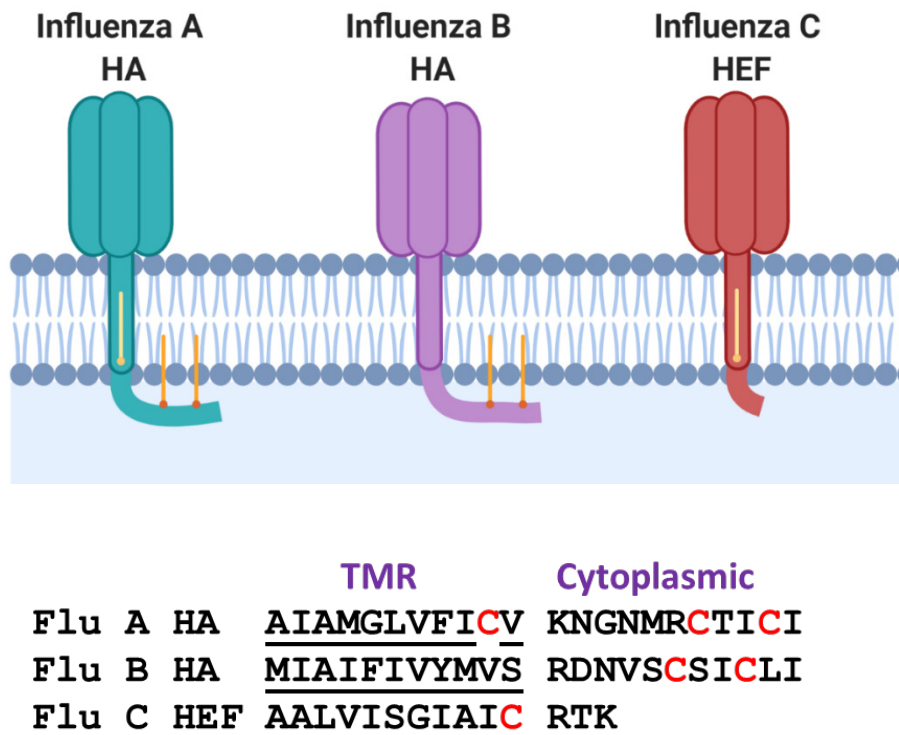


Figure 6. S-acylation pattern of HA glycoprotein in different influenza subtypes. Scheme of proteins with attached fatty acids and amino acid sequences at the end of the transmembrane region and of the cytoplasmic tail. Acylated cysteines are in red.

S-acylation of HA is involved in cell entry of viruses by membrane fusion and virus budding [89]. The fusion of viral and cellular membranes assumingly proceeds via a “hemifusion” stage, which is characterized by mixing of lipids of the two membranes. In the subsequent step a fusion, pore forms, which opens, flickers and dilates allowing entry of viral genome into the target cells to initiate the viral replication cycle [90,91]. Contradictory data have been published concerning the effect of acylation on the ability of HA from different influenza subtypes to mediate full fusion demonstrated by syncytium formation between HA expressing and adjacent cells. [84,92-94]. The exact role of acylation in HA-mediated membrane fusion appears to vary dramatically between different HA subtypes. It was reported that deacylated HA mutants from H1, H7 and H2 subtypes show impaired fusion pore or syncytium formation

[84,95,96] . In contrast, HA acylation mutants from the same H2 subtype, but also from H3 subtype mediate cell-to-cell fusion [78,93,94]. In addition, acylation of HA is one of the key players in influenza virus assembly and budding where it organizes the viral budzone, a large raft domain which provides a platform required for enriching the viral components and facilitate their interactions in preparation for assembly and budding of new virus particles [97,98].

Whatever the role played by s-acylation in the influenza replication cycle might be, this hydrophobic post-translational modification is crucial for virus multiplication, since mutation of 2 or 3 acylation site in HA subtypes H1, H3 and H7 yielded no virus by reverse genetic system. Those with single mutated acylation site can be rescued but showed impaired growth in cell culture [96,99,100]. As an example, deletion of the two cytoplasmic cysteines (modified with palmitate) in HA of WSN (H1N1 strain) of Influenza A virus prevented rescue of infectious virus, whereas viruses with a deletion of the stearylated cysteine at the transmembrane domain showed only slight growth defect in cell culture [101], which is in agreement with other studies on H3 and H7 HA strains. [96,99,100]. Likewise, mutation of the single stearylated cysteine in influenza C HEF protein has no effect on virus rescue and viral infectivity was only slightly (~1log) reduced [102]. Virus mutants were not made with H2 subtype and Influenza B viruses, but exchange of the conserved acylation sites in HA influenza expressed impaired fusion pore formation indicating that palmitoylation significantly contributes to virus replication [95,103]. In summary, palmitoylation of the two cytoplasmic cysteines is essential for virus replication, whereas the stearylated cysteine has only a moderate effect.

This is supported by a comparison of all influenza A HA sequences present in the NCBI-database (≈ 17.000). Each molecule contains three, some even four cysteine residues located in the relevant region [101]. The conservation of cysteines residues in a rapidly mutating molecule like HA supports its essential role in the life cycle of Influenza viruses.

In contrast, the acylation site of M2 does not exist in ~15% of M2 variants. Deletion of acylation site had no effect on virus rescue with no replication impairment in cell culture [104], but acylation of M2 and HA together synergistically affect virus release [105] and viruses mutants having a deleted acylation site in M2 showed reduced pathogenicity in mice [106].

1.2.1.2. S-acylation of proteins from other viruses

Measles, Respiratory syncytial virus, Nipah, Hendra (Paramyxovirus, ss, RNA (-), enveloped)

The F-protein of many paramyxoviruses is S-acylated at one or several cysteines located in the inner part of the TMR, at least in the case of Newcastle Disease virus with stearate [107].

It is controversial whether acylation of F affects its fusion activity; removal of certain (but not each) acylated cysteine residue from the F-protein of measles virus reduced its cell-cell fusion activity, but no such effect was reported for the human respiratory syncytial virus [108,109]. Nipah and Hendravirus contain a cysteine in the middle of the transmembrane region of F but have not been analyzed for S-acylation of its proteins.

Rabies virus (Rhabdoviridae, ss, RNA (-), enveloped)

The G-protein of rabies virus is palmitoylated at least one of the cysteines in its cytoplasmic tail, but no functional studies were performed [110]. In the case of the G-protein of the closely related VSV no effect on its functions was found when the palmitoylation site was removed [111]. Moreover, a natural VSV strain exists that lacks the acylated cysteine in the G-protein indicating that acylation has no essential role.

Ebola- and Marburg viruses (Filoviridae, ss, RNA (-), enveloped)

No function could be attributed to palmitoylation of the filovirus glycoprotein, which also occurs on membrane-near cytosolic cysteines [112,113].

SARS, MERS (Coronaviridae, ss, RNA (+), enveloped)

Coronaviruses contain two S-acylated proteins, the large spike protein S, which is S-acylated at a cluster (8-10) of membrane-near cysteine residues in the cytoplasmic tail and the small envelope protein E, a viroporin and assembly factor that contains three S-acylated cysteines in a cytosolic amphiphilic helix. Palmitoylation is required for S to perform its fusion activity and affects virus assembly [114-116]. S-acylation of E also affects virus assembly and production [117,118] indicating that palmitoylation of both proteins is crucial.

Chikungunya virus (Togaviridae, ss, RNA (+), enveloped)

Chikungunya virus contains a large number of putative S-acylation sites in the E1/E2 glycoprotein complex and in the 6K/TF protein, which have been shown in the closely related Sindbis virus to be required for virus budding [119-124]. In addition and based on previous work with Semliki Forest virus, the non-structural protein 1 of Chikungunya virus requires palmitoylation for its proper localization and for replication of its RNA genome [125,126].

Hepatitis C virus (Flaviviridae, Hepacivirus, ss, RNA (+), envelope)

The highly conserved core protein of Hepatitis C virus (HCV) is palmitoylated at a cysteine residue located close to its single C-terminal membrane-span. Removal of the palmitoylation site prevents the association of the core with ER membranes and impairs virion production [127]. Conflicting data have been reported whether NS4B is palmitoylated, a nonstructural integral membrane protein that serves as a scaffold for the virus replication complex on ER-derived membranes [128,129].

Human Immunodeficiency virus (Retroviridae, RNA, reverse transcribing)

Likewise, whether S-acylation of cysteines in the cytoplasmic tail of the gp41 of HIV has an effect on virus replication is controversial [130,131].

Tat, a non-structural protein, is secreted from HIV-infected cells and enters neighboring host cells by endocytosis and translocation into the cytosol. Tat is palmitoylated at one of several cysteines in its N-terminal domain, but only in the host cell, not in the HIV-infected cell. The palmitoylated version of tat binds with higher affinity to phosphatidylinositol-4,5 phosphate, which inhibits PI(4,5)P₂-dependent membrane traffic, such as phagocytosis and neurosecretion, which partially explains the neurotoxicity of most HIV strains [132].

Hepatitis B virus (Hepadnaviridae, DNA, reverse transcribing, enveloped)

The large version of the envelope glycoprotein is myristoylated at its N-terminus, but apparently not palmitoylated, although the cytoplasmic loop between TMD1 and 2 contains several cysteine residues [133].

Herpes simplex and Cytomegalovirus (Herpesvirales: ds-DNA, enveloped)

The fusion protein gB of Cytomegalovirus is S-acylated at a single cytosolic cysteine located close to its transmembrane region. Palmitoylation affects the fusion activity of gB, probably because it maintains cholesterol-induced clustering. Interestingly, gBs of other herpesviruses do not contain a cysteine residue in a similar position [134]. Glycoprotein gN of cytomegalovirus contains two fatty acids in its short cytoplasmic tail, which affect virus morphogenesis [135]. Using high-throughput mass spectrometry several glycoproteins of herpes simplex virus including gE, gG, gI, gK as well as non-glycosylated proteins (US2, US3, UL56, UL51 and UL24) were shown to be palmitoylated, but no functional studies were performed so far [136].

Hepatitis E virus (Hepeviridae, ss, RNA (+), not enveloped)

ORF-3, a small and hydrophobic protein of hepatitis E virus (HEV) is one of the few palmitoylated proteins hitherto described for a non-enveloped virus. It carries several fatty acids in its N-terminal region, which bind the protein to the cytosolic side of cellular membranes. Mutagenesis of palmitoylation sites causes significant reduction in secretion of viral particles indicating that the modification is required for efficient virus replication [137].

In summary, a large variety of proteins from diverse virus families are palmitoylated and in most cases the modification is beneficial or even essential for virus replication. Previous research has concentrated mainly on viral spike proteins, but recent data revealed that non-structural proteins are also acylated. Presumably, many more await their discovery, especially in the large DNA viruses that encode more than 100 proteins. Progress in mass spectrometry now allows identifying candidates in much shorter time periods [136,138] and the enzymes that mediate their acylation also begin to be elucidated.

1.3. Enzymology of S-acylation

Initially, it was thought that palmitoylation might occur via a non-enzymatic mechanism due to many unsuccessful attempts to identify palmitoylating enzymes using traditional biochemical methods, i.e. incubating purified substrate proteins with cellular extracts as an enzyme source. Although various substrates became acylated *in vitro* if they are incubated with Pal-CoA, however usually at very low stoichiometry or at unphysiologically high pH or acyl-CoA concentrations [139-143]. Stoichiometric auto-acylation has been described for only two proteins: TEAD, a transcription factor and Bet3, which is involved in vesicular transport. Crystal structures of both proteins revealed that the acyl chain is buried inside a hydrophobic tunnel and is attached to a cysteine located at its entrance. Auto-acylation of Bet3 occurs also inside cells since simultaneous knockdown of every ZDHHC protein in yeast did not diminish the modification [144-147]

S-acylation reactions are now thought to be catalyzed by enzymes, namely by members of the ZDHHC family. The discovery of the enzymes responsible for fatty acid attachment represent a great breakthrough in the field of S-acylation. The first protein acyltransferases were described in yeast in 2002. Erf2/Erf4 and Akr1p were identified as palmitoylating enzymes specific for Ras2 [148] and Yck2p [149], respectively. Analysis of amino acid sequence of these two enzymes revealed that they share a conserved Asp-His-His-Cys (DHHC) sequence located within a ~50 aa cysteine-rich domain (CRD), which is responsible for the catalytic activity of these enzymes. Identification of these enzymes and their active site has provided the starting point for the subsequent discovery of genes encoding such proteins in human and other mammalian species [150,151] where they all have the DHHC-CRD signature domain giving the family its characteristic name. The number of ZDHHC family members varies from 5-7 in yeast [146] to 23 in human [71]. Although they are different in molecular size, structure, and substrate interactions, they share a common topology comprising 4-6 transmembrane domains (TM) with the DHHC-CRD domain localized in the cytoplasm within the intracellular loop between TM2 and TM3. This makes the S-acylation process limited to cysteine residues in a protein that have a membrane-near, cytosolic environment.

ZDHHC S-acyltransferase family members have distinct cellular localizations; most of them are localized in the endoplasmic reticulum (ER) and Golgi apparatus, the major intracellular sites of protein palmitoylation. The exception to this are ZDHHC-5, ZDHHC-20 and DHHC-21 who primarily localize to plasma membrane [151]. The parameters and rules that determine how these enzymes choose their respective subcellular localization remain unclear for most ZDHHCs. There is some sort of inconsistency in localization studies of DHHC enzymes, which could be attributed to the lack of specific antibodies against endogenous proteins and the use of epitope tagged ZDHHC proteins, the cell type, stage of cell cycle or even

laboratory differences. For example, ZDHHC20 is localized on the plasma membrane when it is overexpressed in HEK293T cells [151] while remains in the ER in A549 cells (Fig.31). ZDHHCs themselves are palmitoylated in vivo and in vitro, which is part of the 2-step reaction mechanism. [152], A fatty acid chain is first transferred from acyl-CoA to the DHHC domain of the enzyme forming a transient acyl-enzyme intermediate [153], this step is called “auto-acylation” .The second step includes the transfer of fatty acyl moieties to the target protein substrate (Fig.7). No clear motifs on the DHHC proteins for recognition and interaction with target substrates have been identified so far. However, there are some DHHC enzymes that recognize their substrates via distinct binding domains, such as C-terminal ankyrin repeats on ZDHHC13 and 17 [154], SH3 on ZDHHC6 [155,156] and PDZ motifs in the COOH terminus of ZDHHC5 and 8 [157].

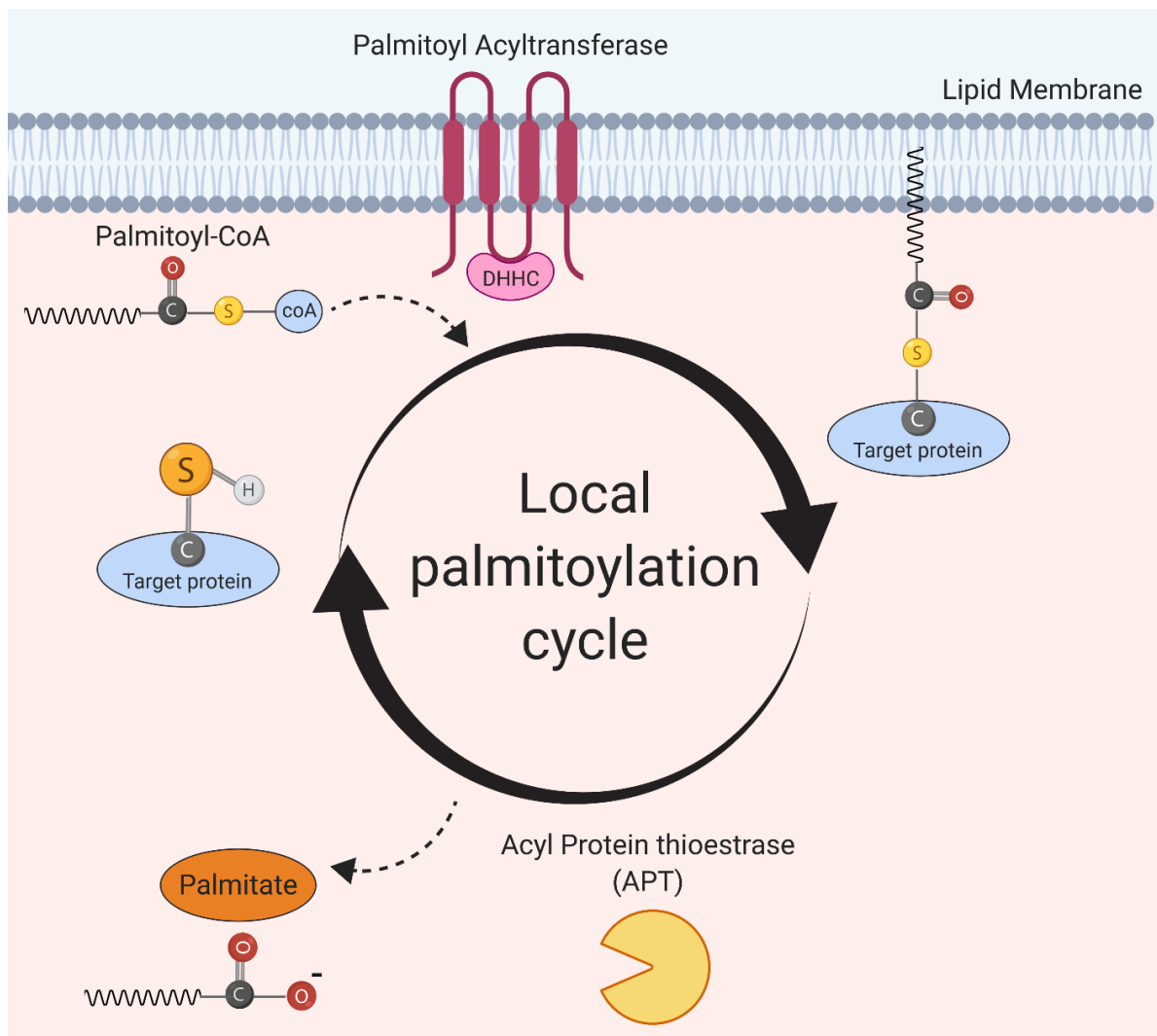


Figure 7. Dynamic protein S-palmitoylation. Fatty acid acyl chain is first transferred from acyl-CoA to DHHC domain of the membrane bound acyl-transferase “Autoacylation” followed by modification of target protein allowing their anchoring to the membranes. Palmitoylated proteins can be also de-acylated by S-acyl-Thioesterases and translocates to the cytoplasm.

Enzyme	Uniprot Accession No.	Synonyms	Molecular Weight (kDa)	No. of TM Domains	Interaction domains	Intracellular localization
ZDHHC1	Q8WTX9	ZNF377, C16orf1	55	4	-	ER
ZDHHC2	Q9UIJ5	REAM, REC, ZNF372	42	4	-	ER, Golgi
ZDHHC3	Q9NYG2	GODZ	34	4	-	Golgi
ZDHHC4	Q9NPG8	ZNF374	40	5	-	ER
ZDHHC5	Q9C0B5	KIAA1748, ZNF375	78	4	PDZ Domain	Plasma membrane
ZDHHC6	Q9H6R6	ZNF376	47	4	SH3 Domain	ER
ZDHHC7	Q9NXF8	SERZ- β	35	4	-	Golgi
ZDHHC8	Q9JLC8	KIAA1292, ZDHHCL1, ZNF378	80	4	PDZ Domain	Golgi
ZDHHC9	Q9Y397	CXorf11, ZDHHC10, ZNF379, ZNF380	41	4	-	ER, Golgi
ZDHHC11	Q9H8X9	ZNF399	40	4	-	ER
ZDHHC12	Q96GR4	ZNF400	25	4	-	ER, Golgi
ZDHHC13	Q8IUH4	HIP14L, HIP3RP	71	6	Ankyrin repeats	ER, Golgi
ZDHHC14	Q8IZN3	NEW1CP	53	4	-	ER
ZDHHC15	Q96MV8	-	40	4	-	Golgi
ZDHHC16	Q969W1	APH2	44	4	-	ER
ZDHHC17	Q8IUH5	HIP3, HIP14, HYPH	73	6	Ankyrin repeats	Golgi
ZDHHC18	Q9NUE0	-	42	4	-	Golgi
ZDHHC19	Q8WVZ1	-	34	4	-	ER
ZDHHC20	Q5W0Z9	-	42	4	-	Golgi, PM
ZDHHC21	Q8IVQ6	-	31	4	-	Plasma membrane
ZDHHC22	Q8N966	C14orf59	29	4	-	ER, Golgi
ZDHHC23	Q8IYP9	NIDD	43	6	-	Nucleus and cytoplasmic vesicle
ZDHHC24	Q6UX98	-	30	5	-	PM, ER, Golgi

Table 2. Structural characteristics, interaction domains and intracellular localization of human ZDHHC S-acyltransferases

1.3.1. Crystal structures of ZDHHC enzymes

Recently, the crystal structures of two ZDHHC-proteins, human ZDHHC20 and zebrafish ZDHHC 15 were determined [158]. The four transmembrane helices form a tent-like structure with the DHHC-motif located at the membrane-cytosol interface. The active site has a catalytic triad like arrangement of aspartic acid and histidine that activate the nucleophile cysteine. The highly conserved cysteine-rich region forms six β -sheets that coordinate two zinc-ions, which impart structural stability [159]. This part of the molecule also contains a patch of positively charged residues that bind the negatively charged phosphates of the CoA moiety. The 3D-structure of the acylated enzyme intermediate, 2-bromo-palmitate attached to Cys of the ZDHHC motif is essentially identical (Fig.8). The fatty acid is inserted into a hydrophobic cavity formed by all four transmembrane regions. The residues in the groove interacting with the acyl chain have been identified for both ZDHHC15 and ZDHHC 20. At the narrow end of the tunnel, Ser29 forms a hydrogen bond with Tyr181, which effectively closes the groove. In contrast to many other amino acids contacting the acyl chain, Ser29 and Tyr181 are not conserved between ZDHHC proteins. All ZDHHCs contain either two bulky residues, one bulky and one small or two small amino acids at the homologues position. The authors hypothesize that the presence of certain amino acids (large or small) determines the lipid binding specificity of a ZDHHC. Indeed, exchanging Tyr181 by a less bulky alanine residue results in a significant increase in the attachment of stearate to ZDHHC20 whereas exchanging Ser29 by Phe increases the preference for palmitate. Likewise, a similar exchange of bulky by small amino acids increases attachment of stearate by ZDHHC3 [160]. Thus, the amino acids at the end of the hydrophobic cavity regulate its deepness and hence presumably determine which fatty acid is accommodated by a given ZDHHC. Although such a mechanism is attractive since it explains whether a certain ZDHHC might be able to use stearate, it is hard to envision how a ZDHHC discriminates against shorter acyl chains. Myristate was never detected as fatty acid bound to HA or to any other viral glycoprotein and cysteines located at the end of the transmembrane of various viral glycoproteins are (almost) exclusively acylated with stearate [86,87,107]. Thus, other mechanism, such as the local concentration of specific acyl-CoAs near a certain ZDHHC protein or acyl-binding proteins [161], some of which might prefer certain acyl-CoAs, might contribute to the observed specificity in fatty acid attachment to some proteins and acylation sites.

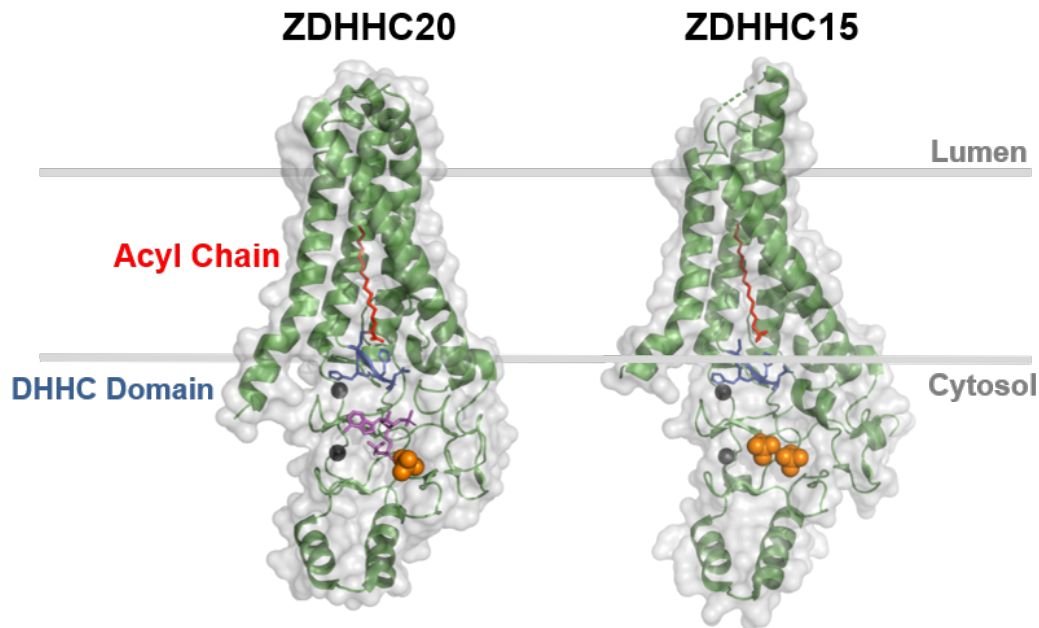


Figure 8. Crystal structure of ZDHHC20 and ZDHHC15 acyltransferases. Surface representation of ZDHHC 20 and 15 revealing also the folding of the polypeptide chain. The membrane-embedded parts are confined by two horizontal lines. The cysteine of the ZDHHC motif (highlighted as blue sticks) is linked to 2-bromo palmitate (highlighted in red) which is embedded in a hydrophobic tunnel. The black balls are zinc ions bound to the cysteine rich domain. The orange balls are phosphate ions probably representing the acyl-CoA binding site

1.3.2. Lipid- and protein substrate specificities of ZDHHC proteins

Mammalian ZDHHC enzymes display distinct fatty acyl preferences [160], meaning that they have the ability to preferentially incorporate and transfer acyl chains of different lengths with distinct efficiencies. ZDHHC3 showed clear preference for attachment of short chain fatty (C:14 myristic acid and C:16 palmitic acid) over long chain fatty acids, while ZDHHC2 displayed affinity for a wide range of acyl-CoA chain lengths with different degrees of saturation [152]. Despite high genetic similarity of ZDHHC3 and ZDHHC7, they have a clear difference in the acyl-chain selectivity due to mutation in single amino acid change (Ile182) in TM3 of ZDHHC enzyme [160]. Most recently, it has been found that such enzymatic selectivity is controlled by the composition of amino acids capping the hydrophobic cavity of the protein [158].

Fatty acids for acylation are intracellularly synthesized by the *fatty acid synthase*, a large, cytosolic multi-enzyme complex. Expression of the enzymes controlling lipid and cholesterol biosynthesis is regulated by the sterol regulatory element binding protein (SREBP). The transmembrane protein SREBP is typically localized in the ER and only transported to the Golgi if the cholesterol concentration in the ER membrane is low. In the Golgi, SREBP is proteolytically cleaved leading to release of the soluble n-SREBP fragment into the cytosol which afterwards translocates to the nucleus where it binds to the sterol-regulatory elements (SRE) in the promotor/enhancer region of multiple lipogenic genes [162]. Interestingly, AM580, a benzoic derivative of retinoic acid, which is known to inhibit MERS-CoV and

Influenza virus replication, binds to the SRE-interaction site in n-SREBP thereby inhibiting the upregulation of lipogenic enzymes. In the case of Influenza virus, it was observed that AM850 reduces palmitoylation of HA [163]. Whether complete palmitoylation of other viral proteins also requires de novo synthesis of fatty acids remains to be shown, but a functional fatty acid synthase is required for efficient replication of many enveloped viruses, such as HCV, HIV, respiratory syncytial virus and Chikungunya virus [126,164-166].

1.3.3. Acylprotein thioesterases and other enzymes that deacylate proteins

Due to the labile nature of the thioester linkage, S-acylation is a reversible and dynamic process. A protein can undergo several cycles of acylation/deacylation which is critical in regulation of the function, trafficking and localization of proteins involved in signal transduction, cell adhesion and cell organelle structure. Despite the large number of palmitoylating enzymes identified in mammalian hosts (23 ZDHHC enzymes). Deacylation is mainly catalyzed by only 3 enzymes known as "S-acyl-thioesterases". Acyl-protein thioesterase 1 (APT-1), Acyl-protein Thioesterase 2 (APT-2) and acyl protein thioesterase like 1 (APTL1). Dynamic acylation cycles is well known and reported for many of cellular palmitoylated proteins however it is not described for any of the viral proteins so far. Acylprotein thioesterases are localized in the cytosolic compartment and responsible for removal of palmitate from membrane bound cytosolic proteins or membrane proteins having their palmitoyl-group in the cytoplasmic side. APT-1 is the major depalmitoylating enzyme involved in dynamic cycles of protein S-acylation [167]. APT is active against several known palmitoylated proteins like heterotrimeric G protein α subunits, H-Ras [167], eNOS [168] and BK potassium channels [169]. APT2, a highly identical analogue of APT1 (68% amino acid sequence Homology) and has been reported to have thioesterase activity against N-Ras and GAP43 [170,171]. APT-1 and APT-2 are palmitoylated on themselves and this was thought to target them to plasma membrane, where they interact and deacylate their target proteins [172]. However, another report showed that unpalmitoylated APT is still able to maintain its deacylation activity on substrate proteins [173]. The activity of APTs can be altered in response to extracellular signals or other stimuli, making them a key player in turnover of palmitoylated proteins.

The activity and stability of (at least one) ZDHHC protein is regulated by dynamic cycles of palmitoylation and deacylation. ZDHHC6, which modifies proteins required for protein folding in the endoplasmic reticulum, is acylated at three cysteines (Cys 328, 329 and 343) located in its C-terminal SH2-like domain by ZDHHC 16. In HeLa cells more than half of all ZDHHC6 molecules are present in a non-palmitoylated and inactive form, but palmitoylation and hence activity of ZDHHC6 increases upon overexpression of ZDHHC16. Interestingly, acylation at individual sites has different effects. If only Cys 328 is palmitoylated ZDHHC6 is highly active, but rapidly inactivated, either by degradation via the ERAD pathway or by

depalmitoylation catalysed by the thioesterase APT2. In contrast, ZDHHC6 forms palmitoylated only at Cys 329 or at Cys 329 plus Cys 343 are moderately active, but long-lived [174].

1.4. Methods to study s-acylation of proteins

S-acylation of proteins can be studied by different approaches, each of which has its own advantages and limitations:

I. Radioactive labeling

It is the oldest technique, but still considered as the “gold standard” for identification and studying s-acylated proteins. It includes incubation of the cells with radioactive palmitic acid ($[^3\text{H}]$ or $[^{14}\text{C}]$), which is metabolically incorporated into palmitoylation sites [175]. This method is ideally suited for studying S-acylation in cultured cells and cannot be used for intact tissues. Briefly, labeled cells are lysed and the target protein is immune precipitated using antibodies followed by SDS and fluorography. The major strength point of this approach is the capability of studying protein palmitoylation dynamics, since it is suitable for pulse chase experiments. However, it has several disadvantages: (1) lengthy exposure time of the X-ray film which can vary from few days to months according to the abundance of target protein and the efficiency of labelling and immunoprecipitation procedures (2) cannot be adapted to perform high throughput palmitoylation analysis.

II. Acyl biotin exchange (ABE) and Acyl-resin assisted capture (Acyl-RAC).

ABE and Acyl-RAC are closely related methods and now the most frequently used assays for studying s-acylation [176,177]. Both utilize the same chemistry for capturing of s-acylated proteins, which can be summarized in three main steps: (1) Reduction of disulfide bonds and irreversible blocking of all free cysteines using NEM (ABE) or MMTS (Acyl-RAC). (2) Selective cleavage of thioester linkages using hydroxylamine at neutral pH. (3) Capture of newly exposed thiol groups, either by biotinylation and subsequent streptavidin-beads capture (ABE) or directly on activated thiopropyl sepharose beads (Acyl-RAC). Acylated proteins are eluted from beads, separated by SDS-PAGE and detected by immunoblotting. These methods can be used for identification of proteins isolated from both tissues and cultured cells and can be also coupled to MS for high throughput proteomic studies. However, these methods cannot determine the nature of the bound lipid, since the resins bind and enrich any protein having a hydroxylamine cleavable thioester bond. Insufficient blocking of free cysteines can give false positive signals. However, this disadvantage can easily be controlled by increasing the reduction time and increasing the concentration of the blocking reagent.

Acyl-PEG exchange (APE) is a modification of the acyl-RAC assay, where thioester-linked fatty acids are cleaved from proteins and the liberated sites subsequently modified by a

cysteine-reactive reagent. In this case, the tag attached to S-acylated proteins is a polyethylene glycol polymer (mPEG) that increases the molecular weight of the modified proteins by 5 kDa per acylation site. This causes a mobility shift in an acylated protein relative to non-acylated ones, which can be readily monitored by SDS-PAGE and Western blot with antibodies [178].

III. Click Chemistry based methods (Isotope free labeling)

Another approach that has been frequently used in recent palmitoylation studies is non-radioactive metabolic labeling of substrate protein with azide-linked fatty acids [179-181]. This method can be used for global and large-scale analysis of acylated proteins using 17-octadecynoic acid (17-ODYA), a fatty acid analogue, which can be attached to palmitoylation sites by the cellular machinery. Afterwards the incorporated fatty acid is conjugated to fluorescent tag having azide group via Cu (I)-catalyzed click chemistry reaction followed by SDS-PAGE and subsequent detection of in-gel fluorescence using typhoon scanner. More than 120 palmitoylated proteins were detected using this approach in Jurkat T cells [182]. This method was also modified to improve both sensitivity and ability to quantify dynamics of protein palmitoylation when it used in combination with stable isotope cell labelling (SILAC) where they are able to identify more than 400 palmitoylated proteins in mouse T-cell hybridoma cells [183].

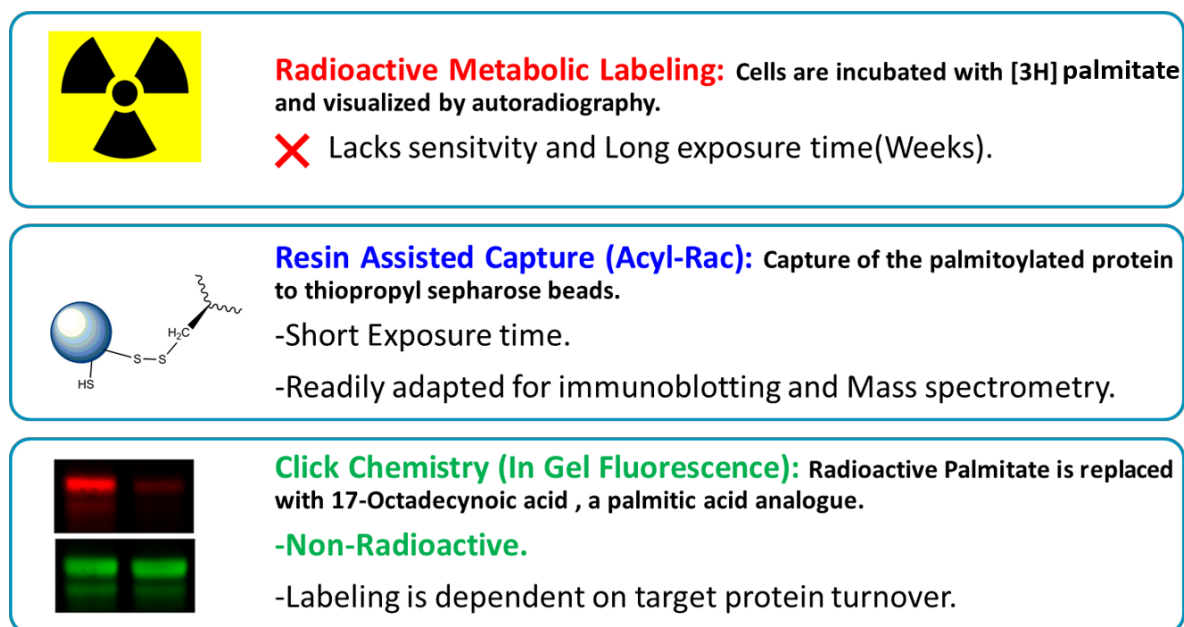


Figure 9. Methods used for studying S-acylation of proteins. (1) Radioactive labelling, which include labeling of target protein with radioactive palmitic acid and visualization with fluorography. (2) Acyl-RAC, which allow enrichment of s-acylated proteins on thio-reactive sepharose beads and detection by immune blotting. (3) Click chemistry-based methods, which include metabolic labeling of the cells using non-radioactive fatty acid analogues having an alkyne group. The alkyne group can be conjugated to azide group on a fluorophore via Cu (I)-catalyzed click chemistry reaction and visualization of target protein in SDS-PAGE using typhoon fluorescence scanner.

1.4.1. Methods to identify ZDHHC substrate pairs

Identification of DHHC enzyme-substrate interaction remains one of the most challenging tasks in the field of S-acylation due to the large number of ZDHHC family members, which have a certain degree of redundancy. Therefore, careful approaches are required to recognize ZDHHC enzyme substrate pairs. There are two main approaches for systematic screening of respective ZDHHC involved in acylation of a specific substrate. The first one is “overexpression” of a target protein along with library of epitope tagged ZDHHC enzyme followed by quantitative analysis of palmitoylation level by radioactive palmitate labeling or ABE/Acyl-RAC methods. A significant increase of the palmitoylation signal in one or more of co-expressed DHHC samples is suggestive that this enzyme(s) is involved in modification of the substrate [150,184]. This approach is unlikely to work with viral glycoproteins, since they are stoichiometrically acylated and hence an increase in acylation is not expected if the relevant enzymes are overexpressed. The second approach includes the use of siRNA libraries targeting single ZDHHC enzymes and functional analysis of target protein in knockout animal or cell line model of identified ZDHHC candidate [185,186]. These two strategies were quite successful in assigning specific ZDHHC enzymes to many substrates in the last 10 years. As an example, postsynaptic density 95 protein (PSD-95), a major palmitoylated protein in the brain is acylated by closely related ZDHHC3/7 and ZDHHC2/15 identified by enhancement of ³H labelling when they co-expressed in HEK293T cells [150]. In the same cell line, Gα subunit protein is palmitoylated by ZDHHC3 and ZDHHC-7 during a co-expression experiment. Individual and simultaneous knockdown of ZDHHC3/7 leads to significant reduction of Gα palmitoylation and interfere with its transport to plasma membrane [187]. Using siRNA library against human ZDHHCs, ZDHHC6 was identified as the major palmitoylating enzyme that interact with Calnexin, an ER chaperone involved in glycoprotein folding and this modification is essential for formation of ribosome translocon complex (RTC) and recruitment of cytoskeleton actin [185].

Due to recent advances in proteomic techniques, comparative palmitoylome analysis of wild type and DHHC2 knockdown Hela cells was able to identify cytoskeleton associated protein 4 (CKAP4) as a major substrate for ZDHHC2 using palmitoyl-cysteine isolation capture and analysis (PICA) approach. Depletion of ZDHHC2 expression impairs trafficking of CKAP4 to the cell surface and consequent interaction with antiproliferative factor (APF) [188]. Using a similar approach where ABE method for enrichment of acylated proteins is coupled with quantitative mass spectrometry, ZDHHC21 was identified to recognize and palmitoylate PECAM1 in endothelial cells [189]. Although these new proteomics-based methods are efficient in identification of enzyme substrate pairs, they are always challenged by the functional redundancy of ZDHHC enzymes in mammalian cells.

2. Aim of the study

S-acylation of influenza virus proteins (HA and M2) is an essential modification and hence blocking the HA-acylating ZDHHC-protein should reduce virus growth. Since 23 ZDHHC proteins with distinct, only partly overlapping substrate specificities are present in humans, only one (or a few) might acylate HA in airway cells of the lung, the site of virus replication in humans. We hypothesize that this ZDHHC-protein is a promising drug target since its blockade might not (or very little) compromise acylation of cellular proteins and thus it might exhibit little cytotoxicity.

Thus, the aim of my study was to identify the ZDHHC-protein(s) that interact and modifies influenza virus HA during infection of human cells. Firstly, I attempted to analyze the expression profile of ZDHHCs in different human cell lines and the effect of influenza virus infection on this expression pattern by quantitative real time PCR (qPCR). To narrow down the number of candidate ZDHHCs, I then used a siRNA library against individual ZDHHCs to knockdown their expression. The identified DHHCs will then be knocked-out using the CRISPR/CAS technology in HAP-1 cells and in influenza susceptible A549 cells to study the effect on acylation of HA and M2 proteins as well as on virus replication. I also aimed to investigate whether the same ZDHHC-protein(s) acylate HA of different subtypes and also HA of Influenza B virus and HEF of Influenza C virus. The acylation pattern of intracellular HA will be analyzed by Acyl-RAC and click chemistry assays while HA in virus particles will be carefully monitored by mass spectrometry. Finally, I will investigate how knockout of a certain ZDHHC-protein(s) affects acylation of cellular proteins. The ZDHHC-protein with the least effect on acylation of cellular proteins and the most effect on virus replication would be the most promising drug target.

3. Materials and Methods

3.1. Materials

The chemicals, enzymes, antibodies, media, and instruments used in this study were used according to the manufacturer's recommendations

3.1.1. Chemicals, consumables and equipment

3.1.1.1. Chemicals

Chemical	Catalog Number	Manufacturer
17-Octadecynoic Acid	90270	Cayman, Michigan
Acetic acid	3738.4	Carl-Roth, Karlsruhe
Acetone	5025.6	Carl-Roth, Karlsruhe
Agar (agar bacteriological)	2266.2	Carl-Roth, Karlsruhe
Agarose-Standard grade	3810.4	Carl-Roth, Karlsruhe
Ammonium chloride	A9493	Sigma-Aldrich, Taufkirchen
Ammoniumpersulfate (APS)	A3678	Sigma-Aldrich, Taufkirchen
Ampicillin Na-salt	K029.2	Carl-Roth, Karlsruhe
Avicel	RC-591 NF I	FMC, Philadelphia
Blasticidin S-Hydrochloride(10mg)	ant-bl-05	Invivogen, California
Bromophenol blue	B1793	Alfa Aesar, Karlsruhe
BSA (Albumin Bovine Fraction V)	A7906	Sigma-Aldrich, St. Louis
Calcium chloride dihydrate	5239.2	Carl-Roth, Karlsruhe
Coomassie Brilliant Blue G250	27815	Fluka, Switzerland
Copper(ii) Sulfate	451657	Sigma-Aldrich, St. Louis
Crystal Violet	T123.1	Carl-Roth, Karlsruhe
D(+) Sucrose	4621.1	Carl-Roth, Karlsruhe
DAPI	62247	Thermo Scientific,USA
DEAE-Dextran	D9885	Sigma-Aldrich, St. Louis
Dimethyl sulfoxide (DMSO)	A3672	AppliChem, Darmstadt
Dithiotheritol (DTT)	3483-12-3	Sigma-Aldrich, St. Louis
dNTP Mix (10mM)	BIO-39053	Bioline, Luckenwalde

MATERIALS AND METHODS

Chemical	Catalog Number	Manufacturer
Dulbecco's MEM (DMEM)	P04-04500	Pan Biotech, Aidenbach
EDTA	A2937	AppliChem, Darmstadt
EMEM (2x)	BE12-668F	Lonza, Köln
Ethanol	E/0650DF/17	Fisher chemical, UK
Ethidium bromide (1%)	2218.2	Carl-Roth, Karlsruhe
Fetal Bovine Serum (FBS)	P30-3306	Pan Biotech, Aidenbach
Fetal Bovine Serum, Dialyzed	P30-2101	Pan Biotech, Aidenbach
Formamide (deionized)	A2156	AppliChem, Darmstadt
Glycerol	4043.3	Carl-Roth, Karlsruhe
Hydrochloric acid (HCl 37%)	4625.2	Carl-Roth, Karlsruhe
Isopropyl alcohol (2- propanol)	20842.330	VWR, France
Magnesium chloride	5883.025	Merck, Darmstadt
Methanol	M/3950/17	Fisher chemical, UK
Monobasic, monohydrate di-Sodium Hydrogenophosphate	A3906	AppliChem, Darmstadt
NP40-50ml	85124	Thermo Scientific, USA
Nuclease Free water	T143.5	Carl-Roth, Karlsruhe
Opti-MEM I	31985070	Thermo Scientific, USA
Paraformaldehyde	P6148	Sigma-Aldrich, St Louis
PMSF	A0999	AppliChem, Darmstadt
Protease Inhibitor "cOmplete Cocktail	11873580001	Roche, Mannheim
Protein G Sepharose Beads	GE17061801	GE Healthcare, Sweden
ProLong Gold antifade mounting buffer	P36930	Thermo Scientific, USA
Puromycin Dihydrochloride	A1113803	Gibco, USA
S-Methyl methanethiosulfonate (MMTS)	64306	Sigma-Aldrich, St. Louis
Sodium chloride	A3597	AppliChem, Darmstadt

Chemical	Catalog Number	Manufacturer
sodium dodecyl sulfate (SDS)	75746	Sigma-Aldrich, St Louis
Sodium hydroxide	1.06462	Merck, Darmstadt
Sodium Phosphate	S9638	Sigma-Aldrich, St Louis
β-mercaptoethanol	28625	Serva, Heidelberg
TAMRA-Azide	T10182	Molecular Probes, USA
TBTA	678937	Sigma-Aldrich, St. Louis
TEMED	2367.3	Carl Roth, Karlsruhe
Thiopropyl–Sepharose® 6B	T8387-5G	Sigma-Aldrich, St. Louis
TPCK-Treated Trypsin	T1426	Sigma-Aldrich, St. Louis
Tris-(2-carboxyethyl) phosphine hydrochloride	HN95.2	Carl-Roth, Karlsruhe
Tris-Salt	A1086	AppliChem, Darmstadt
Triton X-100	8603	Merck, Darmstadt
Trypsin/EDTA 0.05%	P10-021100	Pan Biotech, Aidenbach
Tween-20	9127.2	Carl-Roth, Karlsruhe

3.1.1.2. Consumables

Name	Feature	Manufacturer
Cell culture dishes	6-well, 24-well, 96 well	Sarstedt, Nümbrecht
Cell culture flasks	25 ml, 75 ml	Sarstedt, Nümbrecht
Conical test tubes	17x120 15 ml	Sarstedt, Nümbrecht
Conical test tubes 30x115	50 ml, with and without feet	Sarstedt, Nümbrecht
Cryovials	1.8 ml	Nunc, Roskilde
Eppendorf Tubes 1.5 ml	1.5	Sarstedt, Nümbrecht
Falcon bacteria	13ml	Sarstedt, Nümbrecht
Falcon Tubes	15 ml, 50 ml	Sarstedt, Nümbrecht
Latex gloves Size	S, M, L	Shield Scientific, UK
PCR tube	0.2 ml	Applied Biosystems, UK
Parafilm® M	P7793-1EA	Bemis, Neenah
PVDF membrane	732-3200	VWR, France
Rotilabo® Blotting Papers	CL75.1	Carl-Roth, Karlsruhe

MATERIALS AND METHODS

Petri dish for cell culture	60mm, 100mm, 150mm	Sartstedt, Nümbrecht
Petri dish for bacteria	100mm	Sartstedt, Nümbrecht
Sterile Pipette tips	(10, 200, 1000 µl)	Starlab, Hamburg
Sterile Pipettes for culture	(5, 10, 25 ml)	Sartstedt, Nümbrecht

3.1.1.3. Equipment

Name	Feature / Catalog Number	Manufacturer
1. General Equipment:		
Bacterial incubator	07-26860	Binder, Turtlingen
Bacterial incubator shaker	Innova 44	New Brunswick Scientific, New Jersey
Centrifuge 5424	Rotor FA-45-24-11	Eppendorf, Hamburg
Centrifuge 5804R	Rotors A-4-44	Eppendorf, Hamburg
Centrifuge Sorvall RC 6+	F45-30-11	Thermo Scientific, Dreieich
Chemiluminescence Imaging system	Fusion SL	Peqlab, Erlangen
Electrophoresis power supply	Standard Powepack P25T	Biometra, Göttingen
Fast Real-time PCR system	ABI Prism 7500	Life technologies, Grand Island
Freezer	-20°C	Liebherr, Bulle
Freezer	-80°C	GFL, Burgwedel
Heating, mixing, and cooling thermomixer C		Eppendorf, Hamburg
Heracell 240i CO2 incubator		Thermo Scientific, Dreieich
Ice machine	174059	Ziegra, Isernhagen
Magnetic stirrer	RH basic KT/C	IKA, Staufen
Nanodrop 1000		Peqlab, Erlangen
Nitrogen tank	ARPEGE70	Air liquide, Düsseldorf
Orbital Shaker	OS-10	Peqlab, Erlangen
pH-meter	761-Calimatic	Knick, Berlin
Pipet boy	Pipetus	Hirschmann Laboratories

Name	Feature / Catalog Number	Manufacturer
Pipettes	P1000, P200, P100, P10	Eppendorf, Hamburg
Rotator Tube-Revolver	ATX1.1	Carl-Roth, Karlsruhe
SDS-PAGE System	Mini-Gel Twin	Biometra, Göttingen
Semidry membrane blotter	Blotting System	Peqlab, Erlangen
StepOnePlus Real-Time PCR Systems	StepOnePlus	Life Technologies ,Grand Island
Sterile laminar flow	ScanLaf, Mars, Safety ClassII	Bleymehl, Inden
Thermocyclar Flexcyclar		Analytik Jena, Jena
Thermocyclar T-Gradient		Biometra, Göttingen
Typhoon Scanner	9400	GE Healthcare, Freiburg
UV Transiluminator	Bio-Vision-3026	Peqlab, Erlangen
Vortex Genie 2™		Bender&Hobein AG, Zurich
Water bath shaker	C76	Brunswick Scientific, New Jersey
Water baths	TW2 and TW12	Julabo, Seelbach
<u>2. Microscopes</u>		
Fluorescence microscope	Axiovert S 100	Carl Zeiss MicroImagiJena
Fluorescence microscope	Axio Imager M1	Carl Zeiss MicroImagiJena
VisiScope confocal FRAP System	Confocal Microscope	VisiTron Systems, Puchheim
Inverted microscope	AE20	Motic, Wetzlar

3.1.1.4. Software

Software	Version	Company
AxioVision Microscopy	4.8	Carl Zeiss Micro Imaging, Jena
Chemi-Capt		Vilber-Lourmat, Eberhardzell
Graphpad Prism 7	7	Graphpad Software Inc.
Image J 1.41	1.52a	NIH, Bethesda

MATERIALS AND METHODS

Software	Version	Company
ND-1000	3.0.7	PeqLab, Erlangen
Vision-Capt		Vilber-Lourmat, Eberhardzell
Endnote	X9	Clarivate Analytics
StepOne software	v2.3	Life Technologies

3.1.1.5. Enzymes and markers

Enzyme	Catalog Number	Manufacturer
Antarctic phosphatase	M0289L	New England Biolabs, Ipswich
BbsI	R0539S	New England Biolabs, Ipswich
BsmBI	R0580S	New England Biolabs, Ipswich
CIP	M0290S	New England Biolabs, Ipswich
DpnI	ER1701	New England Biolabs, Ipswich
GeneRuler™ 1kb Plus DNA Ladder	SM1334	Thermo Scientific, USA
Phusion-High Fidelity DNA Polymerase	M0530S	New England Biolabs, Ipswich
Protein Pre-stained plus marker	26619	Thermo Scientific, USA
Proteinase K	7528.2	Carl Roth, Karlsruhe
Q5 High Fidelity DNA Polymerase	M0491S	New England Biolabs, Ipswich
Quick Ligation™ Kit	M2200S	New England Biolabs, Ipswich
RNasin® Ribonuclease Inhibitor	N2511	Promega, Germany
T4 DNA Ligase	M0202	New England Biolabs, Ipswich

3.1.1.6. Kits

Kit	Catalog Number	Manufacturer
peqGOLD plasmid miniprep kit	12-6942-02	Peqlab, Erlangen
RTP® DNA/RNA Virus Mini Kit	1040100300	Stratec, Birkenfeld
GF-1 ambiclean gel extraction kit	GF-GC-200	Vivantis, Malaysia.
QIAGEN® OneStep RT-PCR Kit	210212	Qiagen, Hilden
Roti-Quant universal kit	0120.1	Carl-Roth, Karlsruhe
Pierce™ ECL Plus Western Blotting Substrate	32132	Thermo Scientific, USA
PowerUp™ SYBR® Green Master Mix	A25780	Thermo Scientific, USA
E.Z.N.A. Plasmid Maxi Kit	D6922-04	Omega BioTek , USA
Turbofect Transfection Reagent	R0531	Thermo Scientific, USA
Lipofectamine 3000	L3000015	Thermo Scientific, USA
Interferrin siRNA-Transfection Reagent	409-10	Polyplus , France
One-Step SYBR PrimeScript RT-PCR Kit II	RR086A	Takara, Japan

3.1.2. Primers

3.1.2.1. Primers used for generation of HA acylation mutant by reverse genetics

Purpose	Name	Sequence
FPV-HA Acylation site mutant-2 (Ac2)	Rash-559-F Rash-559-R	CGGAAACATGCGGTCTGACTATTTGTAT ATACAAATAGTCGACCGCATGTTTCCG
FPV-HA Acylation site mutant-3 (Ac3)	Rash-559-F Rash-559-R	CATGCGGTGCACTATTTTCGATATAAGTTTGG CCAACTTATATCGAAATAGTGCACCGCATG
FPV-HA Sequencing primers	FPV-F Seq FPV-R Seq	CAAAAGCACCCAATCGGCAA TGAAAATGGTTGGGAAGGTCTGG

3.1.2.2. Primers used for expression profiling of Human ZDHCs

Gene	Name	Sequence
ZDHC1	ZDHC1-F ZDHC1-R	GTGCGGGACAAGAGCTATG AGTTGCAGTGCAGGTCTTCAA
ZDHC2	ZDHC-2 F ZDHC-2 R	TCTTAGGCGAGCAGCCAAGGAT CAGTGATGGCAGCGATCTGGTT
ZDHC3	ZDHC-3 F ZDHC-3 R	CCACTTCCGAAACATTGAGCG CCACAGCCGTCACGGATAAA
ZDHC4	ZDHC-4 F ZDHC-4 R	CCTGACTTGTGGAACCAATCC GCACCTCACGTTCTTTGGAAAC
ZDHC5	ZDHC-5 F ZDHC-5 R	CACCTGCCGCTTTTACCGT CGGCGACCAATACAGTTATTAC
ZDHC6	ZDHC-6 F ZDHC-6 R	GTTGTGGTATTGGCCCTTACA AAAGCCCGGACCGACAAAC
ZDHC7	ZDHC-7 F ZDHC-7 R	CCCAAAGGAAACGCTACGAAA CGCGCTCGGGTTTAATACAG
ZDHC8	ZDHC-8 F ZDHC-8 R	CTCAAACCCGCCAAGTACATC ACACAGCTCGTGTCAACCAC
ZDHC9	ZDHC-9 F ZDHC-9 R	TCGGGCGCTACCAGATGAA GGGCAGTGATGGTCAAGC
ZDHC11	ZDHC-11 F ZDHC-11 R	GATCTTCTCGTTCCACCTCGT TGTGCATGTTTTGATCTGTCGAA
ZDHC12	ZDHC-12 F ZDHC-12 R	GTGCTGACCTGGGGAATCAC CTGCACATTCACGTAGCCA
ZDHC13	ZDHC-13 F ZDHC-13 R	AGGAAGCCATTAAGGTCCTCC GCCAAAACCTATGCACCGTC
ZDHC14	ZDHC-14 F ZDHC-14 R	TGTGATAACTGCGTAGAACGGT CGTGGGTGATAACGAATGCAA
ZDHC15	ZDHC-15 F ZDHC-15 R	GCCTGCTTGGTCGATCTTCG GGCTCAAACAGTCACCAGGC
ZDHC16	ZDHC-16 F ZDHC-16 R	CGAAAGGCACATCAACAAGAAG AGTTGTCCAAGCAGCCGTAG
ZDHC17	ZDHC-17 F ZDHC-17 R	GATGTACGGCAACCGGACAAA TGATCCACAATAGCACCTTTTCG
ZDHC18	ZDHC-18 F ZDHC-18 R	CACCCCGAACCTCACACTG TGAAGGCCGTCAGGAATGAGA
ZDHC19	ZDHC-19 F ZDHC-19 R	TTGCTGCCTTCAATGTGGTG CGGAGCCTTGATGTAAGATGC
ZDHC20	ZDHC-20 F ZDHC-20 R	CGCACCCACGTTTTTCATACG TCTGGCATACTCATTCTGGTTTG
ZDHC21	ZDHC-21 F ZDHC-21 R	GAGGGCCTCCATAACTGATCC TGGGAACGCTTTGGTCTCATC

Gene	Name	Sequence
ZDHHC22	ZDHHC-22 F ZDHHC-22 R	CCCTGGCGCAAGAACTTACAA CTTCCGACATTGAACATGGGG
ZDHHC23	ZDHHC-23 F ZDHHC-23 R	TCTGGATGAAGGGTGTGATCG GCTCCCCTAAGCCAAGGAA
ZDHHC24	ZDHHC-24 F ZDHHC-24 R	TTCCCTGGCTCATGTTGCTC GACCCAGGTCATAGGAGTGC
Human GAPDH	hGAPDH-F hGAPDH-R	GGAGCGAGATCCCTCCAAAAT GGCTGTTGTCATACTTCTCATGG

3.1.2.3. Guide RNA sequences and screening primers used for generation of CRISPR/Cas9 Knockout cell lines

Cell line	Purpose	Sequence	Annealing T _m
ZDHHC22 Knockout cells	gRNA#1	GCATGCGCGAGGACCCCGC	56°C
	gRNA#2	TTCTTCACCGGCAACTGCAT	
	Genomic DNA Screening Primers (Fo,Re)	GACGCCGTAGTCAGTCAGTCC GAGAAGAACTGGCTGATGGAGGT	
	mRNA Screening Primers (Fo,Re)	GAATGTAATCGAGGATGCTGGC GCTGCCATGGTTTTATGCTCA	58°C

Cell line	Purpose	Sequence	Annealing T _m
ZDHHC2 Knockout cells	gRNA	TATGCACAGCTGGATGGCGT	61°C
	Genomic DNA Screening Primers (Fo,Re)	CTGCGGGATGGGGAGTTAG GCCCGAGGCTGCTTTTA	
	mRNA Screening Primers (Fo,Re)	CTGCGGGATGGGGAGTTAG GCAGTGATGGCAGCGATCTG	

Cell line	Purpose	Sequence	Annealing T _m
ZDHHC8 Knockout cells	gRNA	ACGGCCGCCGCGCTGCTGGT	67°C
	Genomic DNA Screening Primers (Fo,Re)	CTAACTTGAGACAGCCTTAGGGATT CAGTGGTGGTCAAAGTCCTGG	
	mRNA Screening Primers (Fo,Re)	CGCCAAGTACATCCCGGTGG CAGCGTGGTTCAGCACGTAGAC	

MATERIALS AND METHODS

Cell line	Purpose	Sequence	Annealing T _m
ZDHHC15 Knockout cells	gRNA	AGATGGCATGGTAGAGTATG	60°C
	Genomic DNA Screening Primers (Fo,Re)	CCTCTTTTTGTCCTCTTCTTGCTTT CATTATGGCTTGTTTCTGTCACTGT	

Cell line	Purpose	Sequence	Annealing T _m
ZDHHC20 Knockout cells	gRNA	AAACTGTTGCAGCCACGAAA	65°C
	Genomic DNA Screening Primers (Fo,Re)	ATTGTAGCCCTATCTGTCCTCTGAT TATTGCGATTAAAAAGCTCCCCTTC	

3.1.2.4. Sequencing Primers used for validation of gRNA cloning in CRISPR vectors

Gene	Plasmid	Sequence
U6 Promoter	pRP-418	TTTGCTGTACTTTCTATAGTG
	spCas9-EGFP-Blast	ATTTCTTGGGTAGTTTGCAG

3.1.3. Antibodies

Antibody	Dilution	Cat. No	Manufacturer
Rabbit anti- influenza C HEF antiserum (C/JJ/50)	1:1000	----	Home-made
Anti-mouse Alexa Fluor 488	1:1000	A-11004	Thermo Scientific, USA
Anti-Mouse IgG HRP	1:2000	1706516	Biorad, California
Anti-rabbit Alexa Fluor 568	1:1000	A-11034	Thermo Scientific, USA
Anti-rabbit IgG HRP	1:5000	ab191866	Abcam, Cambridge
Mouse monoclonal anti-Flotillin 2 antibody (clone 29)	1:1000	610384	BD Biosciences, New Jersey
Mouse monoclonal anti-HA tag antibody (6E2)	1:1000	2367	Cell signaling, Massachusetts,
Mouse Monoclonal anti-influenza B HA antibodies (B/Lee/1940.)	1:1000	6D12 1B5m	Gift From Dr.Florian Krammer

Antibody	Dilution	Cat. No	Manufacturer
Mouse monoclonal anti-M2 antibody (14C2)	1:2000	ab5416	Abcam, Cambridge
Protein G HRP , 1mg/ml	1:2000	M00090	Genescript, New Jersey
Rabbit anti-Caveolin-1 antibody	1:1000	ab2910	Abcam, Cambridge
Rabbit anti-Caveolin-1 antibody (N-20)	1:1000	SC-894	Santa Cruz, Texas
Rabbit anti-HA2 antiserum (<i>FPV, H7N1 Strain</i>)	1:3000	----	Gift from Prof.Hans Klenk
Rabbit HA antibody (H1N1 Strain)	1:3000	GTX127357	Genetex , California

3.1.4. Prepared solutions and Buffers

Name	Purpose	Composition
Binding Buffer	Acyl-RAC	100 mM HEPES, 1 % SDS, 1 mM EDTA and 1X protease inhibitor cocktail
Blocking Buffer	IF Blocking	5 % BSA in PBS
Blocking Buffer	Western Blot	5% skimmed-milk powder in PBST
Blocking Buffer	Acyl-RAC	100 mM HEPES, 2.5 % SDS, 1 mM EDTA and 1X protease inhibitor cocktail
Coomassie Stain	Protein Gel staining	45% (v/v) ethanol, 10% (v/v) acetic acid, 0.25% (w/v) Coomassie Brilliant Blue G -250
Duplex Buffer	gRNA Annealing	60mM HEPES pH 7.4 + 200mM Sodium Acetate
Fixative	Cell Fixation	4% paraformaldehyde (PFA) in PBS
Infection Medium	Virus Infection	DMEM, 0.1% FBS, penicillin/streptomycin (100 units/mL), 0.2% BSA and 0.25-1 µg/ml TPCK Trypsin
IP buffer	Cell lysis for Immunoprecipitation and Click Chemistry	500 mM Tris-HCl, 20 mM EDTA, 30 mM sodium pyrophosphate decahydrate, 10 mM sodium fluoride, 1 mM sodium orthovanadate, 2 mM benzamidine, 1 mM PMSF, 1 mM NEM and 1X protease inhibitor cocktail
Lysis Buffer	Acyl-RAC	25 mM HEPES, 25 mM NaCl, 1 mM EDTA ,1.5 % Triton X100 and 1X protease inhibitor cocktail

MATERIALS AND METHODS

Name	Purpose	Composition
Non-Reducing SDS loading dye	SDS-PAGE	62.5 mM Tris·HCl, 2% (w/v) SDS, 10% (v/v) glycerin, 0.01% (w/v) bromophenol blue, pH 6.8
PBS	Washing and Dilution buffer	0.8% (w/v) NaCl, 0.02% (w/v) KCl, 0.02% (w/v) KH ₂ PO ₄ , 0.135% (w/v), Na ₂ HPO ₄ ·2H ₂ O
PBST	Western blot washing buffer	PBS+ 0.1% Tween-20
Permeabilization buffer	Permeabilization for florescence microscopy	PBS+ 0.1 % Triton X100
Plaque Medium	Plaque Assay	1XEMEM, 0.6% Avicel, 0.2% BSA, 0.1% FBS, penicillin/streptomycin, 2 µg/ml TPCK-Trypsin, 0.5% DEAE-Dextran, 5% NaHCO ₃
Separating gel solution	SDS-PAGE	10-15% (w/v) acrylamide/bisacrylamide stock solution, 0.1% (w/v) SDS, 375 mM Tris·HCl (pH 8.8), 0.05% (w/v) APS, 0.1% (v/v) TEMED
Stacking-gel solution	SDS-PAGE	5% (w/v) acrylamide/bisacrylamide, 0.1% SDS, 125 mM Tris·HCl (pH 6.8), 0.075% (w/v) APS, 0.15% (v/v) TEMED

3.2. Methods

3.2.1. Molecular biology methods

3.2.1.1. Preparation of chemically competent *E. coli*

Chemically competent bacterial cells are prepared as described before [190], with some modifications. One vial of Top10™ *E. coli* cells (100µl) were thawed on ice, then added to 10 ml LB broth and incubated overnight with shaking (200 rpm) at 37°C. 1 ml of the overnight culture was then inoculated into 99 ml LB broth and incubated with shaking (200 RPM) at 37°C until the mid-log phase (about 3.30 hours) which indicated by turbidity of the broth ($OD_{600}=0.4-0.5$). The 100ml culture was divided into two 50 ml centrifuge tubes, pelleted at 5000 RPM for 5 minutes at 4°C. The supernatant was completely discarded, and the pellet was re-suspended in 10 ml ice cold 100mM MgCl₂ buffer (for each tube). The content of the two tubes were collected in one tube followed by another centrifugation step at 5000 RPM for 5 minutes at 4°C. Afterwards, the pellet was fully re-suspended in 30 ml ice cold 100mM CaCl₂ buffer and kept on ice for 20 minutes. After 5 min centrifugation at 4°C and 3000 RPM, the pellet was gently re-suspended in 5 ml ice-cold 15% glycerol in 100mM CaCl₂ solution. The well-re-suspended cells were then dispensed into sterile ice-cold tubes of 100µl each, stored without disturbance at - 80°C.

3.2.1.2. Transformation of competent bacterial cells

For amplification of plasmid DNA, chemically competent *E. coli* bacteria were transformed either with existing plasmid DNA or with freshly ligated new constructs. 100µl aliquots of competent cells were thawed on ice, mixed with target plasmid DNA (1-100ng) or ligation mixture (1-5µl) and incubated on ice for 30 minutes. After a 45 sec “heat shock” at 42°C cells were directly placed on ice for 2 min. 300µl of pre-warmed (37°C) SOC Medium (ampicillin free) was added and shaken (200 RPM) for 45 min at 37°C to allow expression of the according antibiotic resistance gene. 10-100µl of the transformed bacterial culture were subsequently plated on agar plates containing appropriate antibiotic for selection of bacteria carrying the plasmid. Plates were incubated overnight at 37°C and single colonies were picked for plasmid purification.

3.2.1.3. Plasmid purification

Single colonies from agar plates were picked and amplified through inoculation of LB broth containing selection antibiotic and incubated with shaking at 37°C for 16h. Bacteria were then pelleted, and plasmid DNA were isolated using *peqGOLD* plasmid miniprep kit according to manufacturer instructions. Briefly, bacterial cells were harvested by centrifugation at 5000 rpm for 10 min and the supernatant was discarded. The bacterial pellet was completely re-suspended in 250µl of solution I (With RNaseA) and cells were lysed by addition of 250 µl

solution II (lysis buffer) and incubated for 2 min at RT. To neutralize the lysis reaction and precipitate proteins, 350 µl of solution III (Neutralization buffer) were subsequently added to the mixture followed mix by inverting the tube 6 - 10 times until a flocculent white precipitate is formed. Proteins and cell debris were removed by centrifugation at 10000 rpm for 10 min and cleared supernatant were transferred to a fresh *PerfectBind DNA Column* in a 2.0 ml Collection Tube. Column bound DNA was washed for 2 times with wash buffer (750µl), the residual ethanol was completely removed by centrifugation at 10000 rpm for 2 min. 50-100µl of elution buffer was added to the column and DNA was isolated by centrifugation at 10000 rpm for 1min. Concentration purified plasmid DNA was measured by Nanodrop spectrometer at 260 nm and stored at -20°C until use.

3.2.1.4. Quick Change Site directed mutagenesis

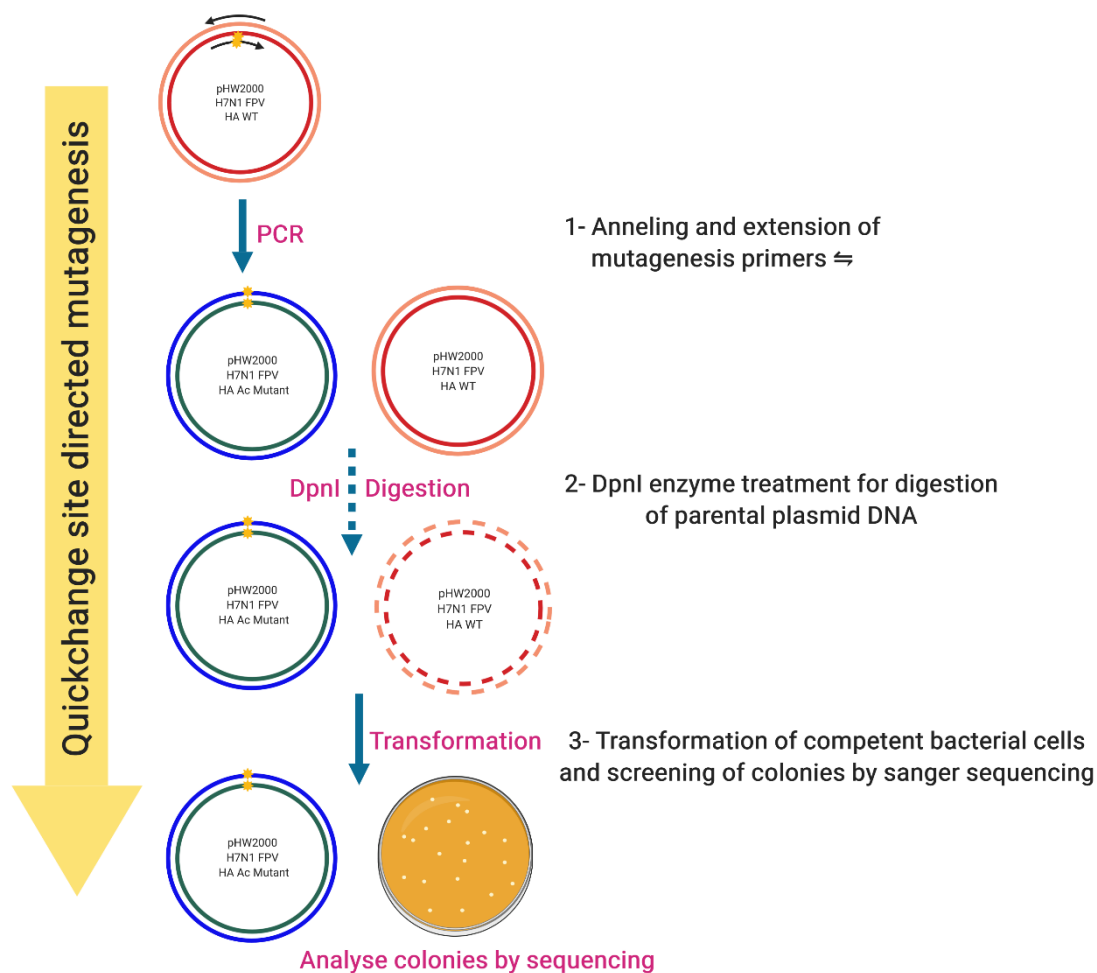


Figure 10. Schematic overview of Quick-change site directed mutagenesis protocol.

Mutations in the acylation sites of influenza virus HA cloned in pHW2000 plasmid DNA was done using PCR based site directed mutagenesis according to strategene quick change protocol (Fig.10). Briefly, a complementary primer pair with desired point mutations were designed so they anneal to the target sequence on the plasmid DNA. These primers have

the mutation(s) at the middle of the primer flanked by 10-15 nucleotides of the matching sequences on both sides and terminated by two or more G and/or C bases. The Cys559 and Cys 562 at the cytoplasmic tail of FPV-HA were individually mutated to serine by changing 2 nucleotides in the amino acid codon (Cysteine **TGT** To Serine **TCG**). This was carried out using 2 step PCR method according to [96] as follows:

PCR Mix	Volume
5x Phusion Buffer	10 µl
dNTPs (10mM)	2 µl
Phusion enzyme	0.5 µl
Plasmid DNA (100ng/µl)	1 µl
Nuclease free water (NFW)	36.5 µl
Total volume	50µl

For each mutation reaction, the above mixture was equally splitted into 2 PCR tubes, then 2µl of each mutation primer was separately added into 1st (F) and 2nd (R) tube respectively. Then the first PCR was performed as follows:

PCR step	Temperature (°C)	Time	Cycles
Initial denaturation	98°C	30s	1x
Denaturation	98°C	10s	
Annealing	57°C	30s	5 x
Extension	72°C	3min	
Final extension	72°C	10 min	1x

**The aim of this step is to allow annealing of mutation primers and individual amplification of each strand to serve as a template in the next step.*


After the first PCR, 25 µl products from both 1st and 2nd tubes were mixed, transferred into a new PCR tube, 0.5µl of fresh Phusion enzyme was added and a second PCR was performed using same protocol but for 30 cycles.

The PCR product is a mixture of both wildtype (methylated DNA) and mutated (Unmethylated DNA). PCR was treated with the restriction endonuclease DpnI (0.2 U/µl) for 2 h at 37°C which digest only methylated DNA leaving the unmethylated PCR products intact. Top10™ E.coli cells were transformed with treated product for amplification (see 3.2.1.2), subsequent purification (3.2.1.3) and sequencing of the mutated plasmids.

3.2.1.5. Screening and Sequencing Polymerase chain reaction (PCR)

To screen for CRISPR induced indels in single cell clones (SCC), Total genomic DNA was isolated from SCC using Invisorb Spin Tissue Mini Kit following manufacturer’s instructions (Stratec). PCR was carried out using specific primers flanking the Cas9 target site of each ZDHHC gene (Section 3.1.2.3). PCR amplifications were performed using Q5 High fidelity DNA polymerase (New England Biolabs) under the following cycling conditions. Amplified PCR products were analyzed by electrophoresis; gel purified using GF-1 ambiclean gel extraction kit (Vivantis) and sequenced (LGC Genomics).

PCR Mix	Volume	PCR Step	Temp	Time
Template DNA	100ng	Initial Denaturation	98°C	30s
5x Q5 Buffer	5 µl	Denaturation	98°C	10s
Primer F (10µm)	0.5 µl	Annealing*	60-69°C	30s
Primer R (10µm)	0.5 µl	Extension	72°C	30s/Kb
dNTPs (10mM)	0.5 µl	Final Extension	72°C	2min
Q5 DNA Polymerase	0.25 µl	Hold	10°C	∞
Nuclease free water	Add to 25 µl	<i>*Annealing temperature varies according to each primer pair.</i>		



3.2.1.6. Agarose gel electrophoresis

For separation and analysis of PCR products, 1% agarose powder was dissolved in 100ml of TAE buffer, boiled in the microwave to dissolve the agarose and left to cool at RT. After cooling, Ethidium bromide was added (0.5µg/ml) and gel mixture was poured in gel trays with pre added comb. The electrophoresis-running chamber was filled with 0.5x TAE buffer, PCR products are loaded and separated at 100v for 20-30 min along with 5µl of DNA ladder in order to determine the size of separated fragments (GeneRuler, 1kb plus DNA Ladder, Thermo). Finally, Gels were visualized and analyzed using UV Trans-illuminator gel documentation system (PeqLab, Erlangen).

3.2.1.7. DNA extraction or clean up from agarose gel

PCR products/DNA fragments separated by agarose gel electrophoresis was extracted using GF1 Ambiclean kit (Vivantis, Malaysia). The target band was visualized by UV light and excised from gel using sterile scalpel. Gel slices were solubilized using equal volume of DNA binding buffer at 55°C with regular vortexing until gel has melted completely. Then Homogenized gel was transferred to GF-1 column, which have high DNA binding capacity. Bound DNA was washed once with ethanol-based washing buffer, eluted in nuclease free water and stored at -20°C for downstream application.

3.2.1.8. CRISPR/Cas9 Technology

CRISPR (clustered regularly interspaced short palindromic repeats)/Cas system is a prokaryotic adaptive immune response that has been identified in a wide range of bacterial and archaeal hosts enabling them to respond and eliminate invading viral or plasmid DNA. It utilizes non-coding RNA to guide the Cas nucleases to induce site specific cleavage of foreign DNA [191]. There are 3 types of CRISPR system (I-III) identified in bacteria, but the type II CRISPR/Cas system is the best characterized and it was modified to be a powerful gene-editing tool in mammalian cells because of precision, efficiency and ease of use. Most of the currently used CRISPR systems for generation of functional knockout cell lines relies on the Cas9 nuclease derived from streptococcus pyogenes bacteria (spCas9). Genome editing using CRISPR/Cas9 comprises two major components, short guide RNA (gRNA) and the Cas9 nuclease. Both work together to recognize and cleave a specific target DNA site [192]. The gRNA recognizes and binds to a target sequence located upstream of a protospacer adjacent motif (PAM motif). The PAM sequence of spCas9 is mainly (NGG) Once Cas9 binds to region of interest; it induces double stranded breaks (DSBs), which are later repaired by one of the following cellular mechanisms: Non-homologous end joining (NHEJ) and homology-directed repair (HDR)[193]. NHEJ is error prone due to imprecise rejoining of genomic DNA ends resulting in different lengths of deletions and insertions (Indels) at the cut site. CRISPR induced indels in the coding sequences can lead to functional knockout of the target gene by introduction of an early stop codon or via disruption of the translational reading frame (Fig.11). The HDR pathway is more precise than NHEJ; it depends on an exogenously added DNA donor template with desired insertions or modifications flanked by sequences of DNA homologous to the blunt ends of the target break site. Gene editing by HDR can be used not only for gene knockout, but also for insertion of marker genes (Knock-In), like antibiotic resistance genes or fluorescent/epitope tagging for generation of reporter cell lines [194,195].

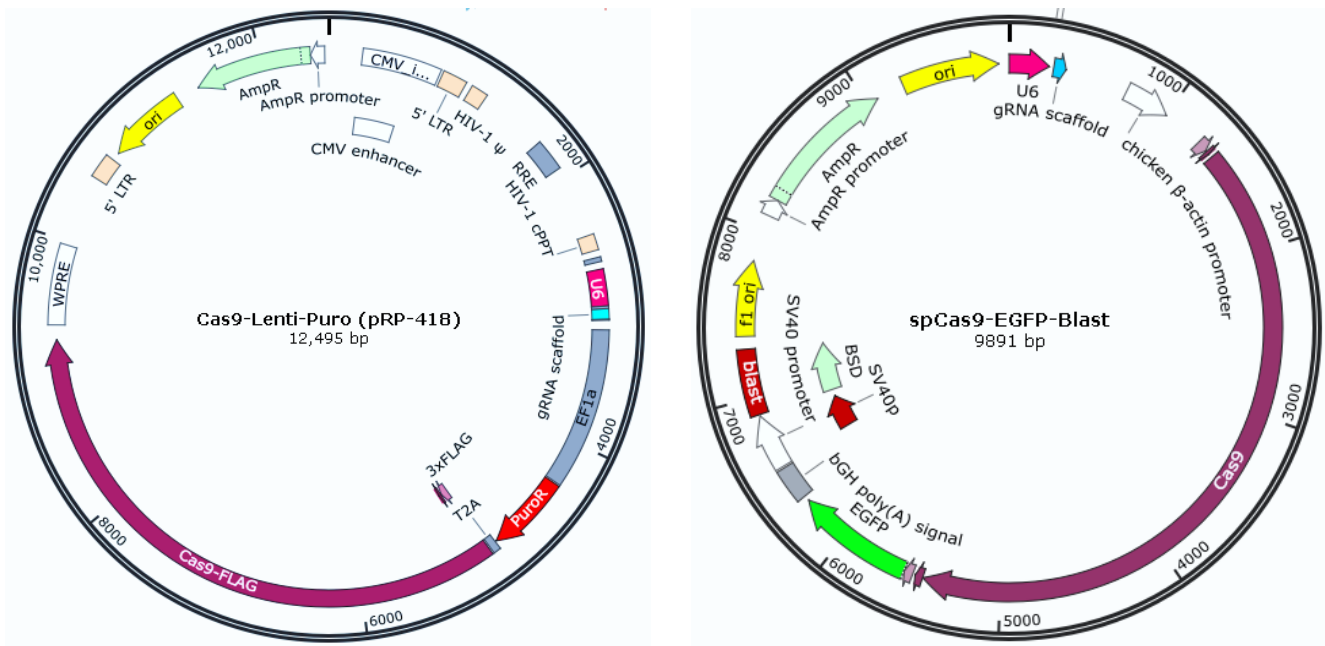
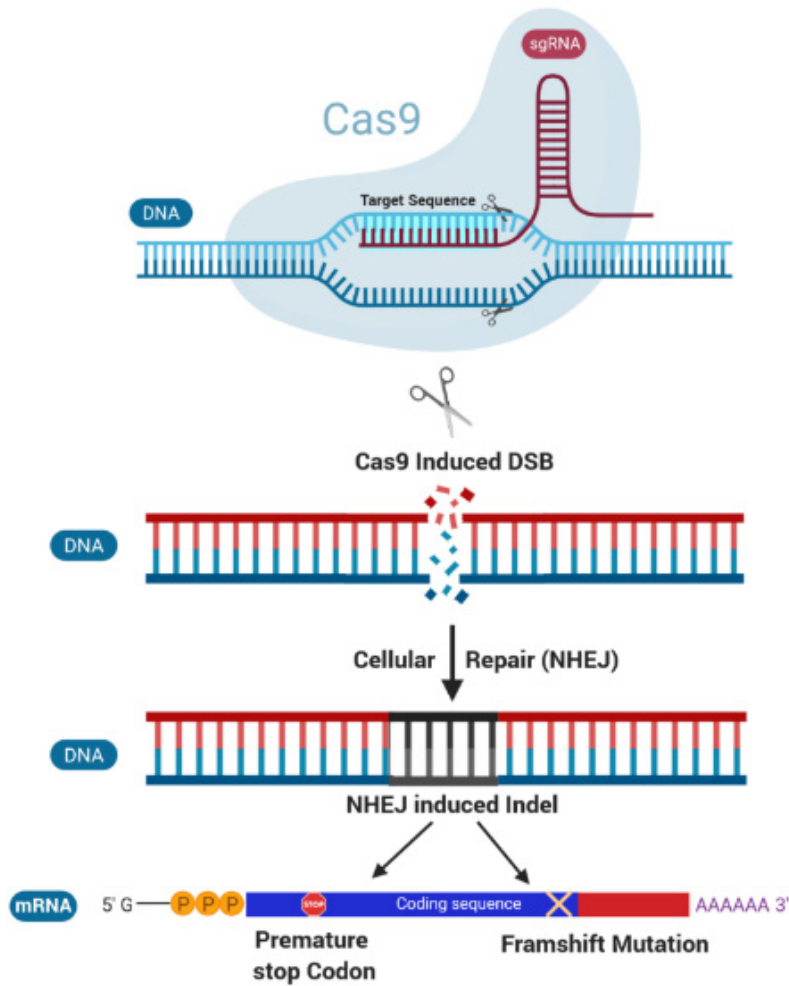


Figure 11. Schematic overview of CRISPR/Cas9 system and plasmids used for generation of knockout cell lines.

3.2.1.8.1. CRISPR/Guide RNA annealing and vector cloning

Guide RNA (gRNA) oligo (19-20nt) specific to different human ZDHHC were selected to minimize the likelihood of off-target cleavage using online MIT CRISPR design tool and Atum DNA 2.0 gRNA designer tool. For cloning in *pRP-418 vector*, “ACCG” overhang was added to the 5’ end of the gRNA-forward specifying oligo sequence and “AAAC” was added to the 5’ end of the reverse complement of the sgRNA-specifying oligo for cloning using the BsmBI restriction enzyme. For *spcas9-EGFP-Blast* vector cloning, cloning was done using BbsI restriction enzyme. The reverse gRNA overhangs remain the same as BsmBI but the forward oligo overhang has to be changed to “CACC”. In both cases, an extra ‘G’ should be added to the 5’ end of the gRNA sequence just after the restriction enzyme overhang. This G was added to ensure efficient initiation of the gRNA transcription of the from U6 promoter. The oligoes were then sent for company for synthesis.

For pRP-418 Plasmid (Bsmbl Cloning)

5'- **ACCGG**-----gRNA Seq.----- '3
 5'- AAAC-----gRNA Seq.----- '3

For spcas9-EGFP Plasmid (BbsI Cloning)

5'- **CACCG**-----gRNA Seq.----- '3
 5'- AAAC-----gRNA Seq.----- '3

The oligos were re-suspended in nuclease free water to 100µM stock solution. Then individually phosphorylated using the following conditions:

Mix	Volume
100µM oligo	2 µl
10x T4 Ligase Buffer	2 µl
T4 PNK enzyme	1 µl
Nuclease free water (NFW)	15 µl
Total volume	20 µl

The components were well mixed and incubated at 37°C for 1hour followed by inactivation step at 65°C/20min. The phosphorylated oligos were then annealed in duplex buffer at 95 °C for 5 min; and then cool down to 30 °C at (0.01°C/sec) in a gradient PCR thermomixer.

Mix	Volume
Forward oligo	10 µl
Reverse oligo	10 µl
Duplex Buffer	30µl
Total volume	50 µl

MATERIALS AND METHODS

CRISPR plasmids were digested, each with respective restriction enzyme according to the following protocol:

Digestion Mix			Volume
Plasmid DNA	<i>pRP-418</i>	<i>spcas9-EGFP-Blast</i>	1-2µg
10x NEB Buffer	3.1	2.1	2.5µl
Enzyme	BsmBI	BbsI	1µl
Total volume			25 µl
Temperature/Time	55°C/2hours	37°C/2hours	
Inactivation	80°C/20 min	65°C/20 min	

The digested vectors were then directly dephosphorylated after inactivation step by adding CIP enzyme (1µl/µg DNA) to the digestion mix and incubated at 37°C for 45min followed by gel purification. The concentration of purified DNA was measured by nanodrop and used for ligation of annealed oligo.

The phosphorylated annealed oligos were cloned into linearized CRISPR plasmids using a Golden Gate assembly with the following conditions:

Ligation Mix	Volume
Linearized Plasmid DNA	100ng
10x T4 DNA ligase buffer	2µl
1:10 Annealed Oligo	2µl
T4 ligase	1µl
Nuclease free water (NFW)	10µl
Total volume	20µl

Ligation was done at 16°C/overnight. Ligation reaction was then transformed into Top10 competent cells. Colonies were picked and analyzed for successful cloning using sequencing by U6 promoter specific sequencing primer (3.1.2.4).

3.2.1.9. Quantitative Real-time PCR (qPCR)

Primer pairs for each ZDHHC gene were selected to generate amplicons of 80-225 base pairs (3.1.2.2). All primer sets were designed with uniform annealing temperatures to allow detection of all ZDHHCs within the same qPCR run. Primers were synthesized by Integrated DNA Technologies (*IDT-DNA, BVBA, Belgium*). qPCR was used to profile the expression level of human ZDHHC in different cell lines and to quantify the fold-change in expression of

ZDHHCs in presence of influenza virus using PowerUp™ SYBR® Green Master Mix (Applied Biosystems, USA). The 10 ul PCR reaction consists of 5ul 2x powerUp SYBR green master mix, 400 nM of each primer and 100 ng cDNA template in qPCR 96-well plate (Eurogentec, Belgium). Non-template controls (NTC) are also included as an indicator for contamination. Plates are loaded into Applied Biosystems 7500 Fast/Step-one Plus Real-Time PCR machines (*Applied Biosystems, USA*). The cycling conditions was performed as follows; UDG (uracil-DNA glycosylase) activation step at 50°C for 2 min, followed by incubation at 95°C for 2 min to activate the Dual-lock™ DNA polymerase. Amplification was then performed using 40 cycles of denaturation at 95°C for 15s, annealing, and extension at 60°C for 30s. Following amplification, amplicon specificity for each ZDHHC was confirmed by melting curve analysis. Relative expression values for each DHHC mRNA were normalized to Human GAPDH. The fold change in relative DHHC expression levels (cDNA) was calculated using the following formula [196] :

$$\text{Fold Change} = 2^{-\Delta\Delta\text{Ct}} = 2^{-(\Delta\text{Ct of influenza infected} - \Delta\text{Ct of Mock infected})}$$

3.2.1.10. siRNA transfection and Knockdown

Hela cells (2×10^6) seeded in 6 well plate 1 day before transfection were transfected with 100 pmol of validated siRNAs against individual human ZDHHCs along with scramble siRNA as a negative control for 48h [185] (Qiagen) using interfeerrin transfection reagent (Polyplus) according to manufacturer instructions. Knockdown cells were again transfected 48h later with a plasmid encoding HA of the FPV mutant (FPV-I). 24 hours later cells were washed with cold PBS and acylation of viral HA was assessed using Acyl-RAC assay and metabolic labelling with radioactive palmitate.

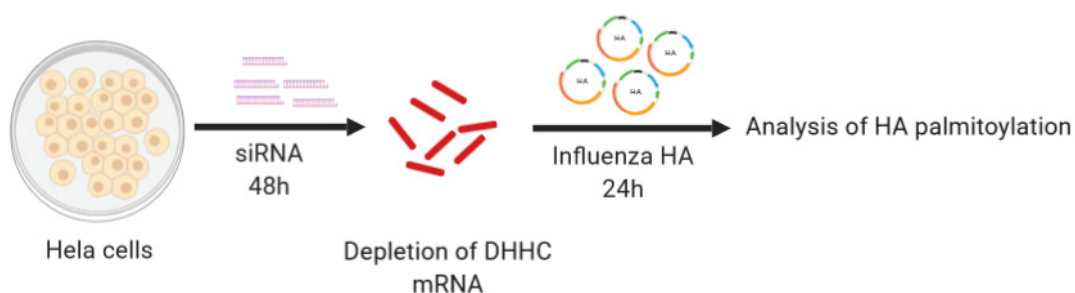


Figure 12. Schematic overview of ZDHHC siRNA knockdown procedures. Hela cells were individually transfected with siRNA against all human using interfeerrin transfection reagent for 48h followed by transfection of H7N1 FPV-I for 24h. Knockdown cells expressing viral HA were washed once with PBS and acylation of HA was analyzed by acyl-RAC or radioactive labeling.

3.2.2. Cell culture and microscopy

3.2.2.1. Cultivation and maintenance of mammalian cells

A549, MDCKII, HAP1 and 293T cells were maintained in DMEM while HeLa was cultured in MEM-Eagle medium. All media were supplemented with 10% FBS, 1x penicillin/streptomycin (PAN-Biotech). Cells were grown under cell culture conditions (5% CO₂, 37°C). They were routinely passaged (Every 3-4 days) in T25-T75 cell culture flasks when reaching confluency (100% for all cells and 70-80% for HAP1 cells). For passaging, cells were washed with sterile PBS and treated with trypsin/EDTA at 37°C until detachment. Then, the cells were mixed with growth medium and seeded into appropriate flasks/plates or used for continued culture (typically 1/5-10).

3.2.2.2. Freezing and thawing of cells

To make liquid nitrogen stocks for long term storage of cells, Healthy and confluent cells were detached from cell culture flasks, resuspended in growth medium, pelleted down at 3000RPM for 5min. Cell pellet was gently resuspended in ice cold freezing medium (60% DMEM, 30%FBS and 10% DMSO) and aliquoted into cryo-vials. Cooled down at -80°C overnight then stored in liquid nitrogen at -196°C.

To thaw cells, an aliquot from liquid nitrogen stock was rapidly thawed in 37 °C water bath. Afterwards, Cells were diluted in 10ml fresh growth medium and pelleted at 3000RPM for 5min, Cell pellet was then resuspended in prewarmed growth medium and transferred to a new cell culture flask and grown under cell culture conditions as described before.

3.2.2.3. Transfection

Transfection of plasmid DNA into mammalian cells (A549, HeLa, HAP1, 293T) was done using the Lipofectamine 3000 or Turbofect transfection reagents according to the manufacturer's instructions. For Lipofectamine 3000, 2 µg plasmid DNA/well was used for transfection of cells grown to 70 % confluency in 6 well plate. The DNA was diluted with Opti-MEM along with P3000 reagent (2µl/µg DNA) to a final volume of 250µl, while 5 µl of Lipofectamine 3000 were added to 125µl of Opti-MEM. Solutions were combined, together and thoroughly mixed. After 15 min incubation at RT, the transfection mixture was added dropwise to the cells covered with 2ml of fresh growth medium. Plate was then gently swirled and incubated at 37°C for 48-72h. Downstream application, Antibiotic selection, immunofluorescence or analysis of cell lysates was done as described in the respective sections.

3.2.2.4. Isolation of single cell clones and generation of knockout cell lines

Antibiotic kill curve was carried out to determine the optimal antibiotic (Puromycin–Blasticidin) concentration required for selection of transfected cells. Confluent A549 cells

were cultured at various concentrations of puromycin (0-5 μ g/ml) or Blasticidin (5-15 μ g/ml). The optimal selection dose is the lowest concentration of puromycin or Blasticidin that kills 100% of non-transfected cells within 5-7 days. Optimal dose was determined to be 2 μ g/ml for puromycin and 10 μ g/ml for Blasticidin). Cells were seeded 16h before transfection in 6 well plate, to be 60-70% at day of transfection. Cells were transfected with recombinant Ca9 plasmids with ZDHHC gene specific gRNA using Lipofectamine 3000 following manufacturer instructions (Thermo Scientific). Transfected cells were incubated in complete growth media for 48h followed by addition of antibiotic selection media and left until death of all control non-transfected cells with change of antibiotic media every 48h. Following antibiotic selection, single-cell clones were isolated by limited dilution in 96 well plate / or by cell culture cloning cylinders.

Limited dilution is a common technique used for isolation of single cell clones (SCC) and generation of stable cell lines. Briefly, Antibiotic resistant polyclonal cells population were trypsinized and re-suspended to 1x10⁴ cells/ml. 100 μ l of antibiotic selection media was added to all wells of 96 well plate except A1. Then 200 μ l of the cell suspension was added to A1 well and 2 fold serially diluted along column 1 from A1-H1 (First dilution series). Using Multi-channel, additional 100 μ l medium was added to each well in column 1 (giving a final volume of cells and medium of 200 μ L/well) and second 2-fold dilution series was horizontally carried out throughout the whole plate from A1-A12, B1 to B12 and so on (Fig.13). All wells were filled up to 200 μ L by adding 100 μ L medium to each well then plate was carefully placed in the incubator at 37°C. Single cell Clones should be visible by microscopy within 8-10 days , wells with single clones are marked and carefully checked every other day to make sure that it has only single clone with no any other contaminating cells on the well edge.

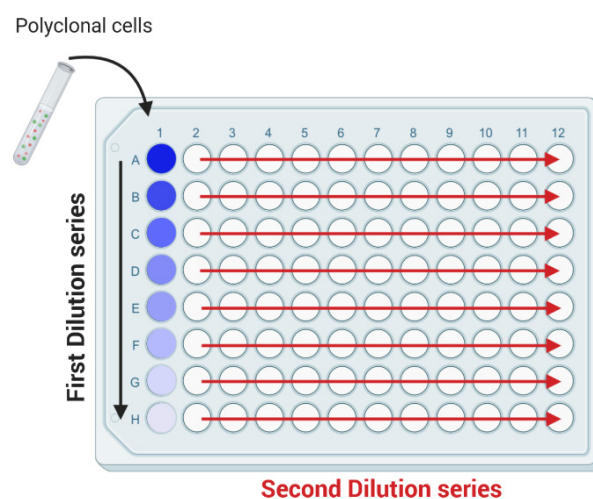


Figure 13. Plate setup for limited dilution method used for isolation of single cell clones: Stock polyclonal cells were placed in well A1 and serially diluted along column 1 from A1-H1 then a second dilution series was carried out from each well of column 1 , horizontally across the plate from 1-12.

Once the single cell clones are large enough, they are gently trypsinized from wells of 96 well plate and transferred into larger area (Usually in 24 well plate then 12 well plate for further propagation).

Cell culture cloning cylinders is another method used for isolation of SCC, simply by seeding cells at very low density in a large surface area (100-150mm Cell culture dishes) so each cell would individually settle down, divide and grow into a cell clones. Each growing cell clones is marked under the microscope and picked up with a small cloning cylinder. The cylinders are made of glass and sealed to the cell culture plate with sterile silicone high vacuum grease to prevent any possible leakage during the picking up procedures. It is quite efficient and clean method for isolation of SCC however, care should be taken that the cell clone has to be average size and widely separated with no any nearby cells to avoid picking of multiple cell clones. Briefly polyclonal cell population were seeded at very low density in 100 or 150mm cell culture dish with antibiotic selection media. 2-3 days later, cells were settled down to the bottom of the plate and starts to divide forming a cell clone. Cell culture dish has to be carefully examined under microscope and once a well-isolated clone is identified, a circle was drawn around it using a marker pen. Once satisfactory number of clones located, Growth media were removed and cells were washed with PBS then using sterile forceps, cloning cylinders were picked up and very gently pressed into the sterile silicone grease in order to make its bottom sticky to the culture plate and avoid leakage. Cloning cylinders were gently placed and pressed over the colony. This procedure has to be very fast in order to avoid dryness of the cell clones and high care should be taken while placing the cylinders by avoiding contact of the grease with cells or sliding of the cylinder across the colony. 150-200 μ l of trypsin were added to into the cylinders and plate was incubated at 37°C for 3-5 min until cells became rounded and come off the dish bottom, Detached cells of each single were gently pipetted and transferred into appropriate cell culture dish (Usually each clone in each well of 24 well plate) with fresh growth medium (Fig.14).

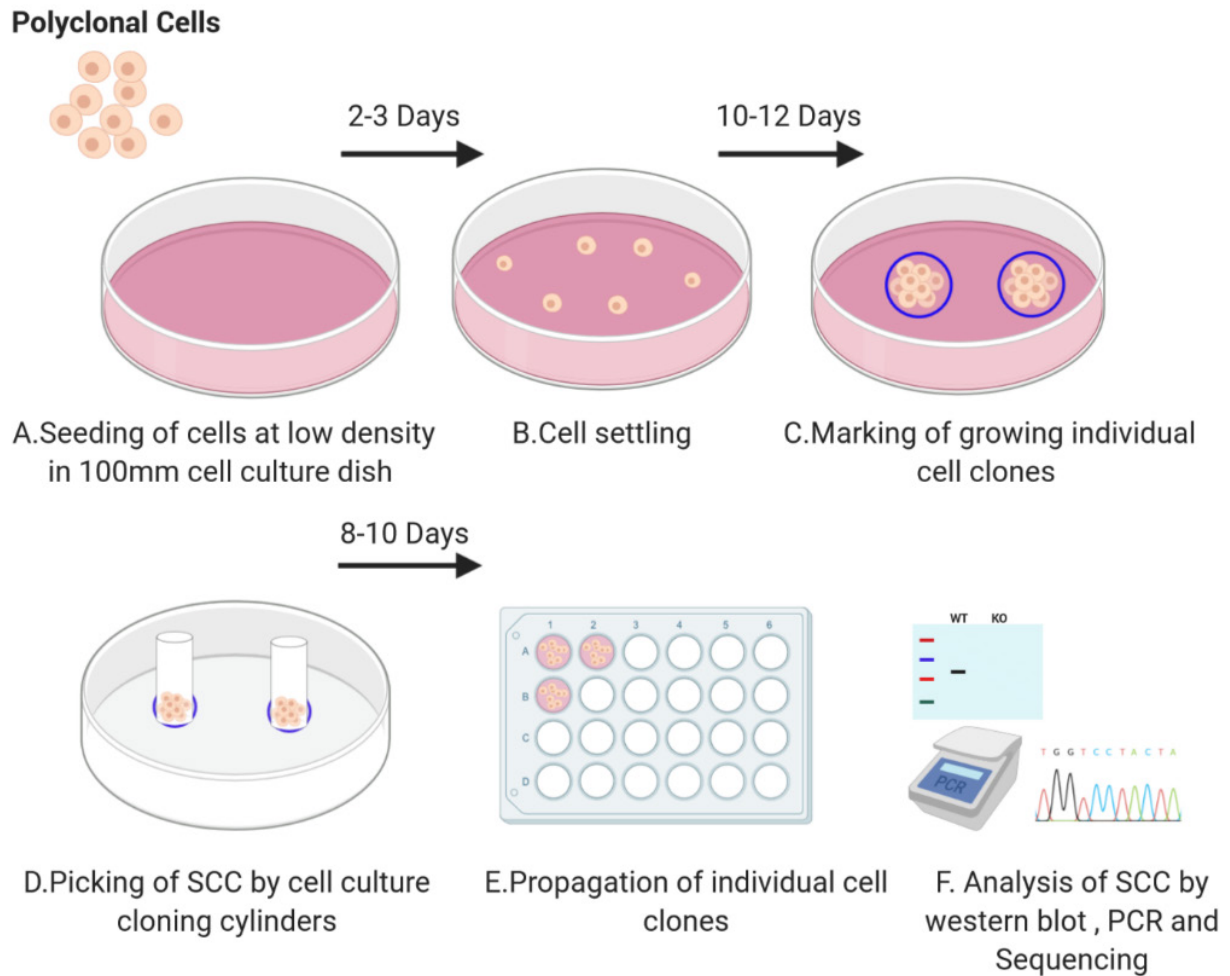


Figure 14. Experimental procedures for Isolation of single cell clones by cell culture cloning cylinders. Polyclonal cell population were seeded at low density in 100mm cell culture dish and left to settle down for 2 days under antibiotic selection media, Once the cell clones are visible and large enough to be picked ,They are marked using permanent marker and carefully picked up using cloning cylinders , bottom of the cylinder was greased with sterile silicone grease and carefully placed on the marker cell clone , 150-200 μ l trypsin was added to the cloning cylinder to detach the cells and each clone was transferred to wells of 24 well cell culture plate with fresh growth medium for propagation. Isolated clones were verified for CRISPR edit using western blot PCR and sequencing.

3.2.2.5. Confocal fluorescence microscopy

To investigate whether the ZDHHCs we identified to be involved in acylation of HA are expressed in a cell line relevant for replication of Influenza virus. A549 cells were seeded at 50% confluency one day before transfection on glass coverslips in 24-well cell culture plates. Cells were co-transfected with plasmids (1 μ g each) encoding HA of FPV along with individual mouse ZDHHCs (2, 8, 15 and 20), each fused to a C-terminal HA-tag using lipofectamine 3000 transfection reagent (ThermoFisher) according to manufacturer instructions. 24h post transfection, cells were fixed with paraformaldehyde (4% in aqua dest.) for 20min at room temperature (RT), permeabilized with Triton X-100 (0.1% in PBS) for 10 min under gentle

shaking and blocked with bovine serum albumin (BSA, 1% in PBS) for 45 min at RT. Cells were stained simultaneously with antiserum against influenza virus FPV (rabbit, 1:3000 diluted in 1% BSA) and mouse monoclonal anti-HA (6E2) tag antibody (1:1000 dilution in 3% bovine serum albumin, Cell signaling) for 1hr at RT. The HA-tag antibody recognizes the amino acid sequence YPYDVPDYA which is not present in the H7 subtype HA. To further exclude any possibility of cross reactivity of our used FPV antiserum with HA tagged proteins. Cells transfected only with GST (HA tag vector control) and stained with both antibodies was used as a negative control. Afterwards, cells were washed 3x for 5 min with PBS and then treated for 1hr protected from light at RT simultaneously with fluorescent secondary antibodies, anti-rabbit Alexa fluor 488 from goat (ThermoFisher) and anti-mouse antibody coupled to Alexa Fluor 568 (ThermoFisher), both at a dilution of 1:1000. Nuclei were then stained with DAPI (4',6- diamidino-2-phenylindole, dihydrochloride, ThermoFisher, 1:1000 dilution in washing buffer) for 5 min on a shaker at RT. Cells were then washed 3 times and coverslips were mounted on glass slides with ProLong Gold antifade mounting buffer (Thermo Fisher) and allowed to cure in a dark place overnight. Cells were illuminated via laser lines at 488 nm (Alex Fluor 488) and 561 nm (Alexa Fluor 568) and visualized with the VisiScope confocal FRAP System (VisiTron Systems GmbH), equipped with iXon Ultra 888 EMCCD camera, using 60X objective and the images were then processed using ImageJ (<https://imagej.nih.gov/ij/>).

3.2.3. Virological Methods

3.2.3.1. Generation of influenza acylation mutants with reverse genetics system

Wild type as well as acylation mutant influenza viruses were reconstituted from cDNA using 12 plasmids reverse genetic system for FPV-I /H7N1 virus strain according to the following protocol [96,197]. Briefly, one day before transfection, both 293T and MDCKII cells were cocultured into 100mm culture dishes to reach 80% confluency at transfection day. This system is more efficient and rapid rescue of viruses than transfection of 293T cells alone since MDCKII cells provide a good matrix to support 293T cells which is great for transfection however they poorly allow influenza replication, Moreover, the rescued virus can infect the MDCKII cells and amplify in case of low reconstitution efficiency. Cells were gently washed once with PBS and overlaid with 10ml fresh growth medium. The transfection mixture was prepared by adding 6 μ g DNA of FPV 12 plasmids (0.5 μ g each), to 12 μ l TurboFect transfection reagent diluted in 600 μ l Opti-MEM and incubated at RT for 20min, followed by dropwise addition of transfection mixture to the cells and incubation at 37°C and 5% CO₂ overnight. 16-24h post-transfection, medium with transfection mixture was removed and changed to virus infection medium (DMEM + 0.1%FBS + 0.3%BSA and 1 μ g TPCK trypsin). 48h post transfection, culture supernatant was collected and centrifuged at 5000 rpm for

5min to remove dead cells and debris. Cleared supernatants were tested for hemagglutination activity using HA assay, then aliquoted and stored at -80°C. Fresh MDCKII cells were infected with rescued viruses for further amplification and generation of virus stocks. Amplified viruses are titrated with plaque assay and stored in small aliquots at -80°C until use.

3.2.3.2. Virus infection and propagation

For infection of eukaryotic cells with Influenza viruses, 80-90 % confluent cells were washed with sterile PBS and overlaid with the virus suspension at different MOI (0.0001-1) according to cell line and experimental objective. After 1h adsorption, the inoculation medium was removed, and cells were washed twice with PBS for removal of non-adsorbed virus particles followed by addition of pre-warmed virus infection medium freshly supplemented with TPCK-trypsin in case of MDCKII (2µg/ml) and A549 (0.25-0.5 µg/ml) cells to allow multiple infection cycles. HAP1 cells are infected in absence of TPCK trypsin because they are very sensitive culture and rapidly detach in presence of trypsin. HAP1 cells can be infected with influenza viruses but without production of infectious virus particles (Infection supernatant tested negative for virus particles by HA and plaque assays). Typically, influenza A viruses produce cytopathic effect (CPE) in MDCKII and A549 cells within 1-3 days post-infection, once CPE reached 80%, culture supernatants were collected, cleared from cell debris at 5000rpm/10min, Aliquoted and stored at -80°C.

3.2.3.3. Plaque assay and virus growth kinetics

Plaque assay is a common technique used for determination of number of infectious virus particles in a given suspension. MDCKII cells were seeded in 6 well plate 1 day before to be 100% confluent in the next day. Cells were washed with PBS during which 10-fold serial dilution of virus was made in DMEM. 500µl of each virus dilution was used for infection single or duplicate wells of 6 well plate for 1hr at 37°C with gentle agitation every 15min. thereafter cells were washed once with PBS and overlaid with freshly prepared prewarmed 0.6% Avicel overlay medium (2ml/well)[198]. Cells were then without any movement in the incubator at 37°C. After 2 days, overlay was removed, cells are washed once with PBS and plaques was visualized using 0.1% crystal violet in 4% paraformaldehyde. Each plaque probably represents a single infection with one virus particle.

$$\text{VirusTiter (PFU/ml)} = \frac{\text{Number of plaques}}{\text{Dilution factor} \times \text{volume of virus used}}$$

For multicycle growth curve of influenza, A viruses in wild type and knockout cell lines, A549 cells were seeded in T25 cell culture flasks 1-2 days before start of growth kinetics. 80% confluent cells were gently washed with PBS and infected with virus at MOI 0.01(WSN, H1N1) or 0.001 (FPV-I, H7N1). After 1hr, cells are washed again with PBS for removal of

unbound viruses and incubated with fresh infection media. Aliquots of infection supernatant were collected 12h, 24h, 36h, 48h and 60h post infection, cleared by centrifugation at 5000RPM/5min and virus titer was measured with HA and plaque assays.

3.2.3.4. Ultracentrifugation and virus purification

For mass spectrometry and electron microscopy experiments, purified virus particles were prepared by infection of A549 and MDCKII cells respectively. Cells were seeded in T175 flasks and infected with WT and mutant viruses at different MOI as described above. Infected cell culture supernatant was cleared from dead cells and debris by low speed centrifugation (5000 RPM, 5min). Influenza virus particles were pelleted down from cleared supernatants by ultracentrifugation at 100000g for 2h 4°C. Virus pellet was resuspended in 500µl 1x TNE buffer. Resuspended virus pellet was further purified through sucrose cushion; 20-60% sucrose gradient was prepared by Gradient Master and the virus pellet was gently added to the top of the tube containing sucrose gradient and centrifuged at 100000g for 4h at 4°C. Virus band was identified against dark background, carefully collected and diluted in PBS and subjected to another ultracentrifugation cycle (100000g for 2h at 4°C). PBS with residual sucrose supernatant was carefully poured off, virus pellet was finally resuspended in 100µl 1X TNE buffer and subjected to SDS-PAGE and mass spectrometry analysis or prepared further for electron microscopy.

3.2.4. Biochemical Methods

3.2.4.1. Determination of protein concentration

Protein content of cellular lysates was quantified using BCA based Roti-Quant universal protein quantification kit (Carl-Roth) according to the manufacturer's instructions. The assay allows detection of protein in the range of 5–1000µg/ml, it is based on the reduction of Cu⁺⁺ (cupric form) by proteins in alkaline solution combined with the colorimetric detection of resulting Cu⁺ ions (cuprous form) by chelation with PCA, a molecule highly similar to bicinchoninic acid (BCA). The resulting chelate complex is strongly colored greenish-blue directly proportional to the number of peptide bonds (Protein) present in the sample. The chelated complex exhibits strong light absorbance at 503nm wavelength measured by microplate-spectrophotometer. Sample protein concentration was determined within a standard curve range made by Bovine serum albumin (BSA) standards.

3.2.4.2. SDS polyacrylamide gel electrophoresis (SDS-PAGE)

SDS-PAGE is a common biochemical procedure used for separation of protein based on their molecular weight through stoichiometric binding to negatively charged sodium dodecyl sulfate (SDS). SDS evenly renders all protein molecules net negative charge so, when the voltage is applied, all the proteins migrate through gel pores towards the positive electrode. Discontinuous gels were prepared and poured into glass casts then assembled into Biometra

Minigel-Twin electrophoresis system (Analytik jena). Acrylamide/bisacrylamide concentration varies between 10-15% in resolving gel (pH 8.8) while 5% in the stacking one (pH 6.8). Exact composition of gel and buffers were specified in the material section (Section 3.1.4). Protein samples were mixed with reducing/or non-reducing SDS sample loading buffer, boiled at 95°C for 10 min; Then electrophoresis was run at constant voltage of 80V (stacking gel) and then raised to 150V in the separating gel. For detection of individual proteins after electrophoresis, the gel was processed by western blot and Coomassie staining.

3.2.4.3. Western blotting

Western were used for specific detection of proteins after SDS-PAGE. Briefly, gels were electrophoretically transferred (200mA for 1hr) onto polyvinylidene difluoride (PVDF) membranes (GE Healthcare) using PerfectBlue™ Semi-Dry blotting system. After blocking (blocking solution: 5% skim milk powder in PBS with 0.1% Tween-20 (PBST)) for 1h at room temperature, membranes were incubated with the primary antibody overnight at 4°C followed by 3x washing, each for 10min with PBST, then membranes were incubated with horseradish peroxidase-coupled secondary antibody, for 1 hour at room temperature. Primary and secondary antibodies with indicated dilutions are listed in the material section (Section 3.1.4). After washing three times, signals were detected by chemiluminescence using the Pierce ECLplus reagent (ThermoFisher) and a Fusion SL camera system (Peqlab, Erlangen, Germany). The density of bands was quantified with Image J software.

3.2.4.4. S-acylation analysis assays

3.2.4.4.1. Acyl-Resin assisted capture (Acyl-RAC)

Acyl-RAC is a faster and more sensitive modification of Acyl biotin exchange (ABE) method for enrichment of s-acylated proteins [146,176,177]. Acyl-RAC principle is based on the labile nature of the thioester bond between the attached fatty acid and the modified cysteine residue. This can be cleaved using hydroxylamine (HA), revealing a free sulfhydryl group on the cysteine residue, which can be directly pulled down with thiopropyl sepharose beads. Prior to beads binding, Methyl methanethiosulphonate (MMTS) was used for irreversible blocking of any existing sulfhydryl groups on unmodified cysteine residues to avoid any nonspecific binding of non-acylated proteins to the beads (Fig.15). Protein S-acylation was analyzed by the Acyl-RAC assay as described [199], with some modifications. Transfected or infected cells in a six well plate was washed with PBS, lysed in 500µl buffer A (0.5% Triton-X100, 25 mM HEPES (pH 7.4), 25 mM NaCl, 1 mM EDTA, and protease inhibitor cocktail). Disulfide bonds were reduced by adding Tris (2-carboxyethyl) phosphin (TCEP, Carl Roth) to a final concentration of 10mM and incubated at RT for 30min. Free SH-groups were blocked by adding methyl methanethiosulfonate (MMTS, Sigma, dissolved in 100 mM HEPES, 1 mM EDTA, 87.5 mM SDS) to a final concentration of 1.5% (v/v) and incubated for 4 h at 40 °C.

Subsequently, 3 volumes of ice-cold 100% acetone was added to the cell lysate and incubated at -20°C overnight. Precipitated proteins were pelleted at 5,000xg for 10 minutes at 4°C. Pelleted proteins were washed five times with 70% (v/v) acetone, air-dried, and then re-suspended in binding buffer (100 mM HEPES, 1 mM EDTA, 35 mM SDS). 20-30 µl of the sample was removed to check for total protein expression by Western blotting. The remaining lysate was divided into two equal aliquots. One aliquot was treated with hydroxylamine (0.5 M final concentration, added from a 2M hydroxylamine stock adjusted to pH 7.4) to cleave thioester bonds. The second aliquot was treated with 0.5M Tris-HCl pH 7.4. 30µl thiopropyl Sepharose beads (Sigma), which were beforehand activated by incubation for 15 min in Millipore water, were added at the same time to capture free SH-groups. Samples were incubated with beads overnight at room temperature on a rotating wheel. The beads were then washed 5x in binding buffer and bound proteins were eluted from the beads with 2x non-reducing SDS-PAGE sample buffer for 5 minutes at 95°C. Samples were then subjected to SDS-PAGE and Western-blotting.

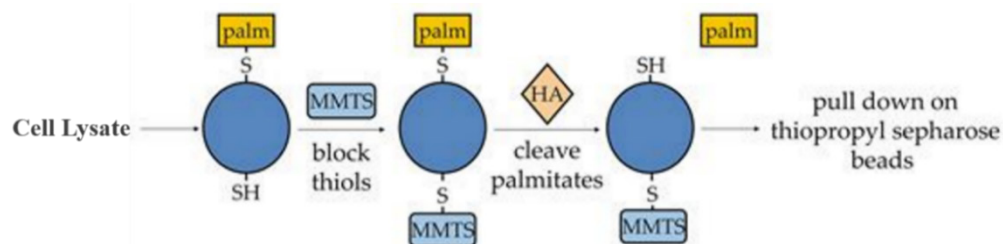


Figure 15. Principle of acyl-resin assisted capture (acyl-RAC) method for enrichment of acylated proteins (modified from [200]). Cells were lysed and all free cysteines were irreversibly blocked using MMTS. Protein sample was concentrated using a single step of Acetone precipitation then cysteine bound fatty acid was cleaved using hydroxylamine (HA) and acylated proteins were directly captured on thiopropyl sepharose beads and analyzed by western blot.

3.2.4.4.2. Radioactive metabolic labelling and fluorography

For ^3H -palmitate labelling, HeLa cells were transfected with siRNAs to knockdown ZDHHCs 1, 2, 8, 15 and 20 as well as with a scrambled siRNA. 48 hours later cells were transfected with a plasmid encoding HA of the FPV mutant using Fugene (Promega). 24 hours later cells were labelled for 2hr. with 200 µCi/ml ^3H -palmitic acid (9, 10- ^3H (N)) (American Radiolabeled Chemicals, Inc.) in IM (Glasgow minimal essential medium buffered with 10 mM HEPES, pH 7.4). For immunoprecipitation (IP), cells were washed 3x in cold PBS, lysed for 30 min at 4°C in IP Buffer, and insoluble material was pelleted for 3 min at 5000 rpm. Supernatants were precleared using 20µl of protein G sepharose beads (GE Healthcare) for 1hr at 4°C. 50-100µl of the lysate was separated for total protein expression by western blotting. The remaining cleared supernatants were incubated with 2µl antiserum against the

HA2 subunit of HA from FPV and with 30 μ l protein G beads overnight at 4°C on a rotating wheel. Sepharose beads were washed 3x with IP buffer and bound proteins were eluted in 4x non-reducing SDS-PAGE sample buffer, boiled at 95°C for 5min and subjected to SDS-PAGE. Gels were treated with Amersham Amplify (GE Healthcare) according to manufactures instructions, dried and exposed to X-ray film.

3.2.4.4.3. Click chemistry and In-Gel fluorescence

Click chemistry is a specific, rapid and radioactive free method used for studying s-acylation of proteins. Wild type, Δ ZDHHC22 ; mock and infected A549 cells are washed 3x with serum free DMEM then metabolically labeled with 17-ODYA palmitic acid analogue (1:1000) (Cayman chemicals) in DMEM supplemented with 5% dialyzed serum for 6h. Labeled cells were washed 3 times with cold PBS, lysed for 30min at 4°C in IP and target proteins are immune-precipitated using specific antibodies as described in 3.2.4.4.2. Beads bound proteins were washed 3x with IP buffer and click chemistry reaction was done directly on the beads for 1hr at room temperature (RT) using (1.25Mm TAMRA Azide, 50 mM TCEP, 1x TBTA and 50 mM CuSo₄) [181]. Click reaction was stopped by 4x sample loading buffer and boiled at 95°C for 5min. Fluorescence labelled proteins are separated with SDS-PAGE and visualized by Typhoon 9400 fluorescence scanner.

4. Results

4.1. Expression of ZDHHC proteins in different tissues of the human respiratory tract and corresponding cell lines

The aim of this project was to determine the palmitoyl acyltransferase(s) from the ZDHHC protein family, which are involved in attaching fatty acids to influenza virus proteins. Replication of human influenza viruses is mainly confined to the respiratory tract so I aimed first to check the expression of different ZDHHCs on the available online databases. The existence of a protein in a tissue is based on UniProt evidence and evidence based on two proteogenomic studies (mass spectrometry evidence). Nasopharynx and bronchus are respiratory epithelial cells from these tissues, lung contains pneumocytes and macrophages. RNA data are shown as 'transcript per million' (TPM).

Tissue	Nasopharynx	Bronchus	Lung	Lung	A549 Cells
Protein/RNA	protein	protein	protein	RNA	RNA
ZDHHC1	-/+	+	-/+	10.5	7.2
ZDHHC2	+	+	-/+	21.3	11.3
ZDHHC3	++	+	+	35.5	22.1
ZDHHC4	+	+	+	34.2	32.9
ZDHHC5	+	n.a.	++	41.5	78.0
ZDHHC6	-	-	++	29.9	35.6
ZDHHC7	+	+	-/+	55.0	50
ZDHHC8	-	-	-	22.5	17
ZDHHC9	+	+	+	26.9	21.4
ZDHHC11	n.a.	n.a.	n. a.	7.5	6.8
ZDHHC11b	-	-/+	-/+	5.9	0.9
ZDHHC12	+	+	+	21.3	135.5
ZDHHC13	+	+	-	8.9	17.2
ZDHHC14	n.a.	n.a.	n.a.	4.4	2.5
ZDHHC15	n.a.	n.a.	n.a.	1.7	0.0
ZDHHC16	-	-	-/+	29.7	52.8
ZDHHC17	-/+	n. a.	+	14.1	7.9
ZDHHC18	+	+	-	21	18.0
ZDHHC19	n.a.	n.a.	n.a.	0	0.0
ZDHHC20	+	-/+	+	27.5	18.3
ZDHHC21	+	+	++	7.6	3.2
ZDHHC22	n.a.	n.a.	n.a.	0	0
ZDHHC23	n. a.	n. a.	n. a.	4.9	3.9
ZDHHC24	+	-/+	+	4.6	6.7

Table 3. Expression of ZDHHC proteins in tissue of the human respiratory tract and in A549 cells. - = not detected; +/-: low, +: medium and ++: high expression level. n. a.: not analyzed. All data were collected from human protein atlas: <https://www.proteinatlas.org/>. DOI: 10.1126/science.1260419

Proteomic analysis data of different tissues of the human respiratory tract revealed that ZDHHC5, 6, 21 are highly expressed in lung tissues while ZDHHC8,13,16 and 18 showed no expression. Data for ZDHHC11,14,15,19,22,23 was not available on the database. On the RNA level, all genes are expressed at different levels except for ZDHHC19 and 22 (Table 4). I also checked the expression of different ZDHHC in human lung tissues using the data available on NCBI based on RNA seq data, which measure RNA abundance in form of “reads per kilobase per million reads” (PRKM). The data was quite similar to what was obtained from protein atlas where it showed that all ZDHHCs (Except ZDHHC19 and 22) are expressed in human lung tissues. ZDHHC4, 5, 7 were the highly expressed ones while ZDHHC14, 15, 23 and 24 showed relatively low expression (Fig.16).

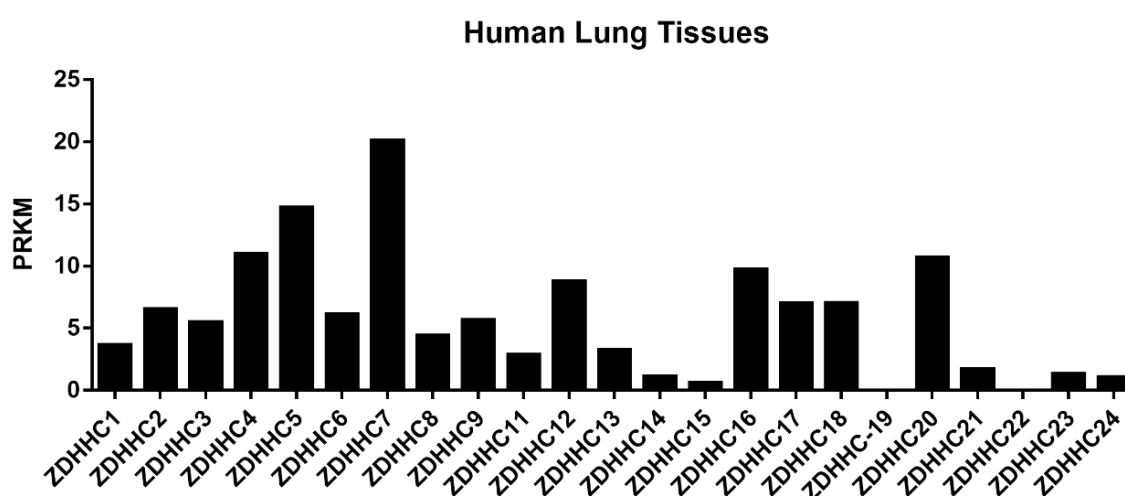


Figure 16. Expression of ZDHHCs in human lung tissues

4.1.1. Expression level of ZDHHCs in different human cell lines

To experimentally profile the expression pattern of ZDHHC family members among different human cell lines used in this study, RNA was isolated from A549, HeLa and HAP1 cells and quantitative RT-PCR (qRT-PCR) was done using primers specific for the mRNA of individual ZDHHCs. mRNA levels were normalized relative to cellular housekeeping genes: GAPDH in A549 cells, TATA-binding protein in HeLa and β -glucuronidase in HAP1 cells. Real-time PCR revealed that all ZDHHC (except 19) are expressed (Fig.17). The relative abundance of the relevant transcripts is very similar in each cell type I used in this study confirming the results collected from the online databases.

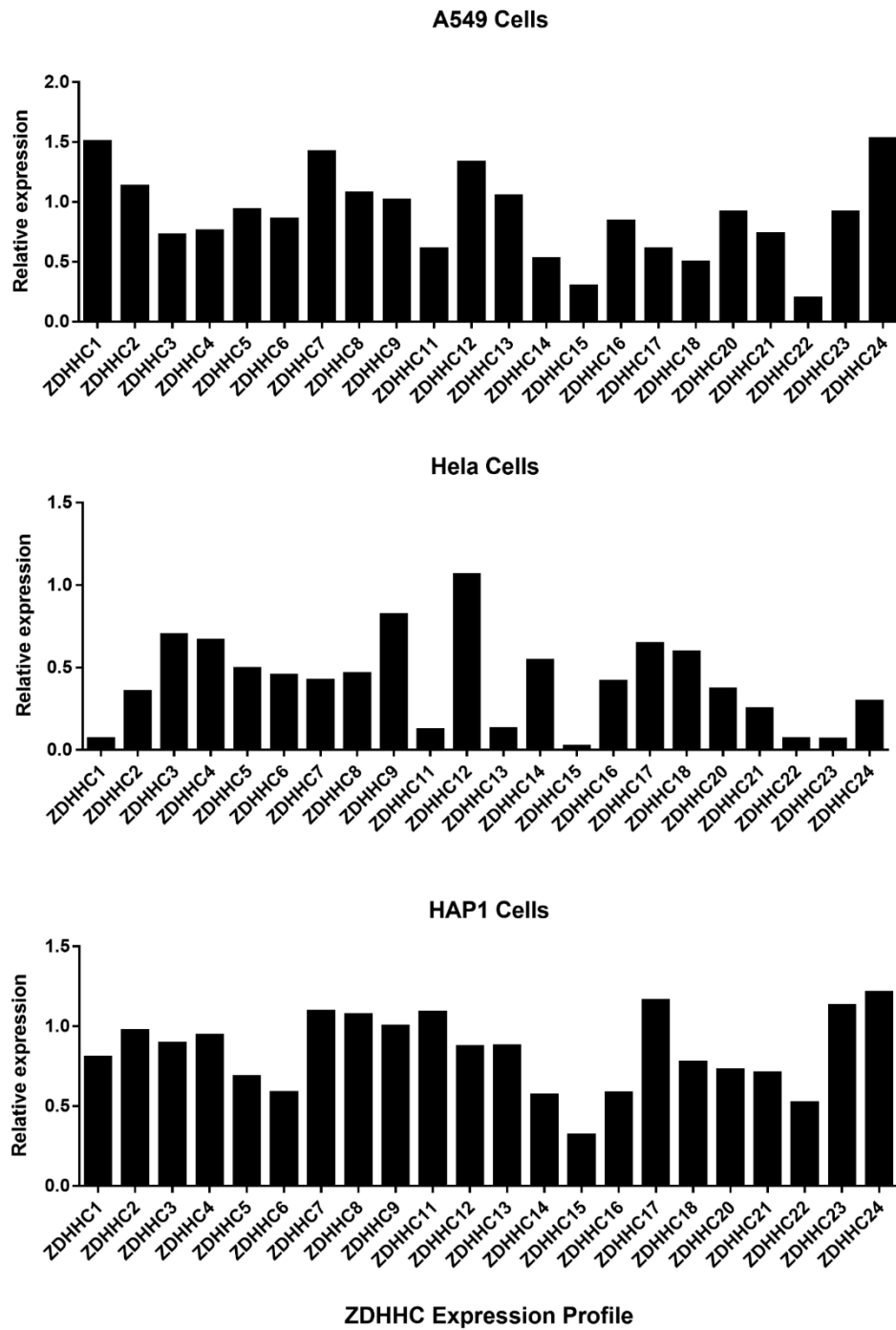


Figure 17. Expression profile of ZDHC enzyme family members by quantitative real-time PCR (qPCR) for the cell lines used in this study. RNA was isolated, reverse transcribed. ZDHC expression was detected using qRT-PCR. mRNA levels of HeLa and HAP1 cells were normalized using human TATA-binding protein and β -glucuronidase while expression in A549 cells was normalized to human GAPDH. Data was analyzed using Livak Method ($2^{-\Delta\Delta CT}$). All ZDHCs (except ZDHC19) are expressed in HeLa, HAP1 and A549 cells but at slightly different levels.

4.1.2. Effect of influenza infection on ZDHHC expression profile

As an initial attempt to narrow down the candidate ZDHHC(s) involved in acylation of HA, I thought that influenza virus could preferentially upregulate one or more ZDHHCs to acylate the viral proteins. One human and one avian influenza virus strain (H1N1-H7N1) was used to infect the human lung cell line A549 at MOI 1 to assure that every cell has received a single viral particle. RNA was extracted 5h post infection from both influenza infected and mock-infected cells, reverse transcribed to cDNA and relative quantification of ZDHHCs was analyzed by qPCR and normalized to GAPDH as a housekeeping gene using Livak Method ($2^{-\Delta\Delta CT}$) [196]. The effect of influenza infection on expression level of individual ZDHHCs is displayed in form of “Fold change” between mock and virus infected cells.

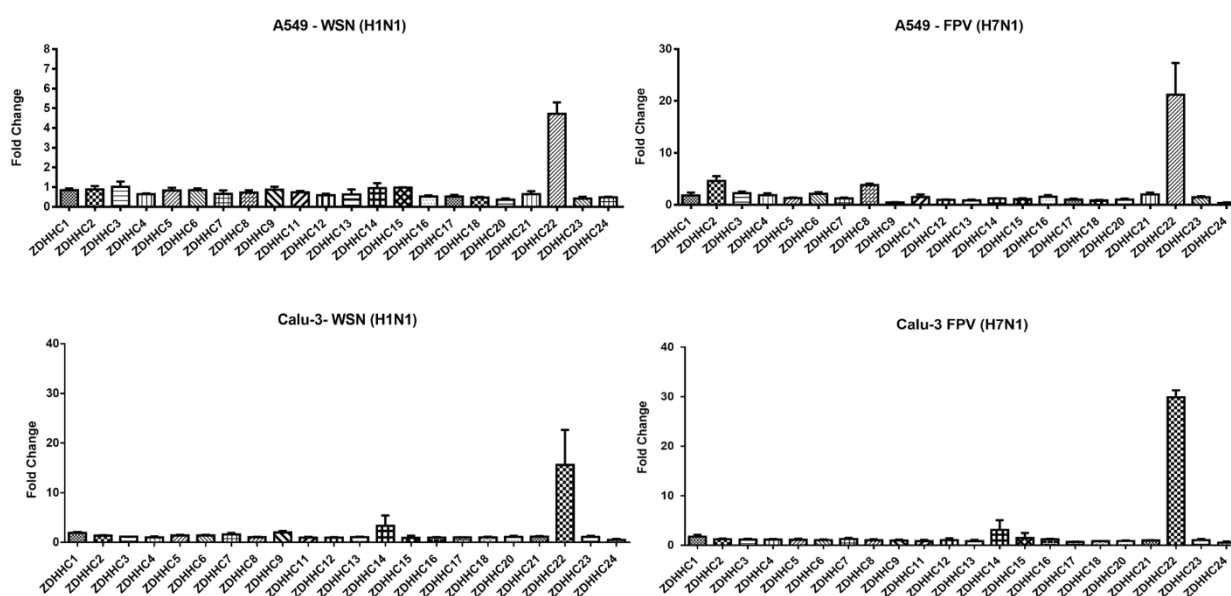


Figure 18. IAV significantly upregulate ZDHHC22 in A549 and Calu-3 human lung cells: A549 cells were infected with WSN (A) or FPV-I (B) at MOI=1 for 5h along with mock infected cells. Total RNA was isolated, reverse transcribed to cDNA and qPCR were performed to determine the expression of different ZDHHCs. WSN (C) and FPV-I (D) influenza A viruses were used for infection of Calu-3 cells at MOI1 for 5 h and relative expression of ZDHHCs was analyzed by qPCR. Relative quantification of ZDHHC gene family was performed using Livak method ($2^{-\Delta\Delta CT}$) to calculate the relative fold change expression of each gene (Infected compared to non-infected control) normalized to GAPDH as a housekeeping gene. Data shown are mean \pm standard deviation from three independent experiments.

Interestingly, I found that only single member of the ZDHHC enzyme family, namely ZDHHC22, was significantly upregulated upon influenza virus infection in human lung cell lines with a fold change of 5 (H1N1) or 20 (H7N1) in A549 cells (Fig.18 a-b). To confirm the specificity of such upregulation, I infected another human lung cell line (Calu-3) using the same influenza strains. The calculated fold change was even higher (15-30) indicating the specific up-regulation of ZDHHC22 mRNA expression during influenza virus infection (Fig.18 c-d).

4.1.3. Influenza virus NS-1 significantly upregulate ZDHHC22 expression

Since NS1 is the key protein of influenza virus that modulates the host innate immune response to viral infection, we hypothesized that NS1 is responsible for induction of ZDHHC22 upregulation. To test this, I expressed NS1 from three different influenza strains (WSN, FPV and PR8) in A549 and checked expression of ZDHHC22. Results showed that expression of FPV-NS1 activated the expression of ZDHHC22 by more than six fold while those of WSN and PR8 by three fold (Fig. 19a). I next validated the specificity of NS1 induced upregulation of ZDHHC22 using NS1 deficient virus mutants from PR8 (H1N1) and Panama (H3N2) influenza virus strains. The results showed no change in the expression level of ZDHHC22 in cells infected with Δ NS1 mutant viruses, whereas the corresponding wild type viruses caused ZDHHC22 upregulation (Fig. 19b). All Together, my results confirmed that NS1 is the key player of ZDHHC22 upregulation observed during IAV infection.

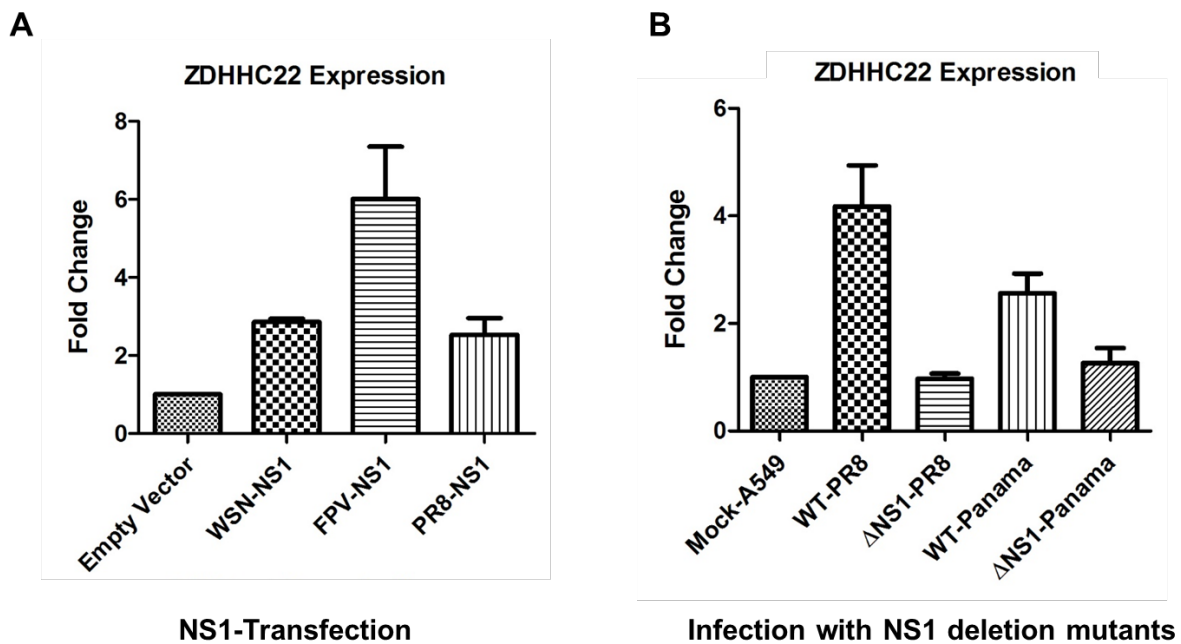


Figure 19. Influenza NS1 significantly induce upregulation of ZDHHC22. (A) NS1 of 3 different influenza virus strains (WSN-FPV and PR-8) cloned in pCAGGS vector was used for transfection of A549 cells for 24h. (B) A549 cells were infected with WT and Δ NS1 mutant viruses for 5h at MOI 1 along with mock infected cells. RNA was isolated and RT-qPCR was carried out to quantify relative expression of ZDHHC22 using Livak method ($2^{-\Delta\Delta Ct}$). Ct values of ZDHHC22 was normalized to GAPDH as the internal control. The $\Delta\Delta Ct$ value was calculated by difference in normalized Ct value (ΔCt) from Transfected cells to the ΔCt from empty vector transfected ones. The $\Delta\Delta Ct$ values is then transformed into $2^{-\Delta\Delta Ct}$ value which represent the fold change of estimated gene expression. The data represents the mean plus standard deviation from 3 independent experiments. NS1-pCAGGS expression vectors and Δ NS1 mutant viruses were kindly provided by Dr.Thorsten Wolff from the Robert Koch institute (RKI).

4.2. Knockout of ZDHHC22 in A549 cells using CRISPR/Cas9

Because IAV significantly upregulate the expression of ZDHHC22 during infection of lung cells, we hypothesized that ZDHHC22 might play a role in acylation of influenza virus proteins (HA and M2). To test this hypothesis, I knocked out ZDHHC22 in A549 cells using CRISPR/Cas9 technology. In order to make a functional knockout of the protein, two guide RNAs (gRNAs) (**Section 3.1.2.3**) were designed targeting exon-2 of the ZDHHC22 gene containing the DHHC domain responsible for catalytic activity of the enzyme. The two gRNAs flanking 260bp region in exon-2 of the target gene were individually cloned into the pRP-418 vector together with cas9 nuclease and used together to co-transfect A549 cells followed by isolation and screening of single cell clones. Due to lack of specific antibodies for most members of ZDHHC family, including ZDHHC22, I relied on genetic approaches to validate the knockout on both the DNA and RNA level. PCR on genomic DNA isolated from wild type (WT) and knockout (KO) cells revealed a bi-allelic 248bp deletion in coding region of exon-2 creating a shift in the codon reading frame of ZDHHC22 (Fig.20). Knockout has been also confirmed on mRNA level by RT-PCR using primers flanking Cas9 target sites, which showed that only mRNA from WT cells could be amplified but not from the KO cells (Fig.20). This could be attributed to none sense mediated decay of synthesized mRNA due to frameshift deletion in the coding region of ZDHHC22 gene.

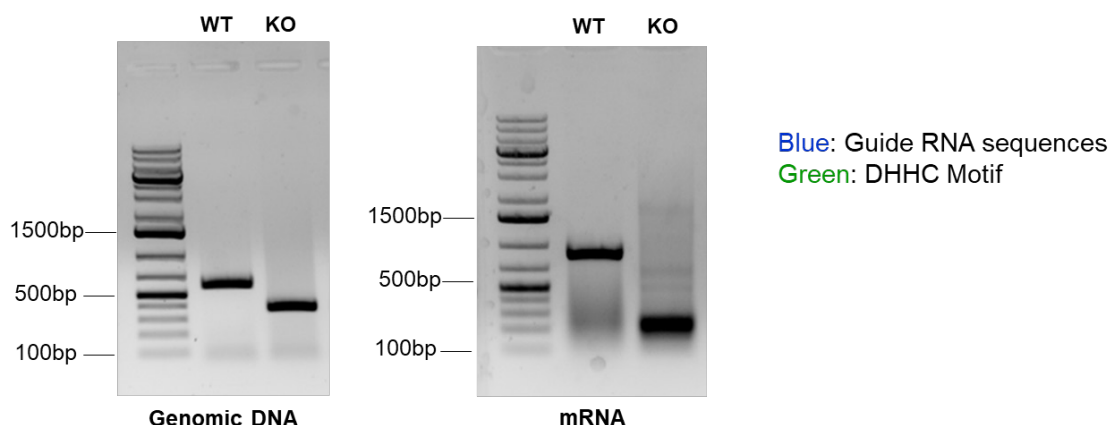
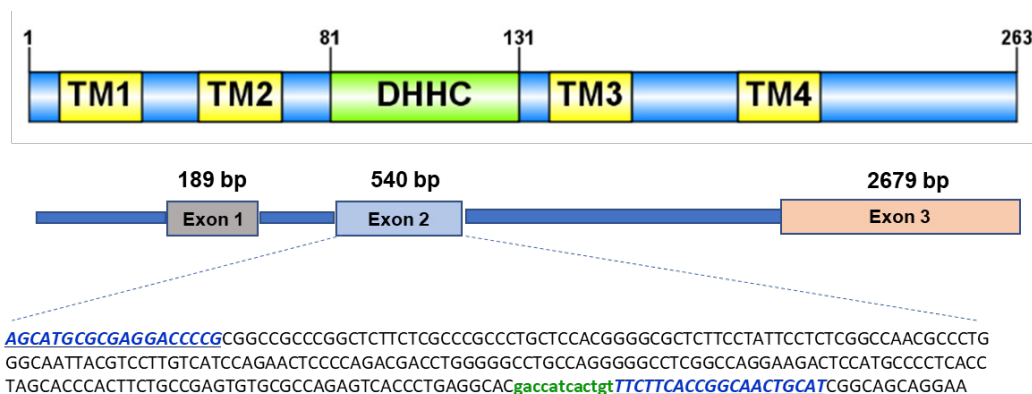


Figure 20. Workflow of CRISPR/Cas9 mediated Knockout of ZDHHC22 in A549 cells. (A) Schematic diagram of human ZDHHC22 protein (263 aa); Four transmembrane domains (TM) with DHHC active domain (81-131) located between 2nd and 3rd TM domains. The 4 TM domains are encoded from 3 Exons of the human ZDHHC22 gene Exons 1, 2 and 3 consists of 189, 540 and 2679 base-pairs. CRISPR/Cas9 guide RNA are designed to target DHHC domain (Green) in Exon 2, The guide RNA target sites are indicated in blue. (B) PCR on genomic DNA (gDNA) isolated from wild type (WT) and Knockout cell line showing biallelic deletion of 248 bp region in Exon-2 of ZDHHC22.

4.2.1. Effect of ZDHHC22 knockout on acylation pattern and growth kinetics of influenza A virus

I next analyzed palmitoylation of influenza virus proteins (HA and M2) in the ZDHHC22 KO cells using Acyl-RAC [199,200] and click chemistry assays. Acyl-RAC is a technique which allows the capture of S-acylated proteins on thioreactive sepharose beads. Briefly, both mock and influenza infected WT and Δ ZDHHC22 A549 cells were homogenized in lysis buffer A, TCEP was used to reduce disulfide bonds and free thiols on unmodified cysteine residues were blocked using MMTS and then treated with hydroxylamine (NH₂OH) to cleave palmitoyl thioester bonds which were subsequently captured by beads (Enriched sample). As a negative control, equal fraction of the same sample was treated with Tris-HCl instead of hydroxylamine so neither cleavage nor beads binding is expected. Proteins from both enriched fraction (+Hydroxylamine) and control fraction (-Hydroxylamine) were eluted, separated by SDS-PAGE, and immune-blotted using antibodies for each protein. Flotillin-2; a well-known palmitoylated protein [201] was used as a cellular control of S-Acylation. The results showed that Hemagglutinin and matrix-2 influenza virus proteins were efficiently enriched as palmitoylated proteins in hydroxylamine treated fraction of lysate (+NH₂OH) along with cellular marker Flotillin-2. However, there was no significant difference in the level of viral protein palmitoylation between the wild type and Δ ZDHHC22 cells (Fig.21a-b).

To further confirm the results of Acyl-RAC, I used click chemistry [181] where mock and influenza virus infected cells were metabolically labeled with the 17-ODYA palmitic acid analogue, which serves as a chemical reporter of protein palmitoylation. Labelled cells were lysed followed by immunoprecipitation of viral hemagglutinin protein (HA) using antibodies and protein G sepharose beads. Labelled immunoprecipitated proteins were reacted with TAMRA-Azide via copper catalyzed click chemistry reaction to allow visualization of in-gel fluorescence analysis of protein palmitoylation. The results revealed that HA protein of 2 different influenza virus strains (WSN and FPV-I) was metabolically labelled in Δ ZDHHC22 cells to the same extent as in wild type cells (Fig.21c). This confirms the acyl-RAC results and suggests that knockout of ZDHHC22 has no effect on acylation of influenza virus proteins (HA and M2).

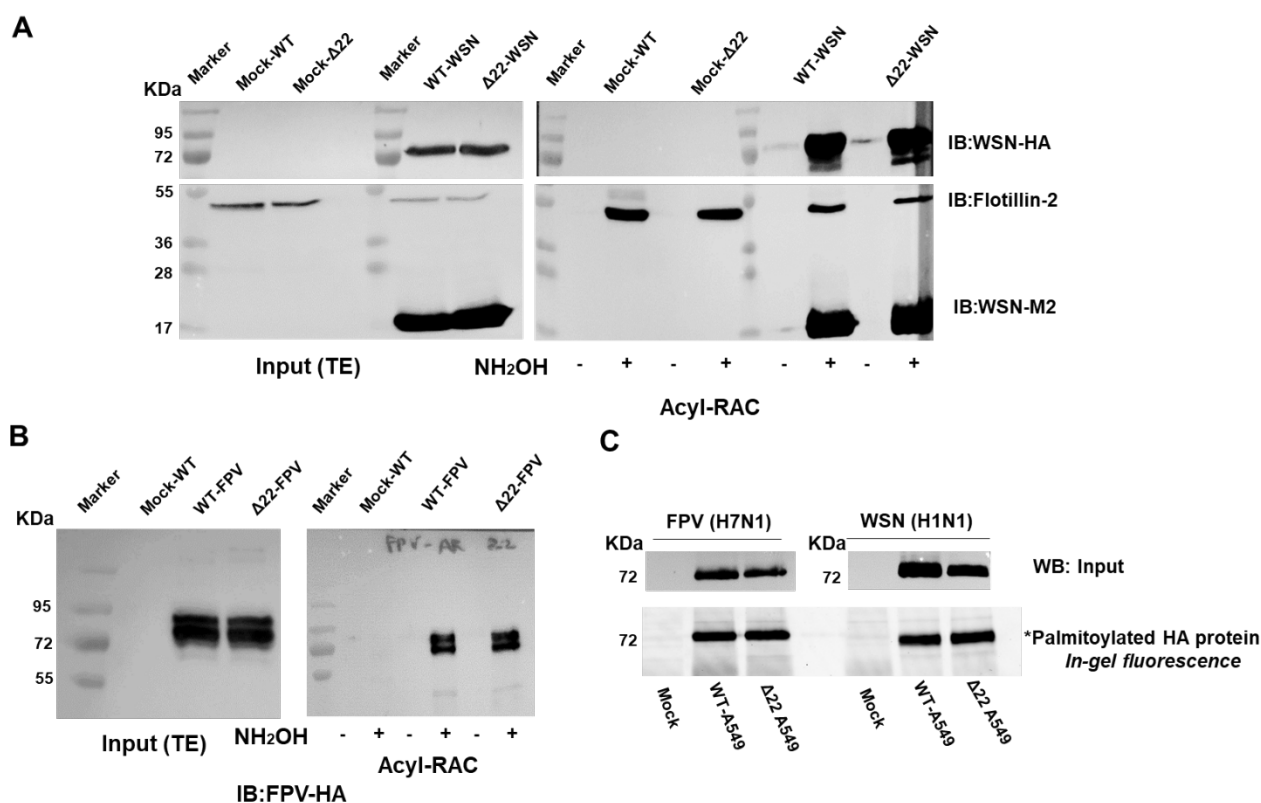


Figure 21. Effect of ZDHHC22 Knockout on palmitoylation of influenza virus HA and M2 proteins. Wild type and DHHC-22 Knockout A549 cells were infected with Both WSN-H1N1 (**A**) and FPV-I-H7N1 (**B**) influenza virus strains. Equal amounts of total protein lysates were subjected to acyl-RAC analysis. 5% of input protein, 100% of +NH₂OH treated and untreated acyl-RAC bound protein were run in SDS-PAGE and analyzed by Western blotting, first with an anti-WSN-HA antibody and subsequently with anti-M2 and anti-flotillin-2 antibodies. The immunoblot analysis of samples purified by acyl-RAC method show did not show any significant reduction in palmitoylation level of both influenza virus proteins (HA and M2) in KO cells compared to WT. No proteins were observed in NH₂OH untreated fractions which confirm the specificity of the acyl-RAC procedures and identity of enriched palmitoylated proteins. (**C**) Influenza as well as mock infected WT and KO cells were metabolically labelled with 17-ODYA for 6h. Viral HA was immunoprecipitated using specific antibodies and 17-ODYA fatty acid labelling and incorporation was detected by click-chemistry via copper catalyzed Tamara azide incorporation. Fluorescently labeled protein was detected by 9400 typhoon scanner.

Multiple-step growth cycles were performed to assess the virus production kinetics in wild type and KO cells. Both cell lines were infected with WSN and FPV-I influenza viruses at 0.01 multiplicity of infection (MOI), the supernatants were collected at various times and virus titers were measured by plaque assay on MDCK-II cells. The growth cycle demonstrated only a slight change in virus titers. For FPV-I, the viruses produced by KO cells was almost one log higher at 12 h after infection but yielded comparable titers at later time points (Fig.22a). However, for WSN strain, the viral growth was quite similar between WT and KO cells (Fig.22b).

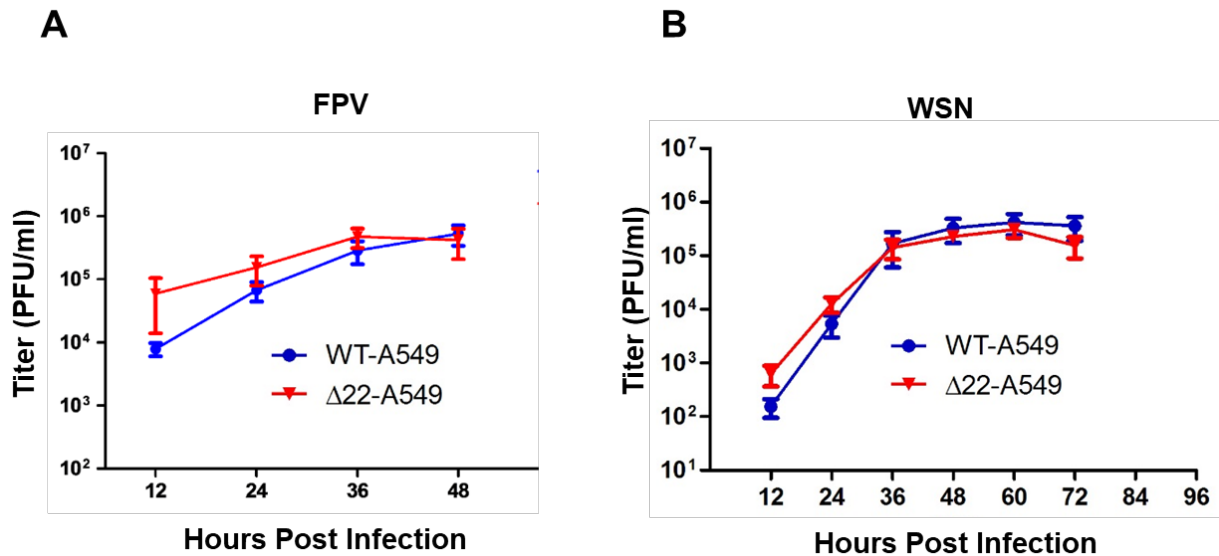


Figure 22. Multistep growth cycle of FPV-I (A) and WSN (B) influenza viruses in wild type and ZDHHC22 Knockout cells. WT and Δ ZDHHC22 A549 cells were inoculated with H7N1 and H1N1 influenza virus strains at MOI of 0.01, incubated at 37°C and supernatants of infected culture were collected at indicated time points (12h,24h,36,48h) for FPV-I (A) or until 72h post infection of WSN (B). The virus titer was determined by plaque assay on MDCKII cells. The data represents the mean including standard error from 3 independent experiments.

4.2.2. MALDI-TOF mass spectrometric analysis of virus particles produced by ZDHHC22 KO cells

Since Acyl-RAC and click chemistry assays only analyze the intracellularly expressed viral proteins, but give no information about fatty acids attached to HA in virus particles we used MALDI-TOF mass spectrometry to quantitatively analyze acylation pattern of virus particles (FPV-I and WSN) produced by WT and ZDHHC22 knockout cell line. The analysis was done by Larisa Kordjukova from the Lomonosow university in Moscow as described before [88]. Virus particles were purified from supernatants of infected WT and KO cells by ultracentrifugation. Pelleted virus particles were separated by non-reducing SDS-PAGE, and electro blotted onto PVDF membranes and visualized by Ponceau S staining. The band corresponding to viral HA was cut from the membrane, fragmented into small pieces with trypsin, and the resulting peptides were eluted and analyzed by MALDI-TOF MS. Two preparations and MS-analysis were performed for each virus, but in each experiment, HA was stoichiometrically acylated. The only difference was an increased stearate content of HA of the WSN virus, that is 18.6% if WSN was grown in WT cells, but 24,4% if produced by Δ ZDHHC22 cells (Fig.23d, e). We also analyzed HA of FPV-I virus particles, but the stearate content remains unchanged between WT (36.9%) and KO cells (40.4%) (Fig.23 a-b)

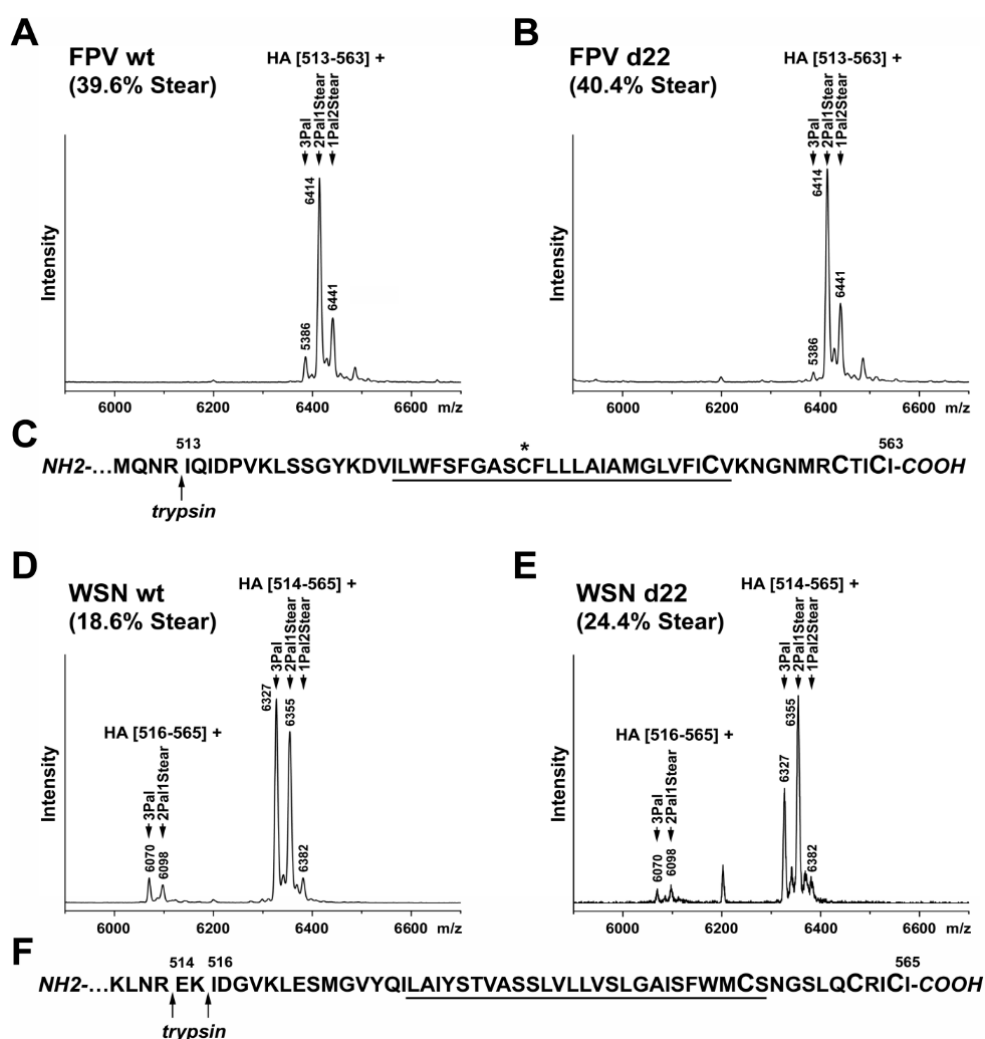


Figure 23. MALDI-TOF MS analysis of hemagglutinin from WSN (A-C) and FPV-I (D-F) viruses grown in wild type or Δ ZDHHC2 A549 cells. A, B, D, E: The results of MALDI-TOF MS analysis of HA bands electro-blotted onto the PVDF membranes are represented. The virus preparations were incubated with 30 mM Iodoacetamide (1 h in dark) before loading onto the gel. Mass spectra obtained in linear mode are depicted. Indicated are the m/z values of the peaks, the first and last amino acid residue of the corresponding peptides and the number and type of HA-bound fatty acid. The stearate amount calculated for the FPV-I HA [513-563] and WSN HA [514-565] peptides are indicated for each virus strain (two preparation and MS-analysis repeats). The mono-carbamidomethylated (CM) FPV HA [513-563] peptide was detected on the mass spectra of both wild type (wt) and ZDHHC2 (d22) preparations (mass shift at 71 units) meaning that the cysteine residue located in the middle of TM region is modified after the reaction with Iodoacetamide. No carbamidomethylated peptides were detected in case of WSN HA peptides possessing no free cysteine in the TM region. The non- and underacylated peptides are not detected after the reaction with Iodoacetamide: neither FPV-I HA [513-563] + 2 Pal (1Pal+1Stear) + 2 CM, m/z 6205 (6233); FPV-I HA [513-563] + 1 Pal (1Stear) + 3 CM, m/z 6024 (6052); FPV-I HA [513-563] + 4 CM, m/z 5843; nor WSN HA [514-565] + 2 Pal (1Pal + 1 Stear) + 1 CM, m/z 6146 (6174); WSN HA [514-565] + 1 Pal (1 Stear) + 2 CM, m/z 5965 (5993). C, F: Amino acid sequences of the C-terminal regions of FPV HA (C) and WSN HA (F) are represented indicating the prevailing sites of cleavage by trypsin. Cysteines as potential acylation sites are enlarged and the TMR is underlined. The non-acylated cysteine residue located in the middle of the FPV-I HA TM region (C) binding the carbamidomethyl-group (m/z equal to 71) after the reaction with Iodoacetamide is marked with an asterisk.

4.2.3. Identification ZDHHC22 acyltransferase potential substrates by LC-MS/MS

Since knockout of ZDHHC22 produced no significant effect on the acylation pattern of both intracellular and virus incorporated hemagglutinin, we hypothesized that ZDHHC22 might be upregulated to modify cellular factors during virus replication cycle. We used Acyl-RAC coupled quantitative mass spectrometry proteomics to identify novel substrates of ZDHHC22 palmitoyl-transferase, which was performed by Eliot Morrison in the group of Prof. Christian Freund (Institute of Biochemistry of the Free University Berlin). Whole lysates of wild type and ZDHHC 22 KO A549 cells were subjected to the acyl-RAC procedure and separated by SDS-PAGE. Separated proteins were subjected to in-gel trypsin proteolysis in the presence of H₂¹⁸O (“heavy” water) and H₂¹⁶O (“light” water) for NH₂OH treated and untreated samples, respectively, and the resulting peptides were eluted and analyzed by (LC-MS/MS) mass spectrometry. For quantification, only unique peptides identified for each protein were included in the analysis, and proteins with fewer than two peptide heavy/light (H/L) ratios were filtered out. Filtered datasets of quantified protein ratios from all four replicates were then normalized by dividing all ratios by the median H/L ratio of each dataset and then combined. MS analysis identified 24 high confidence (identified from two biological replicates) and 36 medium confidence (identified from a single MS measurement) possible substrates of ZDHHC22 (Tables 4-5).

Accession No.	Protein ID	Protein Name
O43776	SYNC	Asparagine-tRNA ligase cytoplasmic
Q96LD4	TRI47	E3 ubiquitin-protein ligase TRIM47
Q9Y6R7	FCGBP	IgGFc-binding protein
Q99959-2	PKP2	Isoform 1 of Plakophilin-2
Q9UNQ0-2	ABCG2	Isoform 2 of ATP-binding cassette sub-family G member 2
Q9H8M5-2	CNNM2	Isoform 2 of Metal transporter CNNM2
P10586-2	PTPRF	Isoform 2 of Receptor-type tyrosine-protein phosphatase F
P84103-2	SRSF3	Isoform 2 of Serine/arginine-rich splicing factor 3
Q15637-2	SF01	Isoform 2 of Splicing factor 1
Q13409-2	DC112	Isoform 2B of Cytoplasmic dynein 1 intermediate chain 2
Q8IWS0-3	PHF6	Isoform 3 of PHD finger protein 6
P49023-2	PAXI	Isoform Alpha of Paxillin
P30419-2	NMT1	Isoform Short of Glycylpeptide N-tetradecanoyltransferase 1
Q07157-2	ZO1	Isoform Short of Tight junction protein ZO-1
P03905	NU4M	NADH-ubiquinone oxidoreductase chain 4
Q8IUH4	ZDH13	Palmitoyltransferase ZDHHC13
O14936	CSK	Peripheral plasma membrane protein CASK
O94992	HEX11	Protein HEXIM1
Q96I34	PP16A	Protein phosphatase 1 regulatory subunit 16A
Q9H2M9	RBGP	Rab3 GTPase-activating protein non-catalytic subunit
P11233	RALA	Ras-related protein Ral-A
Q8IWU2	LMTK2	Serine/threonine-protein kinase LMTK2
P21579	SYT1	Synaptotagmin-1
Q8TD43	TRPM4	Transient receptor potential cation channel subfamily M member 4

Table 4. Possible ZDHHC22 palmitoyltransferase substrates identified from two biological replicates.

RESULTS

Accession No.	Protein ID	Protein Name
Q9Y679	AUP1	Ancient ubiquitous protein 1
P27824	CALX	Calnexin
Q6PJW8	CNST	Consortin
O94923	GLCE	D-glucuronyl C5-epimerase
P33993	MCM7	DNA replication licensing factor MCM7
Q96EP0	RNF31	E3 ubiquitin-protein ligase RNF31
Q9UNN8	EPCR	Endothelial protein C receptor
Q9H9S5	FKRP	Fukutin-related protein
P36915	GNL1	Guanine nucleotide-binding protein-like 1
P18084	ITB5	Integrin beta 5
Q9NP58	ABCB6	Isoform 2 of ATP-binding cassette sub-family B member 6 mitochondrial
Q9UHN6	CEIP2	Isoform 2 of Cell surface hyaluronidase
Q86TI2	DPP9	Isoform 2 of Dipeptidyl peptidase 9
Q14697	GANAB	Isoform 2 of Neutral alpha-glucosidase AB
P46087	NOP2	Isoform 2 of Probable 28S rRNA (cytosine (4447)-C (5))-methyltransferase
Q8N128	F177A	Isoform 2 of Protein FAM177A1
Q9HC56	PCDH9	Isoform 2 of Protocadherin-9
P23470	PTPRG	Isoform 2 of Receptor-type tyrosine-protein phosphatase gamma
P60880	SNP25	Isoform 2 of Synaptosomal-associated protein 25
P14209	CD99	Isoform 3 of CD99 antigen
Q969P0	IGSF8	Isoform 3 of Immunoglobulin superfamily member 8
P40189	IL6RB	Isoform 3 of Interleukin-6 receptor subunit beta
Q969N2	PIGT	Isoform 4 of GPI transamidase component PIG-T
Q86X29	LSR	Isoform 4 of Lipolysis-stimulated lipoprotein receptor
Q96GZ6	S41A3	Isoform 5 of Solute carrier family 41 member 3
Q9HCJ0	TNR6	Isoform 6 of Tumor necrosis factor receptor superfamily member 6
Q9Y446	PKP3	Isoform PKP3b of Plakophilin-3
Q9BWU0	NADAP	Kanadaptin
Q9UIQ6	LCAP	Leucyl-cystinyl aminopeptidase
Q93052	LPP	Lipoma-preferred partner
Q99547	MPP6	MAGUK p55 subfamily member 6
Q10471	GALT2	Polypeptide N-acetylgalactosaminyltransferase 2
Q13464	ROCK1	Rho-associated protein kinase 1
O00161	SNP23	Synaptosomal-associated protein 23
P42685	FRK	Tyrosine-protein kinase FRK

Table 5. Possible ZDHHC22 palmitoyltransferase substrates identified from a single MS measurement.

4.3. siRNA screening for ZDHHC modifying influenza virus HA protein

To narrow down the number of palmitoyl transferases that are involved in acylation of HA from Influenza A virus, I performed a broad siRNA screen in Hela cells. These cells do not produce infectious virus particles [202], but can be transfected with high efficiency. Hela cells were transfected with a commercial siRNA library against individual human ZDHHCs. This was done during my research stay at the global health institute - EPFL, Lausanne using a previously tested siRNA library that reduces synthesis of individual ZDHHC by ~70% to 90% [185]. This approach is well described and commonly used to identify ZDHHCs involved in acylation of substrates [203]. 48 hours after siRNA transfection, knockdown cells were re-transfected with a plasmid encoding a H7 subtype HA. Cells were lysed and a 5% aliquot was used to compare the expression levels of HA in cells transfected with the different siRNAs using western blotting. The remaining protein sample was equally split and subjected to acyl-RAC to determine whether acylation of HA is affected in any of the siRNA transfected cells. All samples were then subjected to western blotting with an antiserum against the HA2 subunit of H7 subtype HA. Blocking expression of ZDHHC2 and 8 completely inhibited acylation of HA but not acylation of the endogenous cellular protein caveolin-1 (Fig.24). siRNAs against the other ZDHHCs had less pronounced effects. Acylation of HA remained unchanged when using siRNAs against some ZDHHCs, e.g. ZDHHC1, 3, 4; other siRNAs slightly reduced (ZDHHCs12, 14, 19) or enhanced levels of HA's acylation (ZDHHCs7, 9, 17).

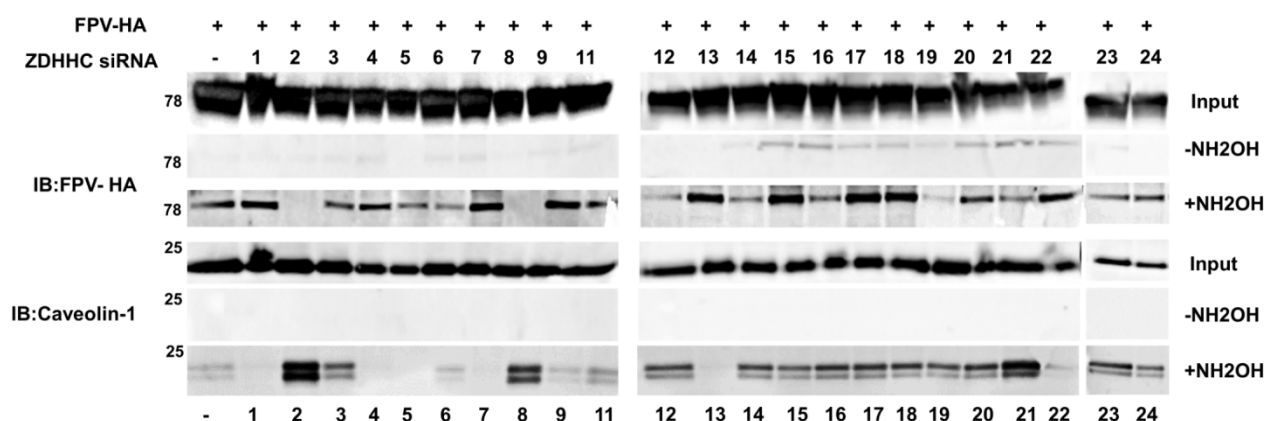


Figure 24. siRNAs against ZDHHC2 and 8 block acylation of HA in transfected Hela cells. Hela cells were transfected with siRNAs against all human ZDHHCs and 48 hours later transfected with a plasmid encoding H7 subtype HA from a variant of FPV. After 24 hours, cells were lysed and subjected to acyl-RAC and western blotting (IB). First with antiserum against the HA2 subunit (upper panel), then the membrane was again blotted with antibody against caveolin-1 as cellular control (lower panel). NH₂OH: samples treated (+) or not treated (-) with hydroxylamine to cleave thioester-bound fatty acids. Input: Western blot of 5% of the lysate to check expression levels of HA. 78 and 25 indicates the mobility of the molecular weight marker. The blots on the left were exposed for the same time as the blots in the middle and on the right. The experiment was performed during my visit of the lab of Prof. Gisou van der Goot at the Global health institute, EPFL, Switzerland.

RESULTS

Since the siRNA screen exhibits some technical flaws, such as reduced acylation of HA in the presence of siRNAs against ZDHHC19, although expression of the protein was not detected by qPCR, we aimed to confirm the main findings by metabolic labelling of transfected cells with [³H]-palmitate followed by immunoprecipitation of HA and fluorography. Blotting an aliquot of immune-precipitated HA ensures that similar amounts of the protein are compared in the fluorogram. We used the same siRNAs against ZDHHC2 and 8, but also against ZDHHC15 and 20. Although the latter had no significant effect on acylation of HA in the first screen, they are phylogenetically closely related to ZDHHC2 (Fig. 25a) and therefore might acylate the same substrates. A scrambled siRNA and a siRNA against ZDHHC1, which had no effect in the siRNA screen, were used as negative controls. Results shown in Fig.25b revealed that [³H]-palmitate labelling of HA is strongly inhibited by siRNAs against ZDHHC2, 15 and 20 and clearly reduced by siRNAs against ZDHHC8. The differing result for ZDHHC15 and 20 between the Acyl-RAC and the [³H]-palmitate assays might be due to the fact that different populations of HA molecules are detected. Acyl-RAC determines all HA molecules synthesized after transfection, i.e. in a time period of 24 hours. In contrast, [³H]-palmitate detects only HA molecules synthesized in a time span of two hours and 24 hours after transfection. Thus, one might speculate that ZDHHC15 and 20 preferentially acylate HA molecules synthesized late after transfection, for example because their activity might be upregulated or because the capacity of ZDHHC2 and 8 might be saturated at late time points.

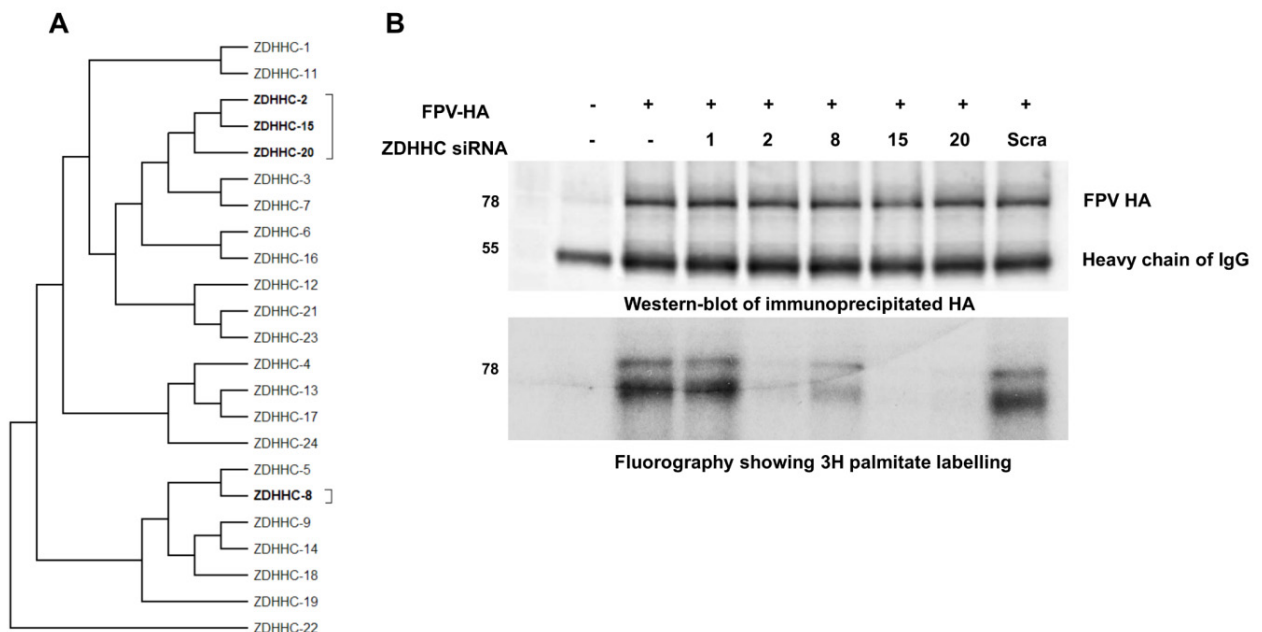


Figure 25. SiRNAs against ZDHHC2, 8, 15 and 20 block acylation of HA as demonstrated by [³H]-palmitate labelling. (A) Phylogenetic tree of human ZDHHCs showing that ZDHHC2, 15 and 20 belong to the same group. **(B)** [³H]-palmitate labelling: HeLa cells were transfected with siRNAs (same sequence and at the same concentration as in Fig.24) against ZDHHC1, 2, 8, 15, with a scrambled siRNA (scra) or remain un-transfected (-) and 48h later with a

plasmid encoding HA from H7 subtype from FPV-I. After 24 hours, cells were labeled for 2 hours with [³H]-palmitate, lysed and subjected to immunoprecipitation with antiserum against the HA2 subunit (lower panel). An aliquot of the sample was subjected to western blotting with the same antibody (upper panel). The lower band in the upper panel is the heavy chain of the antibodies used for immuno-precipitation. This experiment was done by Laurence Abrami, Global health institute, EPFL, Switzerland

4.4. Validation of ZDHHC proteins knockout in HAP1 cells

I next used commercial HAP1 cells, where ZDHHCs2, 8, 15 and 20 were knocked out using the CRISPR/Cas9 technology. HAP1 cells are a human cell line derived from the chronic myelogenous leukemia cell line KBM-7, which have a single copy of almost every chromosome and are therefore ideally suited for the knockout technology. I compared the mRNA levels of individual ZDHHC between the KO and wild type HAP1 cells. Whereas expression of the corresponding mRNAs is decreased in Δ ZDHHC2 to 50% and in Δ ZDHHC20 to 20%. Δ ZDHHC8 and Δ ZDHHC15 cells synthesize slightly more of the relevant mRNAs (Fig.26). Since the Δ ZDHHC HAP1 cells were generated using single guide RNA intended to cause only small deletions or insertions, it is not unexpected that mRNAs are still transcribed.

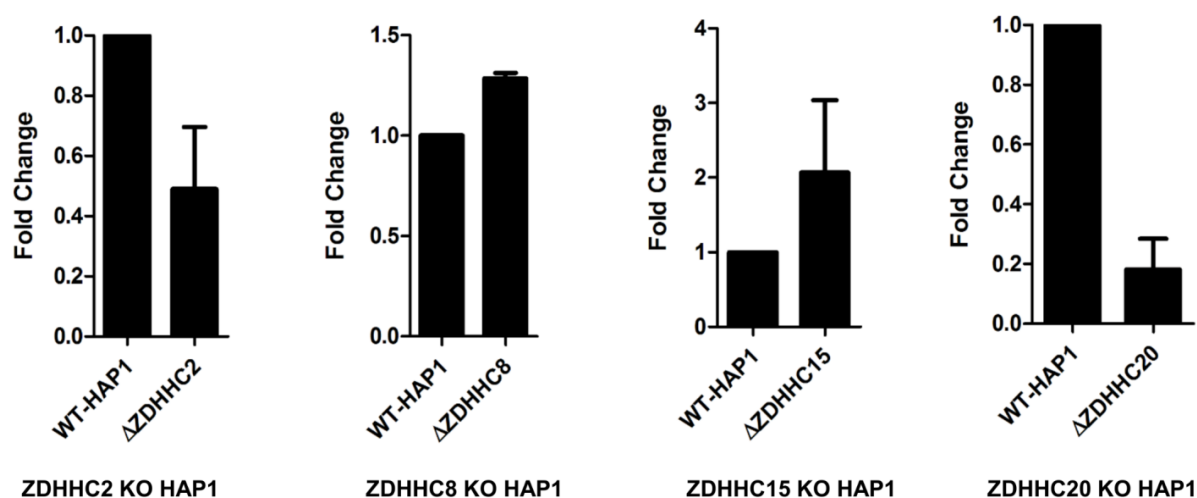


Figure 26. Expression of relevant ZDHHCs in CRISPR/Cas9 knockout relative to wild type HAP1 cells. Graphs showing relative expression level of indicated ZDHHCs determined with qPCR for the specific ZDHHC transcripts, normalized to GAPDH housekeeping gene. Data are the average of two independent experiments.

Therefore, I analyzed by sequencing of chromosomal PCR products whether the ZDHHCs contain frame-shift mutations within their coding exon. All sequencing chromatograms (Fig.27) clearly show a difference in the nucleotide sequences within the Cas9 binding site between wild type and ZDHHC knockout cells. Since the nucleotide differences are all located either before or within the CRD-DHHC domain it is unlikely that the knockout cells are still able to synthesize a functional ZDHHC protein, even if the mRNAs are translated

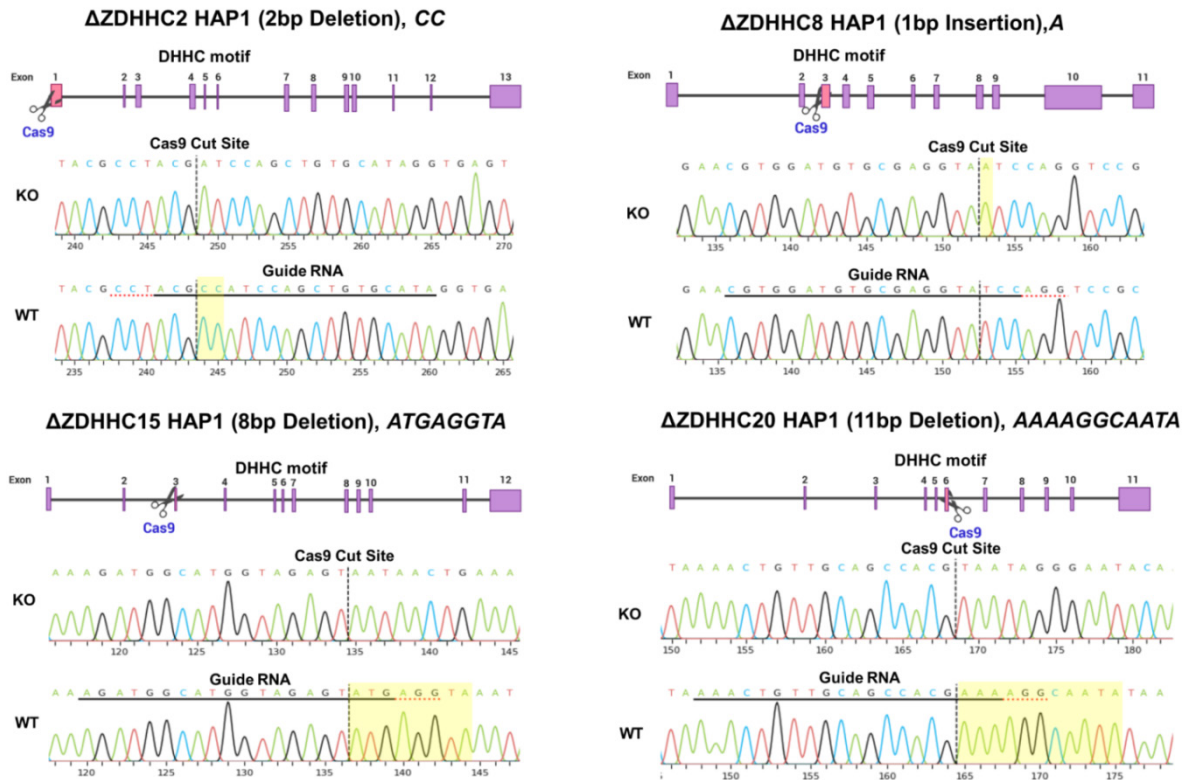


Figure 27. Genotyping of CRISPR/Cas9 induced mutations in ZDHHCs knockout HAP1 cells by PCR and Sanger sequencing. The upper part of each figure shows a scheme of the respective ZDHHC gene. Exons are numbered and marked as purple boxes, the exon which is the target of the guide RNA and hence cleaved by Cas9 is colored pink. The location of the DHHC motif in each ZDHHC gene is also indicated. It is located in exon 6 of ZDHHC2, ZDHHC15 and ZDHHC20 and in exon 4 of ZDHHC8. The lower parts of each figure show two sequencing chromatograms of knockout (KO) and wild type (WT) HAP1 cells. The binding site of the guide RNA is underlined in the sequence. The Cas9 cutting site is indicated by a vertical dotted line. The resulting differences between the WT and KO sequences are highlighted in yellow. The deleted or inserted nucleotides are indicated in the heading of each figure. All induced mutations generate a frameshift in the coding sequence. Parts (330 – 450 bp) of the ZDHHCs gene encompassing the guide RNA binding site were amplified from the genomic DNA by PCR using the primers listed in section 3.1.2.3.

4.4.1. Knockout of ZDHHC2, 8, 15 or 20 in HAP1 cells reduces acylation of HA of influenza A virus

HAP1 cells can be infected with Influenza virus and synthesize HA, which is transported to the plasma membrane as demonstrated by binding of erythrocytes to infected cells. However, HAP1 cells do not release virus particles as analysed by hemagglutination and plaque assays. Acyl-RAC performed on cells infected with the virus that expresses the HA used in the initial siRNA screen (A/chicken/Rostock/8/1934 (H7N1)) confirmed the results. Acylation of HA is strongly inhibited in Δ ZDHHC2, Δ ZDHHC15 and Δ ZDHHC20 and reduced in Δ ZDHHC8 knockout cells, whereas very little (if any) effect was observed in Δ ZDHHC1 cells, which were

used as control (Fig.28a-b). Quantifying relative acylation of HA (band densities of the acylation signal relative to total expression) from this and two identical experiments revealed that acylation is reduced by ~75% in Δ ZDHHC15 and Δ ZDHHC20 and to ~65% in Δ ZDHHC2 cells. Δ ZDHHC8 cells show the tendency to less efficiently acylate HA, but the mean (80%) was not statistically significant different from wild type cells (Fig.28c). Note also that the SDS-PAGE mobilities of HAs synthesized in the various ZDHHC knockout cells is similar to that in wild-type cells indicating that the abolishment of ZDHHC expression has no general effect on vesicular transport of proteins along the exocytic pathway, which would manifest itself as multiple, mainly smaller HA bands due to inhibition or retardation of terminal glycosylation steps. This excludes the possibility that the reduction in acylation of HA is due to its impaired transport to the intracellular site of palmitoylation [204].

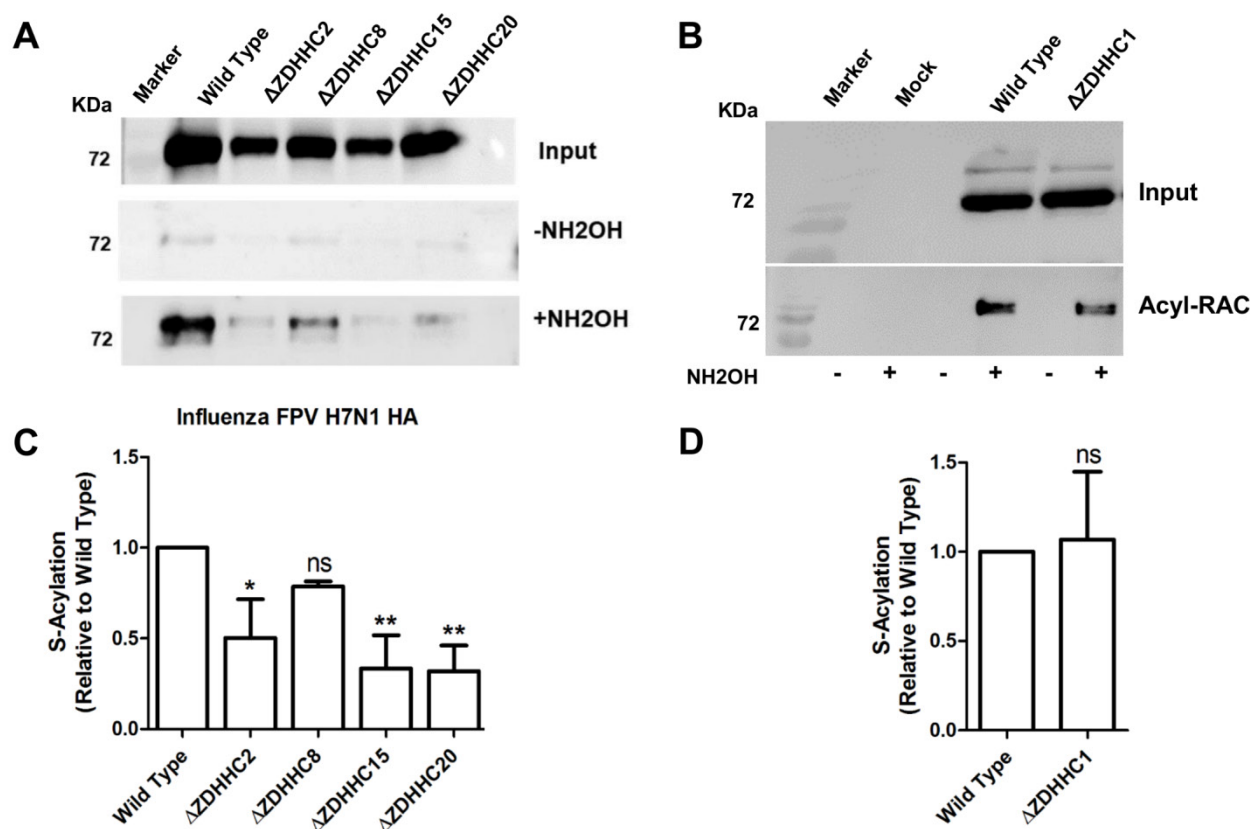


Figure 28. HAP1 cells deficient in ZDHHC2, 8, 15 and 20 show compromised acylation of HA. (A+B) HAP1 cells where the indicated ZDHHCs were knocked-out using the CRISPR/Cas9 technology were infected with FPV-I (Low pathogenic variant of FPV) at MOI of 1. 24 hours later, acylation of HA was analyzed using Acyl-RAC. (C+D) Quantification of the result from this and two other identical experiments. The optical density of the +NH₂OH bands was divided by the density of bands from the input and normalized to wild type (=1). The mean \pm standard deviation is shown. The asterisks indicate statistically significant differences (*P < 0.05, **P < 0.01) between WT and the deficient cells. One-way ANOVA followed by Tukey's multiple comparison test was applied for statistical analysis. ns: non-significant.

4.4.2. HAs of both phylogenetic groups and the viral proton channel M2 are acylated by a similar set of ZDHHC proteins

HA proteins from the various Influenza strains are divided into two phylogenetic groups; the H7 subtype HA from an avian virus we investigated so far belongs to group 2. For a group 1 HA a 3D-structure of most parts of the transmembrane region was resolved by Cryo-EM [205]. However, critical amino acids are not conserved in group 2 HAs suggesting that group 1 and 2 HAs might exhibit different structures. I therefore asked whether they are acylated by the same set of ZDHHC proteins. I infected the Δ ZDHHC HAP1 cells with WSN virus (AWSN/33, H1N1), which was originally isolated from a human patient and performed Acyl-RAC experiments. Quantification of the results from three virus infections revealed that knockout of ZDHHC15 and 20 had the strongest effect (80% reduction) on acylation of HA. Abolishment of the ZDHHC8 protein also led to a significant reduction in HA's acylation to 30%. Δ ZDHHC2 cells showed the tendency to less efficiently acylate HA, but since there were large variation between experiments the mean (50%) was not statistically significant different from wild type cells (Fig.29). Δ ZDHHC1 cells had very little (if any) effect on acylation of the group 1 HA.

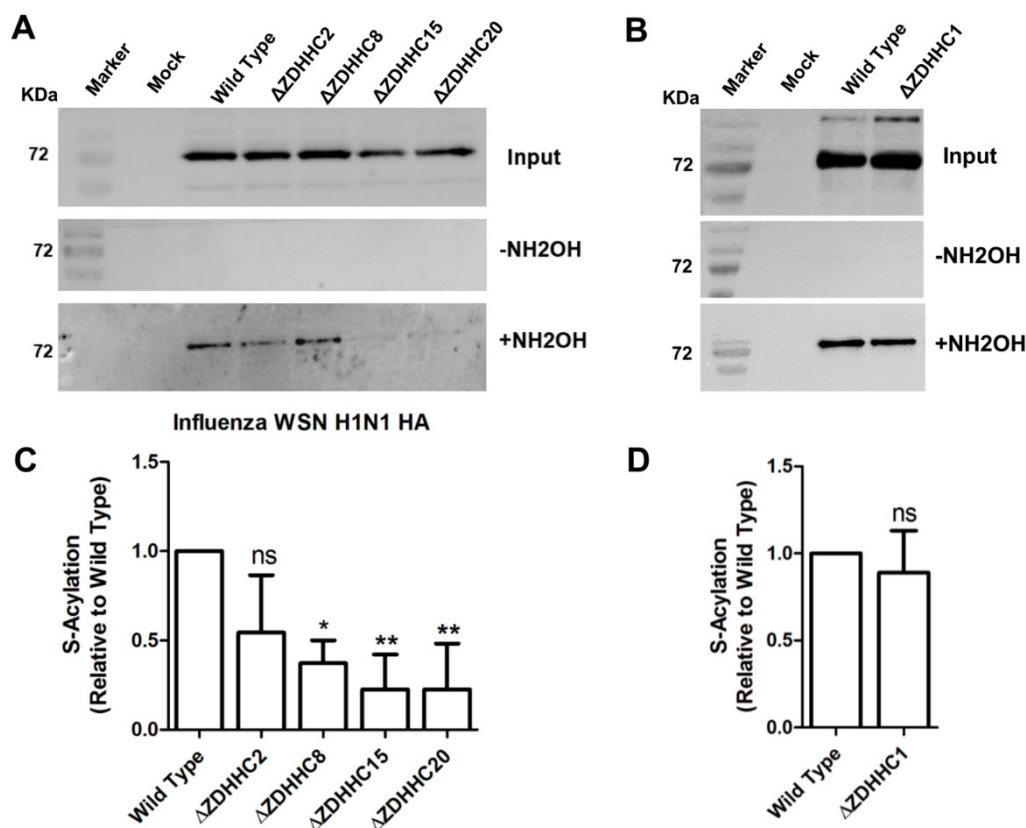


Figure 29. HAP1 cells deficient in ZDHHC2, 8, 15 and 20 show compromised acylation of a group 1 HA. (A+B) HAP1 cells where the indicated ZDHHCs were knocked-out using the CRISPR/Cas9 technology were infected with the WSN virus, which contains a group 1 HA, at MOI of 1. 24 hours later, acylation of HA was analyzed using Acyl-RAC. **(C+D)** Quantification of the result from this and two other identical experiments. Density of the +NH₂OH bands was divided by density of

bands from the input and normalized to wild type (=1)). The mean \pm standard deviation is shown. The asterisks indicate statistically significant differences (* $P < 0.05$, ** $P < 0.01$) between WT and the deficient cells according. One-way ANOVA followed by Tukey's multiple comparison test was applied for statistical analysis. ns: no significant.

Next, we asked whether M2, the second palmitoylated protein of Influenza virus is also acylated by the same set of ZDHHC proteins. This is of interest since a NMR structure of the transmembrane proton channel including the adjacent palmitoylation site is available that might allow drawing conclusions about putative ZDHHC recognition features [206]. Acyl-RAC on HAP1 cells infected with the WSN virus revealed that acylation of M2 was affected in each ZDHHC knockout cells, but to a different extent compared to acylation of HA (Fig.30). M2's acylation is affected the most in Δ ZDHHC15 cells, less prominently in Δ ZDHHC8 and Δ ZDHHC20 cells and the least in Δ ZDHHC2 knockout cells. The reduction in acylation of M2 was statistically significant for each Δ ZDHHC knockout cell. Again, Δ ZDHHC1 cells had no effect on acylation of M2.

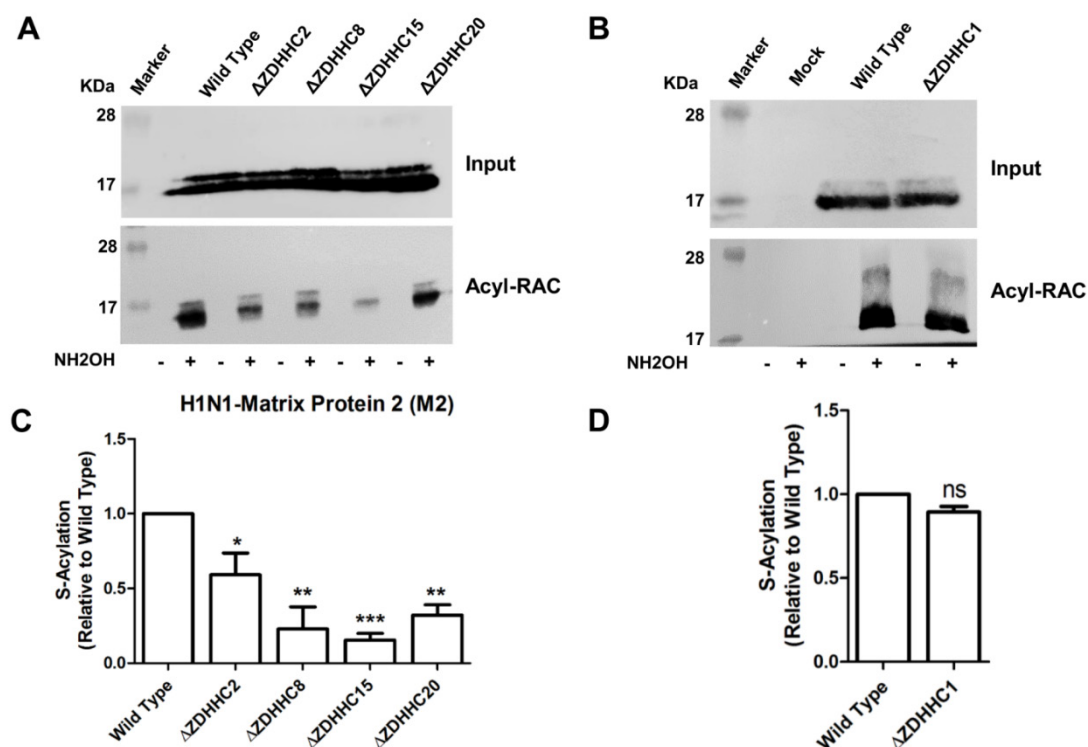


Figure 30. HAP1 cells deficient in ZDHHC2, 8, 15 and 20 show compromised acylation of M2. (A+B) HAP1 cells where the indicated ZDHHCs were knocked-out using the CRISPR/Cas9 technology were infected with the WSN virus. 24 hours later, acylation of M2 was analyzed using Acyl-RAC and an antibody against M2. (C+D) Quantification of the result from this and another identical experiment. Density of the +NH₂OH bands was divided by density of bands from the input (M2 expression) and normalized to wild type (=1). The mean \pm standard deviation is shown. The asterisks indicate statistically significant differences (* $P < 0.05$, ** $P < 0.01$, *** $P < 0.001$) between WT and the deficient cells. One-way ANOVA followed by Tukey's multiple comparison test was applied for statistical analysis.

In summary, the acylated proteins of Influenza A virus are modified by the same set of ZDHHC proteins, but some variation in the relevance of each ZDHHC for acylation of group 1 and 2 HAs and M2 apparently exist.

4.4.3. ZDHHC 2, 8, 15 and 20 have no effect on acylation of Flu B HA and HEF of Flu C

HA of Influenza B virus and HEF of Influenza C virus exhibit the same *overall three-dimensional* folding of their polypeptide chains and play identical roles during virus replication as HA of Flu A, but they differ in their acylation pattern. We were therefore interested whether all hemagglutinating glycoproteins of Influenza viruses are acylated by the same ZDHHC proteins. Only Δ ZDHHC15 and Δ ZDHHC20 cells infected with Influenza C virus revealed a small (but not statistically significant) reduction in acylation of HEF, whereas Δ ZDHHC2 and Δ ZDHHC8 HAP1 cells exhibit no effect (Fig.31 a-b). This result is not unexpected since none of the ZDHHCs identified so far exhibits a very high specificity for stearate and we might have missed a stearate-specific ZDHHC in our siRNA screen since it reduces total acylation of HA at most by one-third. Surprisingly, however, knockout of ZDHHC2, 8, 15 and 20 did also not reduce acylation of HA in HAP1 cells infected with Influenza B virus. The mean of three experiments showed that acylation of HA was even slightly (but not statistically significant) enhanced (Fig. 31 c-d). Thus, HA of Flu B and HEF of Flu C are apparently acylated by other, yet to be identified ZDHHC proteins than HA of Flu A. These results also clearly demonstrate that blocking the expression of ZDHHC2, 8, 15 and 20 in HAP1 cells does not cause a general reduction of acylation of transmembrane proteins that are transported along the exocytic pathway and thus the effect I observed on HA and M2 of Influenza A virus is specific.

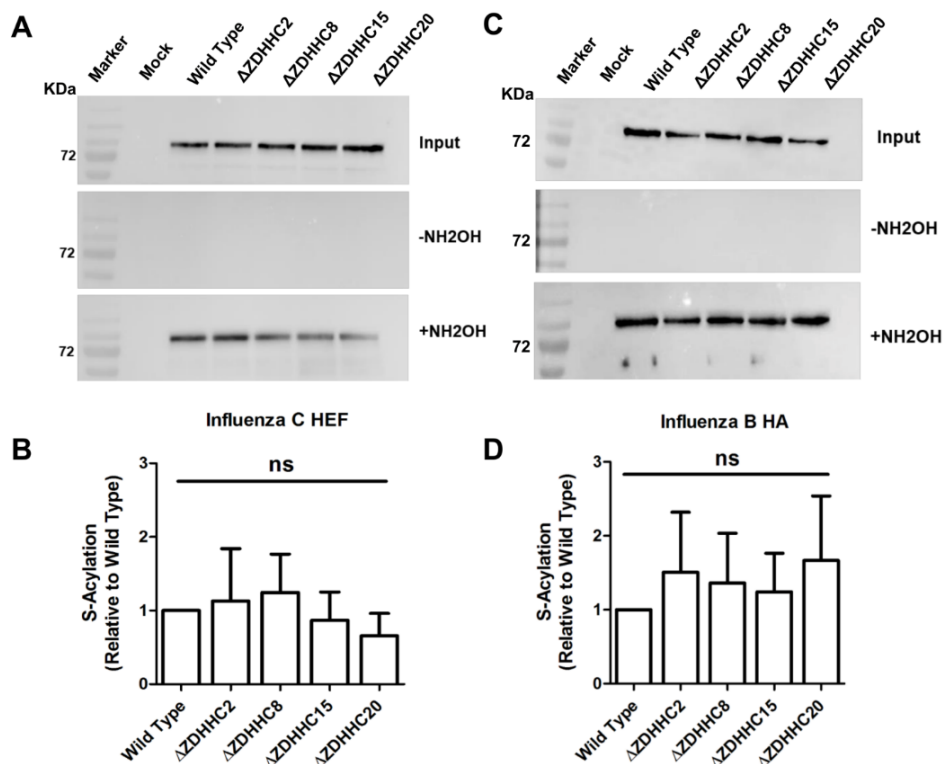


Figure 31. HAP1 cells deficient in ZDHHC2, 8, 15 and 20 exhibit no effect on acylation of HEF from Flu C and HA from Flu B. (A) HAP1 cells where the indicated ZDHHCs were knocked-out using the CRISPR/Cas9 technology were infected with Influenza C virus. 24 hours later acylation of HEF was analyzed using Acyl-RAC. **(B)** Quantification of the result from this and two other identical experiment. Density of bands in the +NH₂OH blot was divided by the density of bands from the input (=HEF expression levels) and normalized to wild type (=1). The mean \pm standard deviation is shown. One-way ANOVA followed by Tukey's multiple comparison test was applied for statistical analysis. **(C)** HAP1 cells where the indicated ZDHHCs were knocked out using the CRISPR/Cas technology were infected with Influenza B virus. 24 hours later acylation of HA was analyzed using Acyl-RAC **(D)** Quantification of the result from this and two other identical experiment revealed no significant difference.

4.5. Co-localization of ZDHHC2, 8, 15 and 20 with HA in a human lung cell line

Next, I investigated whether the intracellular localization of the identified ZDHHCs is consistent with the intracellular site of HA's acylation. Since HA pulse-labeled with ³[H]-palmitate is already trimerized, but its carbohydrates are still Endo-H sensitive it can be concluded that acylation occurs in the late-ER, in the ERGIC and/or in the cis-Golgi region [207]. ZDHHC2, 8 and 15 were previously localized in transfected HEK293T cells to the cis-Golgi, whereas ZDHHC2 also co-localizes with an ER marker [151]. In the same study, ZDHHC20 was detected at the plasma membrane, but others reported that it is also present in a perinuclear compartment [151,208]. To analyze whether HA co-localizes with the ZDHHCs, I co-transfected A549 cells with the H7 subtype HA and with either ZDHHC2, 8, 15 and 20, each fused to a C-terminal HA-tag [150]. Staining of permeabilized cells with an anti-HA-tag antibody showed an intracellular, reticular staining pattern for each ZDHHC, often more concentrated near the nucleus and exhibiting brighter spots throughout the cell (Fig. 32). Staining of HA with anti-Influenza virus serum revealed that it co-localizes with each ZDHHC protein, but only inside cells, not at the plasma membrane where HA is also abundant. In neurons ZDHHC2 cycles between the plasma membrane and endosomes [209]. However, since HA is not endocytosed in transfected cells [210], it is unlikely that the intracellular co-localization of ZDHHC2 with HA takes place in endocytic vesicles. Thus, in A549 cells ZDHHC2, 8, 15 and 20 are present in membranes of the exocytic pathway where they co-localize with HA.

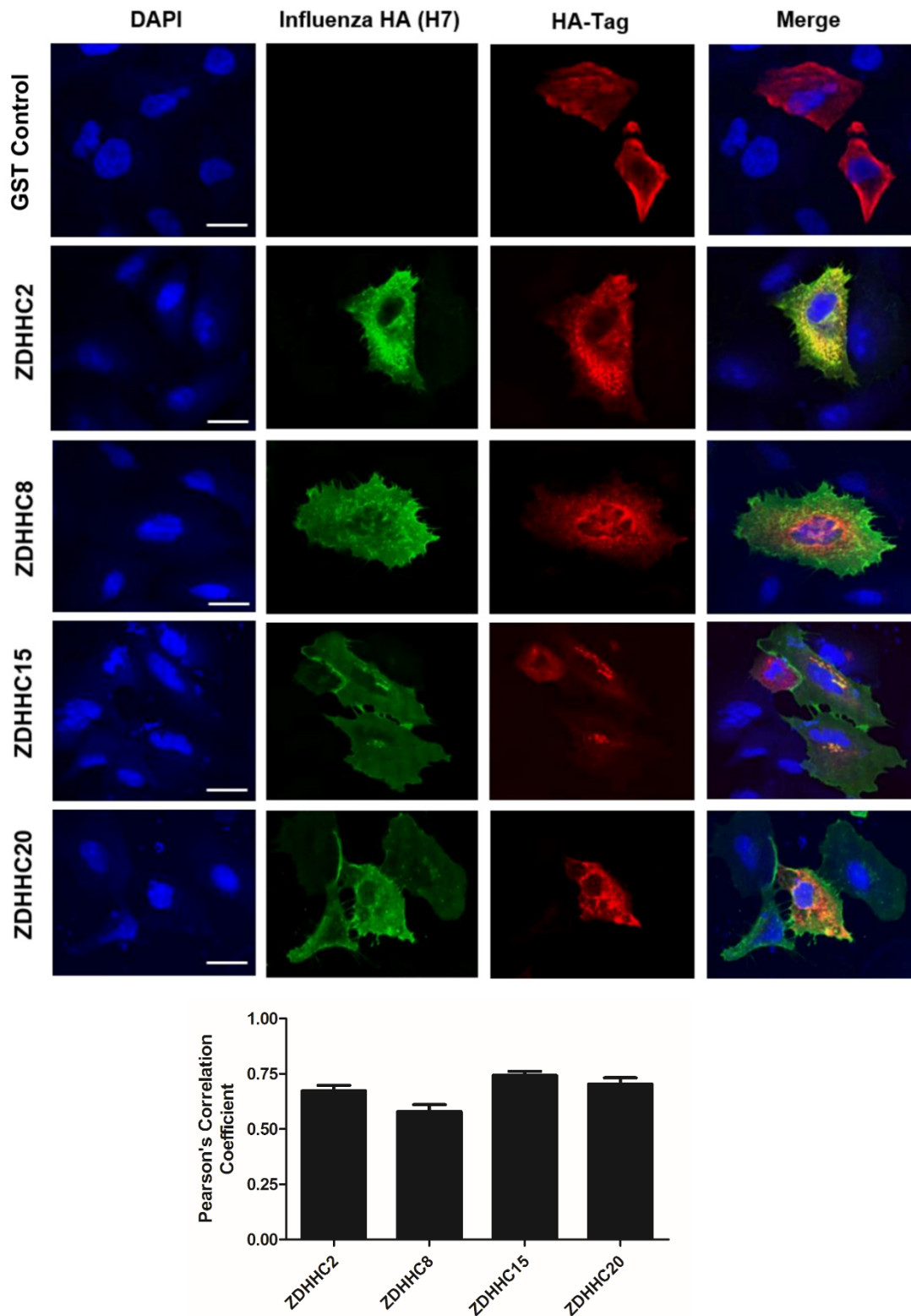
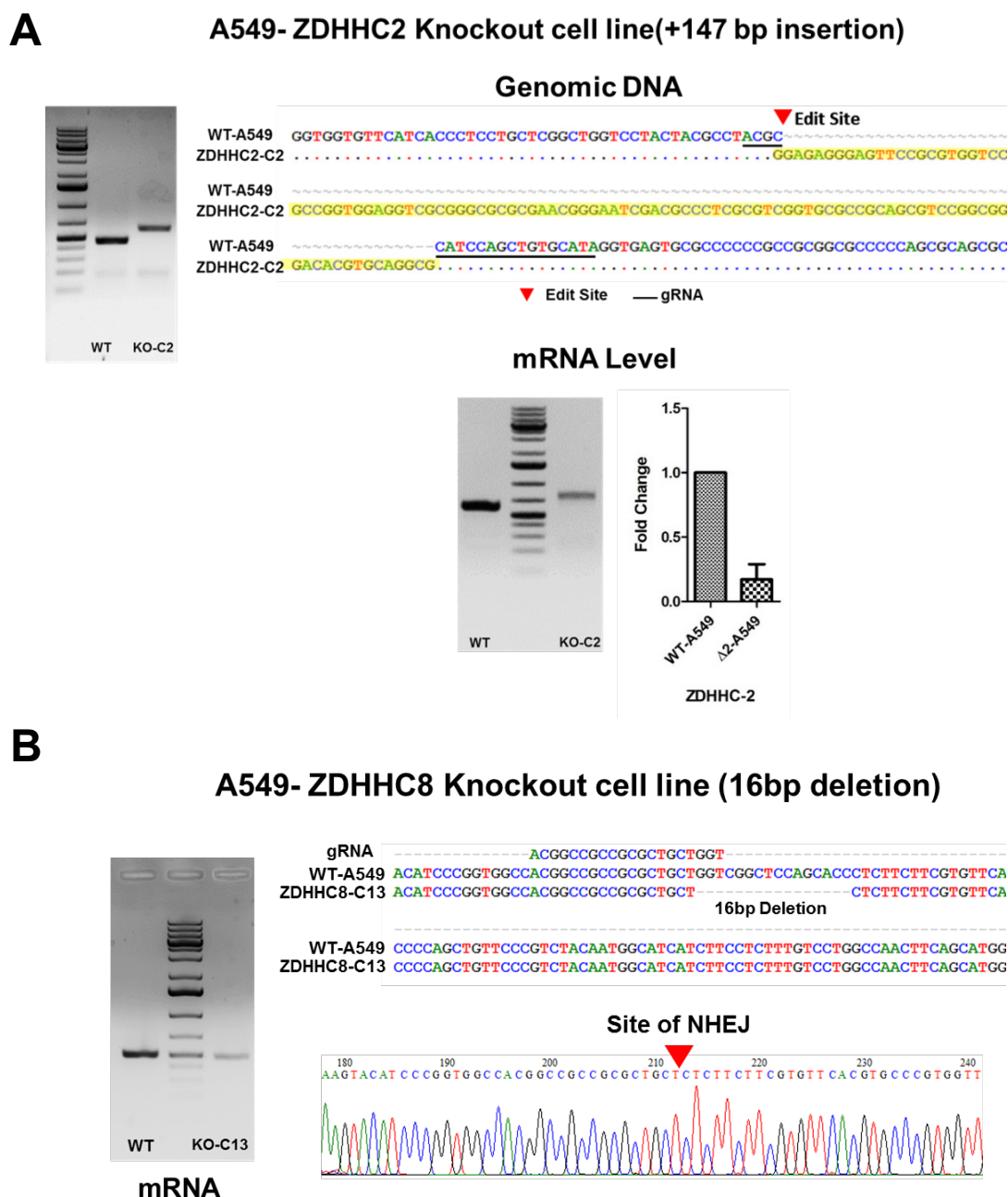


Figure 32. ZDHHCs 2, 8, 15 and 20 co-localize with HA at membranes of the exocytic pathway in human lung cells. A549 human lung cells were transfected with plasmids encoding H7 subtype HA and the indicated ZDHHCs fused to a C-terminal HA-tag. 24 hours later cells were fixed, permeabilized and stained with anti-FPV antiserum, and anti-HA-tag antibodies followed by secondary antibody coupled to Alexa-Fluor 568 (red for ZDHHCs) and Alexa Fluor 488 (green for HA), respectively. Nuclei were stained with DAPI. Scale bar =50 μ m. Cells transfected with a plasmid expressing GST and stained with both antibodies was used as a negative control. Co-localization of FPV-HA with each ZDHHC was analyzed using the JACoP plugin for ImageJ software. At least 40 cells from each condition were quantified. Error bars represent Standard deviation of the mean (SEM)

4.6. Knockout of ZDHHC 2, 8, 15 and 20 in influenza susceptible A549 cells using CRISPR/Cas9

Since HAP1 cells can be infected with Influenza virus and express HA on the cell surface, but do not produce infectious virus particles so the effect on virus replication cannot be determined in these systems. Therefore, I used CRISPR/Cas9 technology to make A549 cell lines where ZDHHC 2,8,15 and 20 were individually knocked out (KO cell lines) in order to study acylation of HA and virus replication in an influenza-susceptible human cell line. PCR of genomic DNA and sequencing of the resulting product from single cell clones revealed that both alleles of each ZDHHC gene had a frameshift mutation within their coding exon. CRISPR/Cas9 induced mutations were 147 bp insertion, a 16bp deletion, a 1bp insertion and a 5bp deletion in ZDHHC2, 8, 15, 20 genes respectively (Fig.33 A-D).



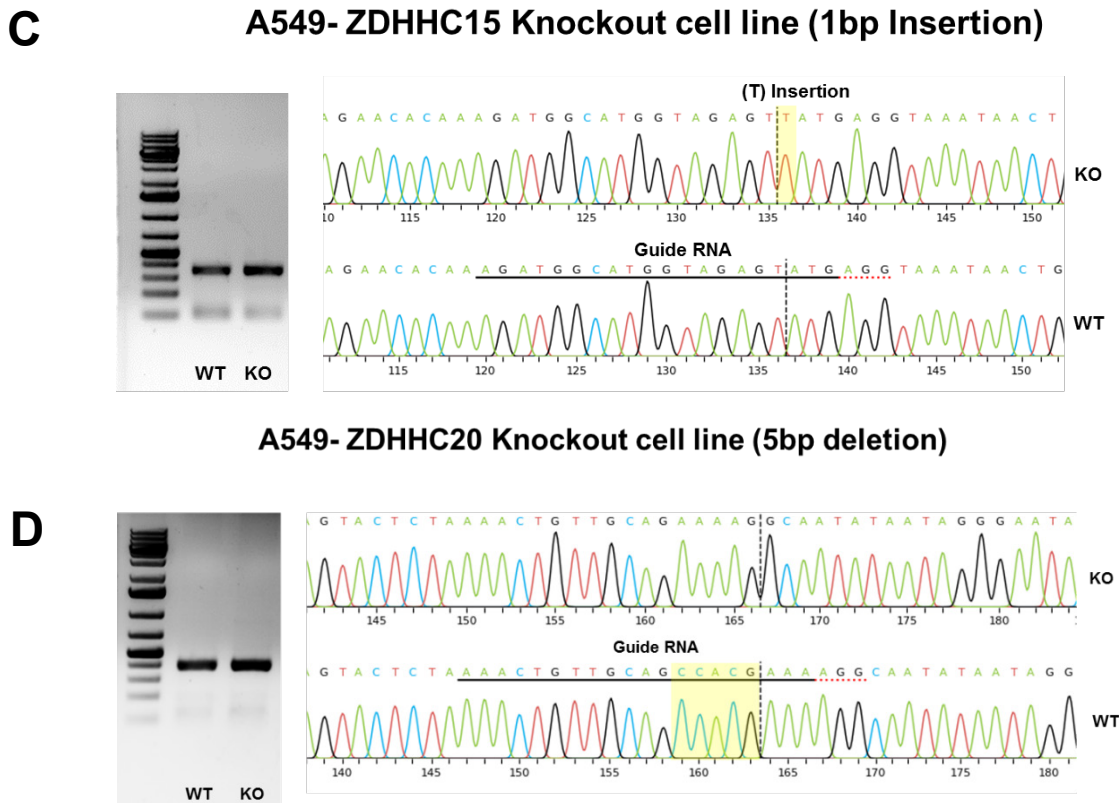


Figure 33. Validation of ZDHHC2, 8, 15 and 20 knockout in A549 cells by PCR, qPCR and Sanger sequencing. (A) PCR on both gDNA and mRNA isolated from WT and KO showing a shift in the size of ZDHHC2 in KO relative to WT. Sanger sequencing of ZDHHC2 KO cells revealed 147 bp insertion (Yellow) in the target site of gRNA. qPCR analysis of the ZDHHC2 KO cells showed ~75% reduction in ZDHHC2 transcript level. (B) PCR and Sanger sequencing analysis of ZDHHC8 gene showing bi-allelic 16bp deletion in target site of CRISPR gRNA with clean peaks at the site of NHEJ. (C-D) PCR and Sanger sequencing of ZDHHC15 and ZDHHC20 knockout cell clones. The binding site of the guide RNA is underlined in the sequence. The Cas9 cutting site is indicated by a vertical dotted line. The induced mutations are highlighted in yellow.

4.6.1. Effect of ZDHHC 2,8,15 and 20 on acylation of HA and virus replication

Acylation of viral HA in individual ZDHHCs knockout A549 cells was analyzed by Acyl-RAC assay. An equal number of WT and KO cells ($\sim 2 \times 10^6$) were infected with FPV-I influenza virus (Low pathogenic variant of FPV) at a MOI=1, cells were lysed 16-24h later, and palmitoylated proteins were enriched on thiopropyl sepharose beads and detected by immune blotting. Results showed minimal differences in acylation level between WT and single ZDHHC knockouts in A549 cells (Fig.34A). Next, I carried out multi-cycle virus growth experiments and virus titers were analyzed at different time points by plaque assay. Results showed a minimal reduction of virus titers in ZDHHC2 and ZDHHC15 knockout cell lines while ZDHHC8 and ZDHHC20 virus titer was comparable to Wild type cells (Fig.34 B-C).

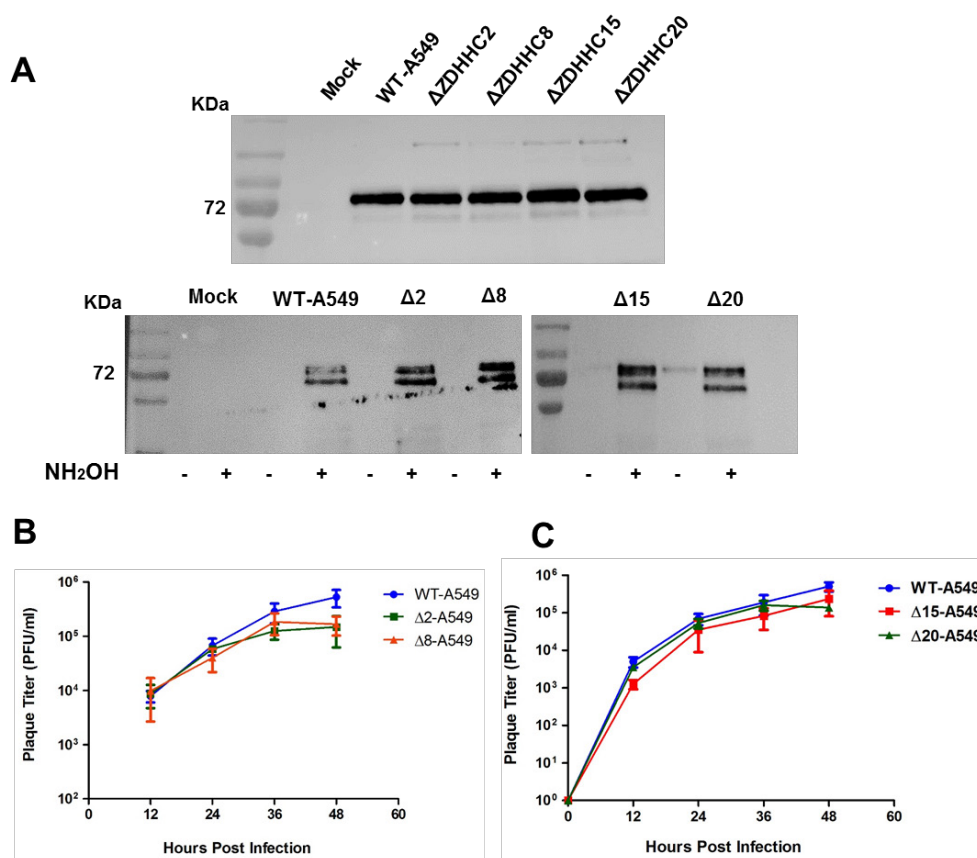


Figure 34. Effect of ZDHHC 2, 8, 15 and 20 knockout on acylation of hemagglutinin and virus growth kinetics in A549 cells. (A) WT as well as KO A549 cells were infected with low pathogenic variant of fowl plaque virus (FPV-I, H7N1 strain) at MOI=1. 24 hours later cells were lysed and palmitoylation of HA was investigated with acyl-RAC. Input: 5% of the lysate was blotted with antibodies against the H7 HA2 subunit; Lower blots were exposed for exactly the same time. (B-C) The indicated cells were infected at a moi of 0.01 with the variant of FPV, aliquots were removed from the supernatant at the indicated time points and titers were determined with a plaque assay. Results are shown as the mean of three experiments including standard deviation.

4.6.2. Generation of double ZDHHC knockout A549 cell lines (Δ 2/15 and Δ 2/20)

One explanation for the non-reduced acylation of HA would be that the virus might utilize another closely related ZDHHC if a single ZDHHC is knocked out. Therefore, I made knockouts of two ZDHHC (2+15 and 2+20) in the same cell. I tried to make a double knockout of 15+20 by starting with Δ ZDHHC15 cell line and knockout the ZDHHC20 or vice versa but no single cell clones with double mutations in both genes (15 and 20) could be isolated. I used the above described ZDHHC2 knockout cell (+147 bp insertion) made by the pRP-418 CRISPR vector (puromycin resistance) to knock-out either ZDHHC15 or ZDHHC20 using the spCas9-EGFP vector (blebbistatin resistance). PCR and Sanger sequencing of single cell clones showed bi-allelic single base pair (A) insertion leading to a frameshift in the ORF of ZDHHC15. For ZDHHC20, I was able to isolate several clones with different

RESULTS

mutations (4bp del, 5 bp del, and 5bp insertion). Single cell clone with 5bp deletion was used in all downstream experiments (Acyl-RAC and Virus replication). All CRISPR induced mutations were bi-allelic demonstrated by absence of any WT sequence in the chromatogram. (Fig.35 A, D).

Interestingly, Acyl-RAC analysis of the acylation status of HA in double knockout cells infected with the FPV-I virus (H7N1 strain) revealed that acylation of HA was significantly reduced (~90%) or even inhibited, but not acylation of the endogenous cellular protein caveolin-1 in both double ZDHHC knockout cells (Fig.34 B, E). I also analyzed growth kinetics of viruses in both double knockout cells and the results showed a reduction of virus titers by almost one log in $\Delta 2/15$ cells and by half a log in $\Delta 2/20$ cells (Fig.34 C, F).

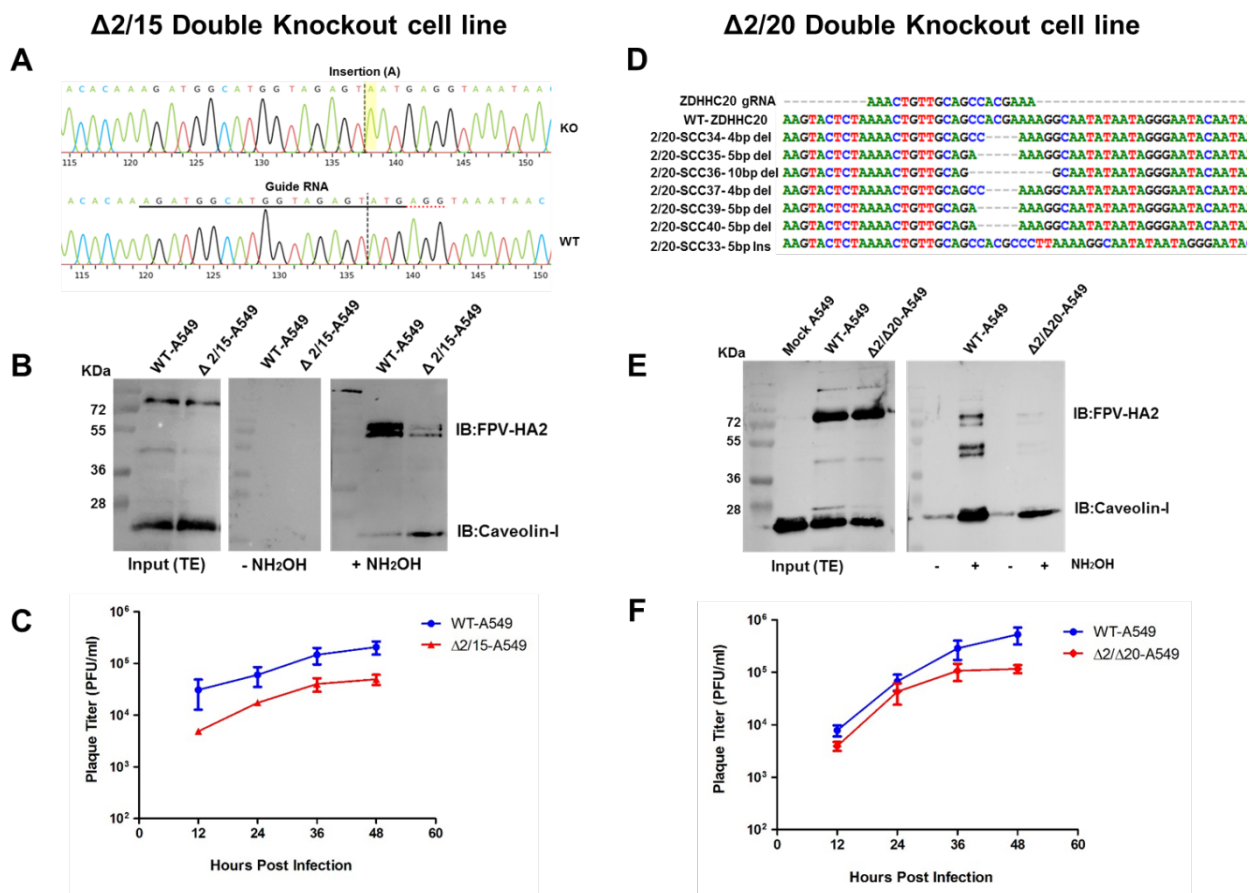


Figure 35. Generation of double knockout A549 cells and its effect on acylation of HA and virus replication. (A&D) Sanger sequencing and alignment of different single cell clones from $\Delta 2/15$ and $\Delta 2/20$ double knockout cells. **(B&E)** WT as well as double KO A549 cells were infected with low pathogenic variant of fowl plaque virus (FPV-I, H7N1 strain) at MOI=1. 24 hours later cells were lysed, and acylation of HA was analyzed with acyl-RAC assay. Input: 5% of the lysate was blotted with antibodies against the H7 HA2 subunit and Caveolin-I as a cellular control. **(C&F)** The indicated cells were infected at a MOI of 0.01 with the variant of FPV, aliquots were removed from the supernatant at the indicated time points and titers were determined with a plaque assay. Results are shown as the mean of three experiments including standard deviation.

5. Discussion

5.1. ZDHHC22 is significantly upregulated during Influenza virus infection but is not involved in acylation of viral proteins

In the first part of this study, I analyzed the expression pattern of ZDHHC palmitoyl-transferases in human cells as well as changes of their expression levels in response to human and avian influenza virus infection as an initial step to identify the ZDHHC enzyme(s) responsible for palmitoylation of influenza virus proteins. The results showed that all ZDHHCs except ZDHHC19 were expressed in uninfected human cells (Fig.17). I also observed that ZDHHC22 was upregulated early after IAV infection (5 hours post infection) (Fig.18), which led me to the hypothesis that ZDHHC22 could be one of the ZDHHCs that contribute to acylation of influenza virus proteins. ZDHHC22 is known to be well expressed in the human brain, eye and lung tissues. It is mainly localized in the ER/Golgi [211]. It has been identified along with ZDHHC23 to be the main palmitoyl-transferase palmitoylating large conductance calcium-activated potassium (BK) channels facilitating its efficient cell surface expression [169]. Most recently, it was reported that ZDHHC22 mediates palmitoylation of Cys241 of a Nephroblastoma overexpressed protein, which is responsible for its secretion and inhibition of S-palmitoylation interferes with neuronal growth [212]. However, the role of ZDHHC22 in influenza virus replication cycle has not been described before.

Therefore, I used CRISPR/Cas9 technology to delete the DHHC domain and make functional knockout ZDHHC22 protein in A549 cells. Then I tested the acylation of both intracellularly expressed HA and viral incorporated HA by acyl-RAC, click chemistry and mass spectrometry assays from WT and Δ ZDHHC22 cells. Analysis of intracellular palmitoylation showed no significant differences in the level of acylation of HA between WT and Δ ZDHHC22 cells (Fig.21).

Influenza viruses showed a tendency for better growth in the ZDHHC22 knockout cells, especially at earlier time points (Fig.22), which might indicate that the observed upregulation of ZDHHC22 could be part of the cellular defense mechanism against viral infection. Thus, I asked which protein is the triggering factor for ZDHHC22 upregulation. Since NS1 protein is one of the key virulence factors of influenza A virus, I assumed it might be the major regulator of ZDHHC22 overexpression. To test this, I expressed NS1 proteins from different influenza virus strains in A549 cells and checked expression of ZDHHC22. Interestingly, the results showed significant increase of ZDHHC22 expression with FPV-NS1 expression (Fig.19a). I also used mutant viruses that have a NS1 deletion, but they were not able to induce expression of ZDHHC22 (Fig.19b) confirming that the ZDHHC22 upregulation is mainly regulated by NS1. The next step would be to figure out the mechanism behind such induced upregulation and further investigate whether this is due to a direct interaction

between NS1 and ZDHHC22 proteins or indirectly through induction of other transcription factor which upregulate ZDHHC22. It has been recently shown that NS1 produce dynamic changes in host genome 3D organization where it induce read through transcription of hundreds of kilobases during IAV infection at the end of highly transcribed genes by inhibition of transcription termination, although this read-through phenomena occur independent of both virus strain and cell type. However its effect on virulence of influenza virus infection still questionable [213].

Since there are only very few substrates identified to be palmitoylated by ZDHHC22, we did LC/MS comparative palmitome analysis of WT and Δ ZDHHC22 cells with the aim to identify novel substrates for ZDHHC22 that might be related to viral infection. Our MS results indeed revealed 50 proteins and thus confirms the identity of ZDHHC22 as an acyltransferase (Table.4-5). However, only one of them, the plakophilin-2 protein (PKP2) has been reported before to be involved in the influenza virus replication cycle. PKP2 is known to be palmitoylated [214] and has an antiviral activity to influenza virus by binding to PB1 preventing its interaction with PB2 and inhibiting assembly of the viral polymerase complex [215]. Palmitoylation is required to increase association and anchor proteins to lipid membranes. PKP2-PB1 interaction occur mainly in the nucleus, thus it is highly unlikely to be controlled by the palmitoylated form of PKP2.

To sum this part up, All ZDHHC palmitoyl-transferases except ZDHHC19 are expressed in human lung cells. The Upregulation of ZDHHC22 early after influenza infection confirmed to be virus specific and regulated by viral NS1 protein but not essential for acylation of influenza HA and M2 proteins. However, the exact role of ZDHHC22 upregulation still unclear and remains as one of the main outlook for this thesis.

5.2. ZDHHC2, 8, 15 and 20 are involved in acylation of HA and M2 of influenza A virus

In the second part of this study, I used a siRNA library to individually knockdown the different human ZDHHCs in HA-transfected HeLa cells (Fig.24). The results showed that expression of ZDHHC2 and 8 along with the closely related ZDHHC15 and 20 (Fig.25) is required for acylation of HA of Influenza A virus. The results were confirmed with CRISPR/Cas9 technology in virus infected HAP1 cells (Fig. 28). Reduction in acylation of HA was analyzed with both [³H]-palmitate-labelling (Fig.25b) and Acyl-RAC assays. Moreover, since quantitative PCR (qPCR) revealed that ZDHHC2, 8, 15 and 20 (as well as every other ZDHHC except ZDHHC 19) are expressed in A549 cells (Human epithelial lung cell line) (Fig.17), the ZDHHCs I identified are probably also relevant for acylation of HA in human lung cells. HA co-localizes with ZDHHC2, 8, 15 and 20 at membranes of the exocytic

pathway in A549 cells (Fig.32), which is consistent with the intracellular site of acylation of HA.

HeLa cells were the cell of choice for the initial screening of candidate ZDHHCs (Fig.24) due to easy handling, high siRNA transfection and knockdown efficiency. Then, I used HAP1 cells in the validation experiments because CRISPR knockout cell lines for individual ZDHHC were commercially available. Unfortunately, both cell lines do not produce infectious virus. Therefore, I used CRISPR/Cas9 technology to make single and double knockout of candidate ZDHHCs (2, 8, 15 and 20) in A549 cells (Fig.34-35) in order to check their effect on palmitoylation of HA and virus replication. Acyl-RAC assay revealed only a slight effect on palmitoylation of HA in all individual ZDHHC-depleted A549 cell clones compared to ZDHHC-depleted HAP1 cells. However, when two ZDHHCs are knocked out simultaneously (2+15, 2+20), palmitoylation of viral HA was almost completely inhibited (Fig.35 b&e). In that case, I also observed a reduction in virus titers, especially in $\Delta 2/15$ cells.

HA of influenza A viruses contain a mixture of palmitate and stearate which might be attached by different ZDHHCs. In HAP1 cells, the virus was only able to infect the cells and express the viral proteins without release of infectious virus particles. Depleting the cells for single ZDHHC by CRISPR/Cas9 showed a significant reduction in acylation of viral HA (70-80% reduction in $\Delta ZDHHC15$ and $\Delta ZDHHC20$ cells (Fig.28-30)). While in A549 cells, where influenza virus can efficiently multiply, the reduction in HA acylation (Fig.34) was not as significant as in HAP1 or HeLa cells (Fig.25&28). It is well known that during replication, the virus hijack the host cell machinery to propagate themselves and since palmitoylation is essential for virus replication, one can assume that once an essential ZDHHC enzyme is silenced or knocked out, the virus can counteract by utilizing another closely related ZDHHC to modify its viral proteins and this could explain why I cannot get an effect in A549 similar to that of HAP1 cells. In agreement with the abovementioned assumption, Virus replication as well as acylation of intracellular HA was significantly affected (80-90% reduction) in A549 cells only when more than one of the candidate ZDHHC is knocked out (Fig.35) which reinforce the hypothesis that multiple ZDHHC are required at the same time to acylate the viral protein during viral replication. One might get a complete suppression of virus replication if we made silencing of all involved candidates, but this would be technically difficult due importance of ZDHHCs for acylation of cellular proteins.

Based on co-expression experiments of various types of substrate proteins with mammalian ZDHHCs in yeast cells it was proposed that ZDHHC2 and ZDHHC20 (but not ZDHHC15) have high activity towards integral membrane proteins [216]. However, ZDHHC2, 8, 15 and 20 are not involved in acylation of HA of Flu B and HEF of Flu C (Fig.31), although all hemagglutinating glycoproteins of Influenza viruses are typical type 1 transmembrane proteins, which exhibit a similar 3D-structure. Furthermore, each of them is transported along

the exocytic pathway to the plasma membrane and thus passes the same set of ZDHHC proteins. One might speculate that the different ZDHHCs hijacked by Influenza A and Influenza B and C viruses might be the result of their different host origins. The reservoirs of Influenza B and C viruses are almost exclusively humans. In contrast, all types of Influenza A viruses constantly circulate in water birds, from where some of them occasionally spread to other animals, such as poultry and swine or to humans. Thus, it might be that the viruses adapted independently from each other to a different set of ZDHHC proteins, i. e. Influenza A viruses adapted in birds to ZDHHC2, 8, 15 and 20, Influenza B and C viruses in humans to other unknown ZDHHCs. This seems contradictory to the finding that the human WSN virus (H1N1) uses the same set of ZDHHCs as the avian fowl plaque virus (H7N1). However, WSN is a successor of the virus that caused the 1918 pandemic, which is likely the result of direct transmission of an avian virus into the human population [217]. The avian viruses likely use the same ZDHHC proteins in both avian and mammalian cells, at least HA from WSN virus purified from embryonated hen's eggs and from mammalian cells are both stoichiometrically acylated. Minor differences were identified in HA's fatty acid pattern; more stearate was attached if the virus was grown in mammalian (20%) compared to avian cells (10%) [88].

I do not want to exclude that other ZDHHCs might also contribute to acylation of HA since the initial screen revealed reduction in HA's acylation by siRNAs directed against various ZDHHC proteins. From an evolutionary point of view, it would be unfavorable for a virus to rely completely on just one (or a few) ZDHHC protein(s) to catalyze a protein modification that is essential for its replication. Such a specialization might restrict virus tropisms to cells and organisms where this ZDHHC is highly expressed and functionally active since a large number of HA molecules need to be acylated. One virus particle contains ~500 trimeric HA spikes and 50 M2 proton channels [218], which correspond to 200 M2-linked and 4500 HA-linked fatty acids because every acylation site is completely filled [86]. Since each cell releases up to 5000 particles in ~10 hours, 20-30 million fatty acid bonds need to be catalyzed in one viral replication cycle. This estimation does not even take into account the large number of HA and M2 molecules still present inside dead cells, which are not able to release more particles. I thus assume that HA has adapted to a ZDHHC machinery that has a high capacity.

Furthermore, I cannot conclude that each of the identified ZDHHCs actually transfers fatty acids to HA. It is possible that they are part of a palmitoylation cascade, similar to the one involved in acylation of ER-resident protein folding factors [174]. In that case, ZDHHC6 catalyzes fatty acid transfer to the protein substrate, but its activity is regulated by ZDHHC16-catalyzed palmitoylation of three cytoplasmic cysteines in ZDHHC6. This generates three versions of the enzyme: non-palmitoylated ZDHHC6 is inactive, palmitoylation at the first site

creates a highly active ZDHHC version that is rapidly degraded and acylation at least one of the two other cysteines generates a moderately active and stable version. Using mass spectrometry both ZDHHC8 and ZDHHC20 appeared to be S-acylated on three cysteine residues within a CCX7–13C(S/T) motif in their cytoplasmic tails suggesting that they might be regulated by acylation [219,220].

5.3. Fatty acid specificities of ZDHHCs involved in acylation of HA

Do the hitherto determined lipid specificities of the ZDHHCs involved in acylation of HA and M2 correspond to the peculiar fatty acid pattern determined for these proteins? ZDHHC2, 15 and 20 use myristate, palmitate and stearate in the auto-acylation reaction and transfer it to protein substrates, but with different efficiency. ZDHHC2 does not show a significant preference for any of the acyl chains, whereas ZDHHC15 and 20 prefer the shorter acyl chains, even myristate is preferred over palmitate [158,160]. However, from previous published data, myristate was never detected as fatty acid bound to HA or to any other viral glycoprotein [86,107].

One factor limiting transfer of myristate to viral proteins might be a low Myr-CoA concentration inside cells. This might be assumed because myristate is a rare acyl-chain, both as free fatty acid and bound to phospholipids. However, at least in HEK293 cells the Myr-CoA content is almost half of the Pal-CoA content and only slightly lower than the amount of Stear-CoA [160]. Nonetheless, the local concentration of Myr-CoA in the vicinity of a ZDHHC protein might be lower and thus limiting myristate transfer to proteins. Pal-CoA has been shown to insert into artificial membranes [221], but Myr-CoA, due to its shorter acyl-chain might have a lower propensity to interact with bilayers, which is reminiscent of myristoylated peptides that have a much lower membrane binding affinity compared to palmitoylated peptides [222]. Alternatively, acyl-CoA binding proteins (ACBP), ubiquitous, mostly cytosolic polypeptides, might control the availability of acyl-CoAs for ZDHHCs. They occur as single domain polypeptide, but the ACBP domain is also present in ~50 different proteins. They bind acyl-CoAs with high affinity (K_D 1-10nM) which keeps the intracellular concentration of free acyl-CoAs in the low nM range. Most of them bind a variety of long chain acyl-CoAs, but at least the parasite *Plasmodium falciparum* encodes an ACBP that is specific for Myr-CoA [161]. It is tempting to speculate that ACBPs might sequester Myr-CoA, which is then not available for ZDHHC proteins. Alternatively, ACBPs might play an active role, e.g. transfer specific lipid substrates from the cytosol to certain ZDHHCs.

The crystal structure of human ZDHHC20 provided a molecular explanation which fatty acids are accepted in the acylated enzyme intermediate [158]. The acyl chain is inserted into a hydrophobic cavity formed by all four transmembrane regions. ZDHHC20 contains at the narrow end of the cavity the small amino acid Ser at position 29 and the large amino acid Tyr

DISCUSSION

at position 181 that form a hydrogen bond, which effectively closes the groove (Fig.36a). Most ZDHHCs contain either two bulky residues, one bulky and one small or two small amino acids at the homologous position and it was postulated that the presence of two large residues would limit the use of stearate. Indeed, exchange of Ser 29 by Phe reduced and of Tyr 181 by Ala enhanced the usage of stearate by ZDHHC20. A similar observation was also reported for the ZDHHC3 enzyme [160].

Based on this model I asked whether the other ZDHHCs we identified to be involved in acylation of HA also accept stearate as lipid donor. Sequence comparison shows that ZDHHC2 and 15 also contain a serine and a tyrosine at the end of the cavity and all other (except one) hydrophobic residues lining the cavity and contacting the acyl chain are conserved between ZDHHC2, 15 and 20. Only ZDHHC2 contains an alanine instead of a valine at position 216, which is located near the end of the tunnel. Since alanine has a shorter side chain, this might explain the increased usage of stearate in autoacylation of ZDHHC2 relative to ZDHHC15 [160].

Lipid preferences have not been experimentally tested for ZDHHC8. We therefore created a 3D-model of ZDHHC8 using the crystal structure of ZDHHC20 as template (Fig. 36b). It revealed identical or similar amino acids in most parts of the hydrophobic cavity of both proteins: Trp136 at the entrance of the tunnel, Phe152, Val192 and Phe196 in TMR 3 and 4 and hydrophobic, but shorter amino acids (Val20, Ala58) in TMR 1 and 2. A cysteine at the end of the cavity is exchanged to methionine 160 in ZDHHC8. Interestingly, the cavity is sealed by two small amino acids, Ser27 and His159 and thus one might speculate that ZDHHC8 might exhibit a higher preference for stearate than ZDHHC20.

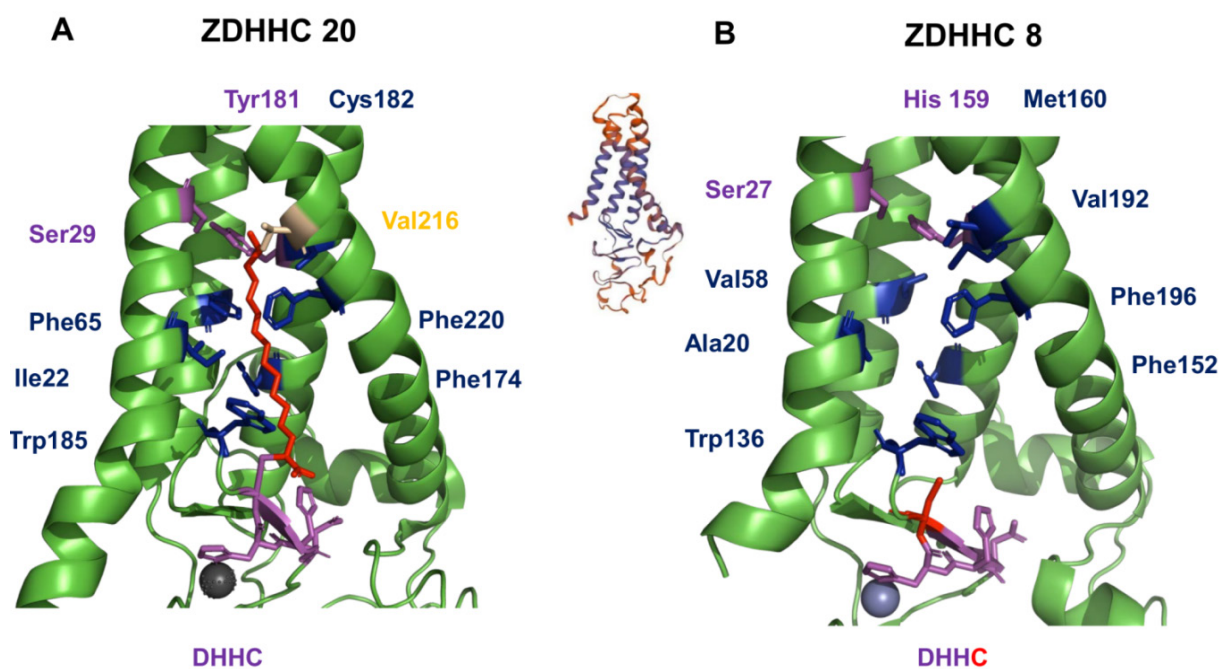


Figure 36. Structure of human ZDHHC20 and a model for ZDHHC8. (A) The figure shows the structure of the hydrophobic cavity of human ZDHHC20. Ser 29 and Tyr 181 (shown as magenta sticks) form a hydrogen bond that seals the tunnel. Amino acids contacting the acyl chain (red) are shown as blue sticks. They are conserved in ZDHHC2, 15 and 20 except Val216 (orange stick) which is replaced by an alanine in ZDHHC2. The DHHC motif is shown as magenta sticks. The figure was created with PyMOI from pdb-file 6bmm.1.A. **(B)** Computational model of ZDHHC8. The structure was created with Swiss-model (<https://swissmodel.expasy.org/>) using the structure of ZDHHC20 as template. Although the quality of the whole model is quite low, the structure of the transmembrane regions is predicted with higher confidence (blue color in the inset). The amino acids supposed to make contact with the acyl chain are shown as blue sticks. Amino acids Ser 27 and His 159 (magenta sticks) are supposed to close the hydrophobic tunnel

In summary, the ZDHHCs I identified to be involved in acylation of HA of Flu A are apparently able to transfer both palmitate and stearate to a substrate. Thus, site-specific acylation of HA can currently not be explained by the activities of two different, acyl-chain specific enzymes. However, it seems possible that the ZDHHC specific for stearate has not been identified in the initial siRNA screen and this ZDHHC might cause the residual acylation of HA in the Δ ZDHHC2, 8, 15 and 20 knockout cells. Unfortunately, the mass spectrometry method used to precisely determine the acyl chain pattern of HA in virus particles [86] cannot be currently applied to intracellular HA due to limited sample amounts. However, assuming that the current model for acyl-chain selectivity applies to all ZDHHC proteins, it is hard to envision a ZDHHC that transfers only stearate. Lengthening the tunnel might allow better access of stearate to the hydrophobic cavity but does not discriminate against the shorter palmitate chain. Interestingly, HEF expressed in insect cells as well as the total pool of S-acylated proteins from these cells contain only minor amounts of stearate [223] suggesting that ZDHHCs have evolved to higher complexity in mammalian cells.

5.4. Protein substrate recognition of ZDHHCs involved in acylation of HA and M2

It was recently proposed that acylation of transmembrane proteins occurs whenever a cysteine is accessible, i.e. located maximally 5-6 helix residues into the inner membrane leaflet [224]. This is consistent with the observation that cysteines located in the middle of the transmembrane region of certain HA-subtypes are not acylated [78]. Since even prokaryotic proteins with cysteines inserted near the transmembrane region become palmitoylated when expressed in mammalian cells it was also proposed that acylation is a random (stochastic) process that does not depend on recognition of a specific sequence or structural motif [224]. However, at least HA of Influenza A viruses must exhibit a certain feature recognized by ZDHHC2, 8, 15 and 20, which is absent in HA of Influenza B virus.

Since the largest part of HA is exposed to the lumen of the ER/Golgi and hence not accessible for a ZDHHC, only a short linker (8 residues), the transmembrane region (26-30

DISCUSSION

residues) and the small cytoplasmic tail (10-11 amino acids) might contain such a signal (Table.6). Common to the cytoplasmic tails of both HAs are two conserved hydrophobic amino acids surrounding the palmitoylated cysteine at the C-terminus (ICI in Flu A, ICL in Flu B). This hydrophobic patch might cause the cytoplasmic tail to run parallel to the membrane bilayer. Exchange of one hydrophobic by a hydrophilic amino acid prevents virus replication, but not palmitoylation of expressed HA from Flu A [88]. Also, otherwise, the HA tails of Flu A and Flu B contain similar amino acids surrounding the acylation sites, such as asparagine in addition to positively and negatively charged residues. Unique for HA of Flu A is a completely conserved glycine in the cytoplasmic tail, which, however, can be exchanged without affecting the stoichiometry of acylation of HA. Since exchange of other amino acids in the cytoplasmic tail also had no effect on acylation and little influence on virus replication [88,101], it seems likely that putative acylation signals are rather located in the transmembrane region.

Protein	TMD	CT
Flu A HA/1	GVKLES MG <u>VYQILAIYSTVASSL VLLVSL</u> G AISFWM C S	NGSLQ C R I C I
Flu A HA/2	PVKLSSGYKD <u>IILWF SFG</u> ASCFLLLAIAM G LVFI C V	KNGNMR C T I C I
Flu B HA	SLNDDGLD <u>NHTILLYYSTAASSLAVTL</u> MIAIFIVYMVS	RDNVS C S I C L
Flu C HEF	DTKIDLQSD <u>PFYW</u> G SSL G LAITATISLAALVIS G IAT C	RTK
Flu A M2	NDSSDP <u>LVIAANII</u> G ILHLILWIL DRL FFK C IYRRLKYGLKR..	

Table 6: Amino acids near the acylation sites of viral substrate proteins. Amino acid sequences of the linker, transmembrane region (underlined) and cytoplasmic tail of the viral proteins analyzed in this study. Cysteines acylated with palmitate and stearate are highlighted in yellow and green, respectively. Glycines in the transmembrane region of HA and M2 of Flu A and HEF of Flu C are indicated as red letters. The C-termini of HAs contain conserved hydrophobic residues around the last palmitoylated cysteine (highlighted in grey). This hydrophobic patch might cause the cytoplasmic tail to run parallel to the membrane.

The structure of the outer part of the TMR has been resolved by Cryo-EM for a group 1 HA from Influenza A virus (Fig 37a). A flexible linker that contains a five-residue α -helix connects the ectodomain to the TMR, which forms a bundle of three α -helices. A leucine is the last residue present in the resolved structure. The next residue is a glycine which causes the chains to splay apart and become less ordered, suggesting that the glycine causes a kink in the TMR α -helix [205]. No such detailed structures are available for any other HA, but most likely, they also form trimeric helices [225]. Interestingly, HA from every subtype of Flu A contains a glycine in the middle of the TMR, whereas none of the Flu B HAs present in the database contain any glycine in their TMR (Table 6). In a previous study from our lab, they were not able to change this glycine in HA of Flu A to a large and hydrophobic isoleucine, since the nucleotides rapidly reverted to a triplet encoding a serine, an amino acid also

having a short side chain. The resulting viruses contain stoichiometrically acylated HA, but with marginally increased stearate content [88,101].

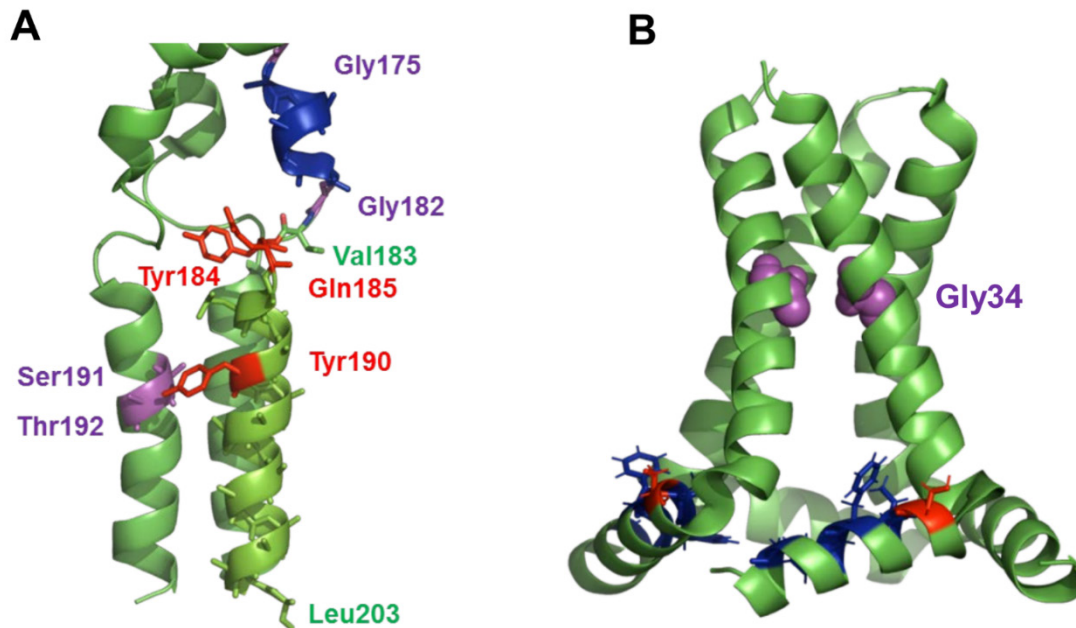


Figure 37. Structure of the viral substrate proteins HA and M2. (A) C-terminal part of the full-length structure of a group 1 HA. The ectodomain of HA (not shown) is connected by a linker region which contains a short α -helix (blue) to the trimeric transmembrane region. The helix is confined by two glycine residues, which allows the ectodomain to tilt against the membrane anchor. Tyr 190 in the TMR probably forms a hydrogen-bond with Ser 191 or Thr 192 in another helix. The last resolved amino acid in the TMR is Leu 203, the next residue, a glycine causes the helices to splay apart. Note that important residues, such as Tyr190, are not present in group 2 HAs suggesting that it might exhibit a different structure. The figure was created with PyMol from pdb-file 6HJ0. **(B)** Structure of amino acids 22-62 of the viral proton channel M2. The tetrameric transmembrane region (residues 26-46) is kinked around the highly conserved glycine 34, which is highlighted as magenta spheres in two TMR regions. Residues 46-49 form a tight turn, which connects the TMR to an amphiphilic helix. Residues interacting with the membrane are shown as blue sticks. Shown as red stick is the acylation site. Cys is replaced by a serine in the peptide used to make the NMR structure. The figure was created with PyMol from pdb-file 2L0J.

Does M2, the other identified substrate of ZDHHC2, 8, 15 and 20, exhibit a similar feature? The NMR structure of the tetrameric proton channel embedded in a lipid bilayer revealed that the acylation site is located at the beginning of a 15 amino acid long amphiphilic helix that runs perpendicular to the membrane. The helix is connected by a short and tight linker to an 18 residue long transmembrane region, which is indeed kinked around a conserved glycine (Fig. 37b, [206]). I thus suggest that ZDHHCs involved in acylation of HA and M2 of Influenza A virus might recognize proteins with kinked transmembrane regions. This might allow the protruding part of the TMR of a prospective substrate protein to interact with specific ZDHHCs, perhaps by insertion into a pocket between two of their transmembrane regions. Alternatively, due to the absence of a side chain, a glycine in the TMR helix of a substrate provides a flat surface for tight packing of a large, hydrophobic side chain present in the TMR

6. Summary

Influenza viruses are negative sense segmented enveloped RNA viruses covered with 2 surface peplomers: the trimeric hemagglutinin (HA), which catalyzes virus entry by binding to sialic acid containing receptors and by performing fusion of viral with endosomal membranes and the neuraminidase (NA), which is required for release of virus particles from infected cells. Among the influenza virus proteins, only HA and the proton-channel M2 are site-specifically modified with fatty acids (S-acylated), which is essential for virus replication. Whereas two cysteines in the short cytoplasmic tail of HA contain only palmitate, stearate is exclusively attached to one cysteine located close to the cytoplasmic border of the transmembrane region (TMR). M2 is palmitoylated at a cysteine positioned in an amphiphilic helix near the TMR. The enzymes catalyzing acylation of HA and M2 have not been identified, but ZDHHC enzyme family who acylate cellular proteins are obvious candidates.

In the first part of this thesis, the expression of 23 ZDHHC family members was analyzed in human lung cells using qPCR. Results showed that all ZDHHCs (except ZDHHC19) are expressed. Interestingly, ZDHHC22 was upregulated during influenza virus infection suggesting that it might be involved in acylation of viral proteins. However, CRISPR/Cas9 mediated knockout of ZDHHC22 did not affect acylation of both intracellularly expressed HA and M2 as revealed by Acyl-RAC and click chemistry as well as HA incorporated into virus particles as shown by MALDI-TOF MS analysis. However, I confirmed that ZDHHC22 is an acyltransferase using LC/MS comparative palmitome analysis, which identified more than 50 proteins as substrates of ZDHHC22. Furthermore, I identified the nonstructural protein 1 (NS1) as the triggering factor for ZDHHC22 upregulation during influenza infection using expression vectors and virus deletion mutants.

In the second part, I identified for the first time 4 ZDHHC enzymes that are involved in acylation of hemagglutinin (HA). For screening, I used a siRNA library to knockdown expression of each of the 23 human ZDHHCs in HA-expressing Hela cells. siRNAs against ZDHHC2 and 8 had the strongest effect on acylation of HA as demonstrated by acyl-RAC and confirmed by 3H-palmitate labelling. The subsequent CRISPR/Cas9 knockout of ZDHHC2 and 8 in HAP1 cells, but also of the phylogenetically related ZDHHCs 15 and 20 strongly reduced acylation of group 1 and group 2 HAs and of M2, but individual ZDHHCs exhibit slightly different substrate preferences. These ZDHHCs co-localize with HA at membranes of the exocytic pathway in a human lung cell line. ZDHHC2, 8, 15 and 20 are not required for acylation of the hemagglutinin-esterase-fusion protein of Influenza C virus that contains only stearate at one transmembrane cysteine. Surprisingly, knockout of these ZDHHCs also did not compromise acylation of HA of Influenza B virus that contains two palmitoylated cysteines in its cytoplasmic tail.

7. Zusammenfassung

“Identifizierung von ZDHHC-Enzymen, die die Acylierung des Influenzavirus Hämagglutinin katalysieren”

Influenzaviren sind negativsträngige, segmentierte und umhüllte RNA-Viren, die mit zwei Oberflächen-Peplomeren bedeckt sind: dem trimeren Hämagglutinin (HA), das den Viruseintritt durch Bindung an Sialsäure-haltige Rezeptoren und durch Fusion von Viren mit endosomalen Membranen katalysiert und der Neuraminidase (NA) die für die Freisetzung von Viruspartikeln aus infizierten Zellen benötigt wird. Unter den Influenzavirus-Proteinen sind nur HA und der Protonenkanal M2 ortsspezifisch mit Fettsäuren (S-acyliert) modifiziert, was für die Virusreplikation essentiell ist. Während zwei Cysteine in der kurzen zytoplasmatischen Schwanz von HA nur Palmitat enthalten, ist Stearat ausschließlich an ein Cystein gebunden, das sich nahe der zytoplasmatischen Grenze der Transmembranregion (TMR) befindet. M2 wird an einem Cystein palmitoyliert, das sich in einer amphiphilen Helix in der Nähe des TMR befindet. Die Enzyme, die die Acylierung von HA und M2 katalysieren, wurden nicht identifiziert, aber Mitglieder der ZDHHC-Enzymfamilie, die zelluläre Proteine acylieren, sind offensichtliche Kandidaten.

Im ersten Teil dieser Arbeit wurde die Expression von 23 Mitgliedern der ZDHHC-Familie in menschlichen Lungenzellen mittels qPCR analysiert. Die Ergebnisse zeigten, dass alle ZDHHCs (außer ZDHHC19) exprimiert werden. Interessanterweise wurde ZDHHC22 während einer Influenzavirusinfektion hochreguliert, was darauf hindeutet, dass es an der Acylierung viraler Proteine beteiligt sein könnte. Das CRISPR / Cas9-vermittelte Knockout von ZDHHC22 wirkte sich jedoch nicht auf die Acylierung sowohl von intrazellulär exprimiertem HA als auch von M2 aus, wie durch Acyl-RAC- und Klick-Chemie sowie HA in Viruspartikeln nachgewiesen wurde, wie durch MALDI-TOF-MS-Analyse gezeigt. Ich bestätigte jedoch, dass ZDHHC22 eine Acyltransferase ist, indem ich eine LC / MS-Vergleichspalmitomanalyse durchführte, bei der mehr als 50 Proteine als Substrate von ZDHHC22 identifiziert wurden. Darüber hinaus identifizierte ich das nichtstrukturelle Protein 1 (NS1) als auslösenden Faktor für die ZDHHC22-Hochregulation während einer Influenza-Infektion unter Verwendung von Expressionsvektoren und Virus-Deletionsmutanten.

Im zweiten Teil habe ich erstmals 4 ZDHHC-Enzyme identifiziert, die an der Acylierung von Hämagglutinin (HA) beteiligt sind. Für das Screening verwendete ich eine siRNA-Bibliothek, um die Expression von jedem der 23 humanen ZDHHCs in HA-exprimierenden Hela-Zellen auszuschalten. siRNAs gegen ZDHHC2 und 8 hatten den stärksten Effekt auf die Acylierung von HA, wie es durch Acyl-RAC gezeigt und durch 3H-Palmitat-Markierung bestätigt wurde. Der anschließende CRISPR / Cas9-Knockout von ZDHHC2 und 8 in HAP1-Zellen, aber auch der phylogenetisch verwandten ZDHHCs 15 und 20 reduzierte die Acylierung von HAs der

Gruppen 1 und 2 und von M2 stark. Einzelne ZDHHCs weisen jedoch geringfügig unterschiedliche Substratpräferenzen auf. Diese ZDHHCs lokalisieren in einer menschlichen Lungenzelllinie zusammen mit HA an Membranen des Exozytoseweges. ZDHHC2, 8, 15 und 20 werden für die Acylierung des Hämagglutinin-Esterase-Fusionsproteins des Influenza C-Virus, das nur Stearat an einer Transmembran-Cystein enthält, nicht benötigt. Überraschenderweise beeinträchtigte das Knockout dieser ZDHHCs auch nicht die Acylierung von HA des Influenza B-Virus, das zwei palmitoylierte Cysteine in seinem cytoplasmatischen Schwanz enthält.

8. References

1. **Palese, S., and In, M.** (2007) *Fields Virology*. Knipe DM, Howley PM, editors. Lippincott Williams & Wilkins, Philadelphia
2. **Hause, B. M., Collin, E. A., Liu, R., Huang, B., Sheng, Z., Lu, W., Wang, D., Nelson, E. A., and Li, F.** (2014) Characterization of a novel influenza virus in cattle and Swine: proposal for a new genus in the Orthomyxoviridae family. *MBio* **5**, e00031-00014
3. **Kibenge, F. S., Munir, K., Kibenge, M. J., Joseph, T., and Moneke, E.** (2004) Infectious salmon anemia virus: causative agent, pathogenesis and immunity. *Anim Health Res Rev* **5**, 65-78
4. **Kuno, G., Chang, G. J., Tsuchiya, K. R., and Miller, B. R.** (2001) Phylogeny of Thogoto virus. *Virus Genes* **23**, 211-214
5. **Presti, R. M., Zhao, G., Beatty, W. L., Mihindikulasuriya, K. A., da Rosa, A. P., Popov, V. L., Tesh, R. B., Virgin, H. W., and Wang, D.** (2009) Quarantfil, Johnston Atoll, and Lake Chad viruses are novel members of the family Orthomyxoviridae. *J Virol* **83**, 11599-11606
6. **Swayne, D. E. J. A. I.** (2008) The global nature of avian influenza. 177-201
7. **Tong, S., Zhu, X., Li, Y., Shi, M., Zhang, J., Bourgeois, M., Yang, H., Chen, X., Recuenco, S., Gomez, J., Chen, L. M., Johnson, A., Tao, Y., Dreyfus, C., Yu, W., McBride, R., Carney, P. J., Gilbert, A. T., Chang, J., Guo, Z., Davis, C. T., Paulson, J. C., Stevens, J., Rupprecht, C. E., Holmes, E. C., Wilson, I. A., and Donis, R. O.** (2013) New world bats harbor diverse influenza A viruses. *PLoS Pathog* **9**, e1003657
8. **Wright, P., and Webster, R. J. P. L.-R. p.** (2001) *Fields virology*. 1533-1579
9. **Fouchier, R. A., Munster, V., Wallensten, A., Bestebroer, T. M., Herfst, S., Smith, D., Rimmelzwaan, G. F., Olsen, B., and Osterhaus, A. D.** (2005) Characterization of a novel influenza A virus hemagglutinin subtype (H16) obtained from black-headed gulls. *J Virol* **79**, 2814-2822
10. **Chu, C. M., Dawson, I. M., and Elford, W. J.** (1949) Filamentous forms associated with newly isolated influenza virus. *Lancet* **1**, 602
11. **Kilbourne, E. D., and Murphy, J. S.** (1960) Genetic studies of influenza viruses. I. Viral morphology and growth capacity as exchangeable genetic traits. Rapid in ovo adaptation of early passage Asian strain isolates by combination with PR8. *J Exp Med* **111**, 387-406
12. **Webster, R. G., Bean, W. J., Gorman, O. T., Chambers, T. M., and Kawaoka, Y.** (1992) Evolution and ecology of influenza A viruses. *Microbiol Rev* **56**, 152-179
13. **Chen, W., Calvo, P. A., Malide, D., Gibbs, J., Schubert, U., Bacik, I., Basta, S., O'Neill, R., Schickli, J., Palese, P., Henklein, P., Bennink, J. R., and Yewdell, J. W.** (2001) A novel influenza A virus mitochondrial protein that induces cell death. *Nat Med* **7**, 1306-1312
14. **Krumbholz, A., Philipps, A., Oehring, H., Schwarzer, K., Eitner, A., Wutzler, P., and Zell, R.** (2011) Current knowledge on PB1-F2 of influenza A viruses. *Med Microbiol Immunol* **200**, 69-75
15. **Wise, H. M., Foeglein, A., Sun, J., Dalton, R. M., Patel, S., Howard, W., Anderson, E. C., Barclay, W. S., and Digard, P.** (2009) A complicated message: Identification of a novel

- PB1-related protein translated from influenza A virus segment 2 mRNA. *J Virol* **83**, 8021-8031
16. **Jagger, B. W., Wise, H. M., Kash, J. C., Walters, K. A., Wills, N. M., Xiao, Y. L., Dunfee, R. L., Schwartzman, L. M., Ozinsky, A., Bell, G. L., Dalton, R. M., Lo, A., Efstathiou, S., Atkins, J. F., Firth, A. E., Taubenberger, J. K., and Digard, P.** (2012) An overlapping protein-coding region in influenza A virus segment 3 modulates the host response. *Science* **337**, 199-204
17. **Muramoto, Y., Noda, T., Kawakami, E., Akkina, R., and Kawaoka, Y.** (2013) Identification of novel influenza A virus proteins translated from PA mRNA. *J Virol* **87**, 2455-2462
18. **Wise, H. M., Hutchinson, E. C., Jagger, B. W., Stuart, A. D., Kang, Z. H., Robb, N., Schwartzman, L. M., Kash, J. C., Fodor, E., Firth, A. E., Gog, J. R., Taubenberger, J. K., and Digard, P.** (2012) Identification of a novel splice variant form of the influenza A virus M2 ion channel with an antigenically distinct ectodomain. *PLoS Pathog* **8**, e1002998
19. **Selman, M., Dankar, S. K., Forbes, N. E., Jia, J. J., and Brown, E. G.** (2012) Adaptive mutation in influenza A virus non-structural gene is linked to host switching and induces a novel protein by alternative splicing. *Emerg Microbes Infect* **1**, e42
20. **Skehel, J. J., and Wiley, D. C.** (2000) Receptor binding and membrane fusion in virus entry: the influenza hemagglutinin. *Annu Rev Biochem* **69**, 531-569
21. **Varghese, J. N., McKimm-Breschkin, J. L., Caldwell, J. B., Kortt, A. A., and Colman, P. M.** (1992) The structure of the complex between influenza virus neuraminidase and sialic acid, the viral receptor. *Proteins* **14**, 327-332
22. **Bui, M., Whittaker, G., and Helenius, A.** (1996) Effect of M1 protein and low pH on nuclear transport of influenza virus ribonucleoproteins. *J Virol* **70**, 8391-8401
23. **Holsinger, L. J., and Lamb, R. A.** (1991) Influenza virus M2 integral membrane protein is a homotetramer stabilized by formation of disulfide bonds. *Virology* **183**, 32-43
24. **Elleman, C. J., and Barclay, W. S.** (2004) The M1 matrix protein controls the filamentous phenotype of influenza A virus. *Virology* **321**, 144-153
25. **Roberts, P. C., Lamb, R. A., and Compans, R. W.** (1998) The M1 and M2 proteins of influenza A virus are important determinants in filamentous particle formation. *Virology* **240**, 127-137
26. **Noda, T., and Kawaoka, Y.** (2010) Structure of influenza virus ribonucleoprotein complexes and their packaging into virions. *Rev Med Virol* **20**, 380-391
27. **Pons, M. W., Schulze, I. T., Hirst, G. K., and Hauser, R.** (1969) Isolation and characterization of the ribonucleoprotein of influenza virus. *Virology* **39**, 250-259
28. **Connor, R. J., Kawaoka, Y., Webster, R. G., and Paulson, J. C.** (1994) Receptor specificity in human, avian, and equine H2 and H3 influenza virus isolates. *Virology* **205**, 17-23
29. **Suzuki, Y., Ito, T., Suzuki, T., Holland, R. E., Jr., Chambers, T. M., Kiso, M., Ishida, H., and Kawaoka, Y.** (2000) Sialic acid species as a determinant of the host range of influenza A viruses. *J Virol* **74**, 11825-11831

30. **Chen, C., and Zhuang, X.** (2008) Epsin 1 is a cargo-specific adaptor for the clathrin-mediated endocytosis of the influenza virus. *Proc Natl Acad Sci U S A* **105**, 11790-11795
31. **de Vries, E., Tscherne, D. M., Wienholts, M. J., Cobos-Jimenez, V., Scholte, F., Garcia-Sastre, A., Rottier, P. J., and de Haan, C. A.** (2011) Dissection of the influenza A virus endocytic routes reveals macropinocytosis as an alternative entry pathway. *PLoS Pathog* **7**, e1001329
32. **Rossman, J. S., Leser, G. P., and Lamb, R. A.** (2012) Filamentous influenza virus enters cells via macropinocytosis. *J Virol* **86**, 10950-10960
33. **Rust, M. J., Lakadamyali, M., Zhang, F., and Zhuang, X.** (2004) Assembly of endocytic machinery around individual influenza viruses during viral entry. *Nat Struct Mol Biol* **11**, 567-573
34. **Lakadamyali, M., Rust, M. J., Babcock, H. P., and Zhuang, X.** (2003) Visualizing infection of individual influenza viruses. *Proc Natl Acad Sci U S A* **100**, 9280-9285
35. **Helenius, A.** (1992) Unpacking the incoming influenza virus. *Cell* **69**, 577-578
36. **Martin, K., and Helenius, A.** (1991) Transport of incoming influenza virus nucleocapsids into the nucleus. *J Virol* **65**, 232-244
37. **O'Neill, R. E., Jaskunas, R., Blobel, G., Palese, P., and Moroianu, J.** (1995) Nuclear import of influenza virus RNA can be mediated by viral nucleoprotein and transport factors required for protein import. *J Biol Chem* **270**, 22701-22704
38. **Dias, A., Bouvier, D., Crepin, T., McCarthy, A. A., Hart, D. J., Baudin, F., Cusack, S., and Ruigrok, R. W.** (2009) The cap-snatching endonuclease of influenza virus polymerase resides in the PA subunit. *Nature* **458**, 914-918
39. **Braam, J., Ulmanen, I., and Krug, R. M.** (1983) Molecular model of a eucaryotic transcription complex: functions and movements of influenza P proteins during capped RNA-primed transcription. *Cell* **34**, 609-618
40. **Luo, G. X., Luytjes, W., Enami, M., and Palese, P.** (1991) The polyadenylation signal of influenza virus RNA involves a stretch of uridines followed by the RNA duplex of the panhandle structure. *J Virol* **65**, 2861-2867
41. **Shapiro, G. I., Gurney, T., Jr., and Krug, R. M.** (1987) Influenza virus gene expression: control mechanisms at early and late times of infection and nuclear-cytoplasmic transport of virus-specific RNAs. *J Virol* **61**, 764-773
42. **Perez, J. T., Varble, A., Sachidanandam, R., Zlatev, I., Manoharan, M., Garcia-Sastre, A., and tenOever, B. R.** (2010) Influenza A virus-generated small RNAs regulate the switch from transcription to replication. *Proc Natl Acad Sci U S A* **107**, 11525-11530
43. **Umbach, J. L., Yen, H. L., Poon, L. L., and Cullen, B. R.** (2010) Influenza A virus expresses high levels of an unusual class of small viral leader RNAs in infected cells. *MBio* **1**
44. **Perez, J. T., Zlatev, I., Aggarwal, S., Subramanian, S., Sachidanandam, R., Kim, B., Manoharan, M., and tenOever, B. R.** (2012) A small-RNA enhancer of viral polymerase activity. *J Virol* **86**, 13475-13485

-
45. **Robb, N. C., Te Velthuis, A. J., Wieneke, R., Tampe, R., Cordes, T., Fodor, E., and Kapanidis, A. N.** (2016) Single-molecule FRET reveals the pre-initiation and initiation conformations of influenza virus promoter RNA. *Nucleic Acids Res* **44**, 10304-10315
46. **Nobusawa, E., Aoyama, T., Kato, H., Suzuki, Y., Tateno, Y., and Nakajima, K.** (1991) Comparison of complete amino acid sequences and receptor-binding properties among 13 serotypes of hemagglutinins of influenza A viruses. *Virology* **182**, 475-485
47. **Bullough, P. A., Hughson, F. M., Skehel, J. J., and Wiley, D. C.** (1994) Structure of influenza haemagglutinin at the pH of membrane fusion. *Nature* **371**, 37-43
48. **Wilson, I. A., Skehel, J. J., and Wiley, D. C.** (1981) Structure of the haemagglutinin membrane glycoprotein of influenza virus at 3 Å resolution. *Nature* **289**, 366-373
49. **Steinhauer, D. A.** (1999) Role of hemagglutinin cleavage for the pathogenicity of influenza virus. *Virology* **258**, 1-20
50. **Koshikawa, N., Hasegawa, S., Nagashima, Y., Mitsuhashi, K., Tsubota, Y., Miyata, S., Miyagi, Y., Yasumitsu, H., and Miyazaki, K.** (1998) Expression of trypsin by epithelial cells of various tissues, leukocytes, and neurons in human and mouse. *The American journal of pathology* **153**, 937-944
51. **Horimoto, T., Nakayama, K., Smeekens, S. P., and Kawaoka, Y.** (1994) Proprotein-processing endoproteases PC6 and furin both activate hemagglutinin of virulent avian influenza viruses. *J Virol* **68**, 6074-6078
52. **Stieneke-Grober, A., Vey, M., Angliker, H., Shaw, E., Thomas, G., Roberts, C., Klenk, H. D., and Garten, W.** (1992) Influenza virus hemagglutinin with multibasic cleavage site is activated by furin, a subtilisin-like endoprotease. *The EMBO journal* **11**, 2407-2414
53. **Swayne, D. E.** (2007) Understanding the complex pathobiology of high pathogenicity avian influenza viruses in birds. *Avian Dis* **51**, 242-249
54. **Wiley, D. C., Wilson, I. A., and Skehel, J. J.** (1981) Structural identification of the antibody-binding sites of Hong Kong influenza haemagglutinin and their involvement in antigenic variation. *Nature* **289**, 373-378
55. **Doms, R. W., Lamb, R. A., Rose, J. K., and Helenius, A.** (1993) Folding and assembly of viral membrane proteins. *Virology* **193**, 545-562
56. **Hammond, C., Braakman, I., and Helenius, A.** (1994) Role of N-linked oligosaccharide recognition, glucose trimming, and calnexin in glycoprotein folding and quality control. *Proc Natl Acad Sci U S A* **91**, 913-917
57. **Segal, M. S., Bye, J. M., Sambrook, J. F., and Gething, M. J.** (1992) Disulfide bond formation during the folding of influenza virus hemagglutinin. *J Cell Biol* **118**, 227-244
58. **Cerioti, A., and Colman, A.** (1990) Trimer formation determines the rate of influenza virus haemagglutinin transport in the early stages of secretion in *Xenopus* oocytes. *J Cell Biol* **111**, 409-420
59. **Roth, M. G., Compans, R. W., Giusti, L., Davis, A. R., Nayak, D. P., Gething, M. J., and Sambrook, J.** (1983) Influenza virus hemagglutinin expression is polarized in cells infected with recombinant SV40 viruses carrying cloned hemagglutinin DNA. *Cell* **33**, 435-443

60. **Brewer, C. B., and Roth, M. G.** (1991) A single amino acid change in the cytoplasmic domain alters the polarized delivery of influenza virus hemagglutinin. *J Cell Biol* **114**, 413-421
61. **Barman, S., Adhikary, L., Kawaoka, Y., and Nayak, D. P.** (2003) Influenza A virus hemagglutinin containing basolateral localization signal does not alter the apical budding of a recombinant influenza A virus in polarized MDCK cells. *Virology* **305**, 138-152
62. **Scheiffele, P., Roth, M. G., and Simons, K.** (1997) Interaction of influenza virus haemagglutinin with sphingolipid-cholesterol membrane domains via its transmembrane domain. *The EMBO journal* **16**, 5501-5508
63. **Simons, K., and Gerl, M. J.** (2010) Revitalizing membrane rafts: new tools and insights. *Nat Rev Mol Cell Biol* **11**, 688-699
64. **Zhang, J., Pekosz, A., and Lamb, R. A.** (2000) Influenza virus assembly and lipid raft microdomains: a role for the cytoplasmic tails of the spike glycoproteins. *J Virol* **74**, 4634-4644
65. **Takeda, M., Leser, G. P., Russell, C. J., and Lamb, R. A.** (2003) Influenza virus hemagglutinin concentrates in lipid raft microdomains for efficient viral fusion. *Proc Natl Acad Sci U S A* **100**, 14610-14617
66. **el-Husseini Ael, D., and Brecht, D. S.** (2002) Protein palmitoylation: a regulator of neuronal development and function. *Nat Rev Neurosci* **3**, 791-802
67. **Linder, M. E., and Deschenes, R. J.** (2007) Palmitoylation: policing protein stability and traffic. *Nat Rev Mol Cell Biol* **8**, 74-84
68. **Towler, D., and Glaser, L.** (1986) Acylation of cellular proteins with endogenously synthesized fatty acids. *Biochemistry* **25**, 878-884
69. **Salaun, C., Greaves, J., and Chamberlain, L. H.** (2010) The intracellular dynamic of protein palmitoylation. *J Cell Biol* **191**, 1229-1238
70. **Fukata, Y., Brecht, D. S., and Fukata, M.** (2006) Protein Palmitoylation by DHHC Protein Family. in *The Dynamic Synapse: Molecular Methods in Ionotropic Receptor Biology* (Kittler, J. T., and Moss, S. J. eds.), Boca Raton (FL). pp
71. **Mitchell, D. A., Vasudevan, A., Linder, M. E., and Deschenes, R. J.** (2006) Protein palmitoylation by a family of DHHC protein S-acyltransferases. *J Lipid Res* **47**, 1118-1127
72. **Ivanov, S. S., and Roy, C.** (2013) Host lipidation: a mechanism for spatial regulation of Legionella effectors. *Curr Top Microbiol Immunol* **376**, 135-154
73. **Schmidt, M. F., and Schlesinger, M. J.** (1979) Fatty acid binding to vesicular stomatitis virus glycoprotein: a new type of post-translational modification of the viral glycoprotein. *Cell* **17**, 813-819
74. **Veit, M.** (2012) Palmitoylation of virus proteins. *Biol Cell* **104**, 493-515
75. **Ernst, A. M., Syed, S. A., Zaki, O., Bottanelli, F., Zheng, H., Hacke, M., Xi, Z., Rivera-Molina, F., Graham, M., Rebane, A. A., Bjorkholm, P., Baddeley, D., Toomre, D., Pincet, F., and Rothman, J. E.** (2018) S-Palmitoylation Sorts Membrane Cargo for Anterograde Transport in the Golgi. *Dev Cell* **47**, 479-493 e477

76. **Ernst, A. M., Toomre, D., and Bogan, J. S.** (2019) Acylation - A New Means to Control Traffic Through the Golgi. *Front Cell Dev Biol* **7**, 109
77. **Engel, S., de Vries, M., Herrmann, A., and Veit, M.** (2012) Mutation of a raft-targeting signal in the transmembrane region retards transport of influenza virus hemagglutinin through the Golgi. *FEBS Lett* **586**, 277-282
78. **Veit, M., Kretzschmar, E., Kuroda, K., Garten, W., Schmidt, M. F., Klenk, H. D., and Rott, R.** (1991) Site-specific mutagenesis identifies three cysteine residues in the cytoplasmic tail as acylation sites of influenza virus hemagglutinin. *J Virol* **65**, 2491-2500
79. **de Vries, M., Herrmann, A., and Veit, M.** (2014) A cholesterol consensus motif is required for efficient intracellular transport and raft association of a group 2 HA from influenza virus. *Biochem J* **465**, 305-314
80. **Hu, B., Hofer, C. T., Thiele, C., and Veit, M.** (2019) Cholesterol binding to the transmembrane region of a group 2 HA of Influenza virus is essential for virus replication affecting both virus assembly and HA's fusion activity. *J Virol*
81. **Veit, M., Herrler, G., Schmidt, M. F., Rott, R., and Klenk, H. D.** (1990) The hemagglutinating glycoproteins of influenza B and C viruses are acylated with different fatty acids. *Virology* **177**, 807-811
82. **Veit, M., Klenk, H. D., Kendal, A., and Rott, R.** (1991) The M2 protein of influenza A virus is acylated. *J Gen Virol* **72 (Pt 6)**, 1461-1465
83. **Holsinger, L. J., Shaughnessy, M. A., Micko, A., Pinto, L. H., and Lamb, R. A.** (1995) Analysis of the posttranslational modifications of the influenza virus M2 protein. *J Virol* **69**, 1219-1225
84. **Naeve, C. W., and Williams, D.** (1990) Fatty acids on the A/Japan/305/57 influenza virus hemagglutinin have a role in membrane fusion. *The EMBO journal* **9**, 3857-3866
85. **Sugrue, R. J., Belshe, R. B., and Hay, A. J.** (1990) Palmitoylation of the influenza A virus M2 protein. *Virology* **179**, 51-56
86. **Kordyukova, L. V., Serebryakova, M. V., Baratova, L. A., and Veit, M.** (2008) S acylation of the hemagglutinin of influenza viruses: mass spectrometry reveals site-specific attachment of stearic acid to a transmembrane cysteine. *J Virol* **82**, 9288-9292
87. **Kordyukova, L. V., Serebryakova, M. V., Polyansky, A. A., Kropotkina, E. A., Alexeevski, A. V., Veit, M., Efremov, R. G., Filippova, I. Y., and Baratova, L. A.** (2011) Linker and/or transmembrane regions of influenza A/Group-1, A/Group-2, and type B virus hemagglutinins are packed differently within trimers. *Biochim Biophys Acta* **1808**, 1843-1854
88. **Brett, K., Kordyukova, L. V., Serebryakova, M. V., Mintaev, R. R., Alexeevski, A. V., and Veit, M.** (2014) Site-specific S-acylation of influenza virus hemagglutinin: the location of the acylation site relative to the membrane border is the decisive factor for attachment of stearate. *J Biol Chem* **289**, 34978-34989
89. **Veit, M., Serebryakova, M. V., and Kordyukova, L. V.** (2013) Palmitoylation of influenza virus proteins. *Biochem Soc Trans* **41**, 50-55
90. **Chernomordik, L. V., and Kozlov, M. M.** (2005) Membrane hemifusion: crossing a chasm in two leaps. *Cell* **123**, 375-382

91. **Nikolaus, J., Warner, J. M., O'Shaughnessy, B., and Herrmann, A.** (2011) The pathway to membrane fusion through hemifusion. *Curr Top Membr* **68**, 1-32
92. **Simpson, D. A., and Lamb, R. A.** (1992) Alterations to influenza virus hemagglutinin cytoplasmic tail modulate virus infectivity. *J Virol* **66**, 790-803
93. **Steinhauer, D. A., Wharton, S. A., Wiley, D. C., and Skehel, J. J.** (1991) Deacylation of the hemagglutinin of influenza A/Aichi/2/68 has no effect on membrane fusion properties. *Virology* **184**, 445-448
94. **Naim, H. Y., Amarneh, B., Ktistakis, N. T., and Roth, M. G.** (1992) Effects of altering palmitoylation sites on biosynthesis and function of the influenza virus hemagglutinin. *J Virol* **66**, 7585-7588
95. **Sakai, T., Ohuchi, R., and Ohuchi, M.** (2002) Fatty acids on the A/USSR/77 influenza virus hemagglutinin facilitate the transition from hemifusion to fusion pore formation. *J Virol* **76**, 4603-4611
96. **Wagner, R., Herwig, A., Azzouz, N., and Klenk, H. D.** (2005) Acylation-mediated membrane anchoring of avian influenza virus hemagglutinin is essential for fusion pore formation and virus infectivity. *J Virol* **79**, 6449-6458
97. **Hess, S. T., Gould, T. J., Gudheti, M. V., Maas, S. A., Mills, K. D., and Zimmerberg, J.** (2007) Dynamic clustered distribution of hemagglutinin resolved at 40 nm in living cell membranes discriminates between raft theories. *Proc Natl Acad Sci U S A* **104**, 17370-17375
98. **Leser, G. P., and Lamb, R. A.** (2005) Influenza virus assembly and budding in raft-derived microdomains: a quantitative analysis of the surface distribution of HA, NA and M2 proteins. *Virology* **342**, 215-227
99. **Chen, B. J., Takeda, M., and Lamb, R. A.** (2005) Influenza virus hemagglutinin (H3 subtype) requires palmitoylation of its cytoplasmic tail for assembly: M1 proteins of two subtypes differ in their ability to support assembly. *J Virol* **79**, 13673-13684
100. **Zurcher, T., Luo, G., and Palese, P.** (1994) Mutations at palmitoylation sites of the influenza virus hemagglutinin affect virus formation. *J Virol* **68**, 5748-5754
101. **Siche, S., Brett, K., Moller, L., Kordyukova, L. V., Mintaev, R. R., Alexeevski, A. V., and Veit, M.** (2015) Two Cytoplasmic Acylation Sites and an Adjacent Hydrophobic Residue, but No Other Conserved Amino Acids in the Cytoplasmic Tail of HA from Influenza A Virus Are Crucial for Virus Replication. *Viruses* **7**, 6458-6475
102. **Wang, M., Ludwig, K., Bottcher, C., and Veit, M.** (2016) The role of stearate attachment to the hemagglutinin-esterase-fusion glycoprotein HEF of influenza C virus. *Cell Microbiol* **18**, 692-704
103. **Ujike, M., Nakajima, K., and Nobusawa, E.** (2004) Influence of acylation sites of influenza B virus hemagglutinin on fusion pore formation and dilation. *J Virol* **78**, 11536-11543
104. **Thaa, B., Tiesch, C., Moller, L., Schmitt, A. O., Wolff, T., Bannert, N., Herrmann, A., and Veit, M.** (2012) Growth of influenza A virus is not impeded by simultaneous removal of the cholesterol-binding and acylation sites in the M2 protein. *J Gen Virol* **93**, 282-292
105. **Veit, M., and Siche, S.** (2015) S-acylation of influenza virus proteins: Are enzymes for fatty acid attachment promising drug targets? *Vaccine* **33**, 7002-7007

106. **Grantham, M. L., Wu, W. H., Lalime, E. N., Lorenzo, M. E., Klein, S. L., and Pekosz, A.** (2009) Palmitoylation of the influenza A virus M2 protein is not required for virus replication in vitro but contributes to virus virulence. *J Virol* **83**, 8655-8661
107. **Kordyukova, L. V., Serebryakova, M. V., Baratova, L. A., and Veit, M.** (2009) Site-specific attachment of palmitate or stearate to cytoplasmic versus transmembrane cysteines is a common feature of viral spike proteins. *Virology* **398**, 49-56
108. **Branigan, P. J., Day, N. D., Liu, C., Gutshall, L. L., Melero, J. A., Sarisky, R. T., and Del Vecchio, A. M.** (2006) The cytoplasmic domain of the F protein of Human respiratory syncytial virus is not required for cell fusion. *J Gen Virol* **87**, 395-398
109. **Caballero, M., Carabana, J., Ortego, J., Fernandez-Munoz, R., and Celma, M. L.** (1998) Measles virus fusion protein is palmitoylated on transmembrane-intracytoplasmic cysteine residues which participate in cell fusion. *J Virol* **72**, 8198-8204
110. **Gaudin, Y., Tuffereau, C., Benmansour, A., and Flamand, A.** (1991) Fatty acylation of rabies virus proteins. *Virology* **184**, 441-444
111. **Whitt, M. A., and Rose, J. K.** (1991) Fatty acid acylation is not required for membrane fusion activity or glycoprotein assembly into VSV virions. *Virology* **185**, 875-878
112. **Funke, C., Becker, S., Dartsch, H., Klenk, H. D., and Muhlberger, E.** (1995) Acylation of the Marburg virus glycoprotein. *Virology* **208**, 289-297
113. **Ito, H., Watanabe, S., Takada, A., and Kawaoka, Y.** (2001) Ebola virus glycoprotein: proteolytic processing, acylation, cell tropism, and detection of neutralizing antibodies. *J Virol* **75**, 1576-1580
114. **McBride, C. E., and Machamer, C. E.** (2010) Palmitoylation of SARS-CoV S protein is necessary for partitioning into detergent-resistant membranes and cell-cell fusion but not interaction with M protein. *Virology* **405**, 139-148
115. **Petit, C. M., Chouljenko, V. N., Iyer, A., Colgrove, R., Farzan, M., Knipe, D. M., and Kousoulas, K. G.** (2007) Palmitoylation of the cysteine-rich endodomain of the SARS-coronavirus spike glycoprotein is important for spike-mediated cell fusion. *Virology* **360**, 264-274
116. **Shulla, A., and Gallagher, T.** (2009) Role of spike protein endodomains in regulating coronavirus entry. *J Biol Chem* **284**, 32725-32734
117. **Boscarino, J. A., Logan, H. L., Lacny, J. J., and Gallagher, T. M.** (2008) Envelope protein palmitoylations are crucial for murine coronavirus assembly. *J Virol* **82**, 2989-2999
118. **Lopez, L. A., Riffle, A. J., Pike, S. L., Gardner, D., and Hogue, B. G.** (2008) Importance of conserved cysteine residues in the coronavirus envelope protein. *J Virol* **82**, 3000-3010
119. **Gaedigk-Nitschko, K., Ding, M. X., Levy, M. A., and Schlesinger, M. J.** (1990) Site-directed mutations in the Sindbis virus 6K protein reveal sites for fatty acylation and the underacylated protein affects virus release and virion structure. *Virology* **175**, 282-291
120. **Gaedigk-Nitschko, K., and Schlesinger, M. J.** (1990) The Sindbis virus 6K protein can be detected in virions and is acylated with fatty acids. *Virology* **175**, 274-281

REFERENCES

121. **Ivanova, L., and Schlesinger, M. J.** (1993) Site-directed mutations in the Sindbis virus E2 glycoprotein identify palmitoylation sites and affect virus budding. *J Virol* **67**, 2546-2551
122. **Ryan, C., Ivanova, L., and Schlesinger, M. J.** (1998) Effects of site-directed mutations of transmembrane cysteines in sindbis virus E1 and E2 glycoproteins on palmitoylation and virus replication. *Virology* **249**, 62-67
123. **Ramsey, J., Chavez, M., and Mukhopadhyay, S.** (2019) Domains of the TF protein important in regulating its own palmitoylation. *Virology* **531**, 31-39
124. **Ramsey, J., Renzi, E. C., Arnold, R. J., Trinidad, J. C., and Mukhopadhyay, S.** (2017) Palmitoylation of Sindbis Virus TF Protein Regulates Its Plasma Membrane Localization and Subsequent Incorporation into Virions. *J Virol* **91**
125. **Kiiver, K., Tegen, I., Zusinaite, E., Tamberg, N., Fazakerley, J. K., and Merits, A.** (2008) Properties of non-structural protein 1 of Semliki Forest virus and its interference with virus replication. *J Gen Virol* **89**, 1457-1466
126. **Zhang, N., Zhao, H., and Zhang, L.** (2019) Fatty Acid Synthase Promotes the Palmitoylation of Chikungunya Virus nsP1. *J Virol* **93**
127. **Majeau, N., Fromentin, R., Savard, C., Duval, M., Tremblay, M. J., and Leclerc, D.** (2009) Palmitoylation of hepatitis C virus core protein is important for virion production. *J Biol Chem* **284**, 33915-33925
128. **Paul, D., Bartenschlager, R., and McCormick, C.** (2015) The predominant species of nonstructural protein 4B in hepatitis C virus-replicating cells is not palmitoylated. *J Gen Virol* **96**, 1696-1701
129. **Yu, G. Y., Lee, K. J., Gao, L., and Lai, M. M.** (2006) Palmitoylation and polymerization of hepatitis C virus NS4B protein. *J Virol* **80**, 6013-6023
130. **Bhattacharya, J., Peters, P. J., and Clapham, P. R.** (2004) Human immunodeficiency virus type 1 envelope glycoproteins that lack cytoplasmic domain cysteines: impact on association with membrane lipid rafts and incorporation onto budding virus particles. *J Virol* **78**, 5500-5506
131. **Chan, W. E., Lin, H. H., and Chen, S. S.** (2005) Wild-type-like viral replication potential of human immunodeficiency virus type 1 envelope mutants lacking palmitoylation signals. *J Virol* **79**, 8374-8387
132. **Chopard, C., Tong, P. B. V., Toth, P., Schatz, M., Yezid, H., Debaisieux, S., Mettling, C., Gross, A., Pugniere, M., Tu, A., Strub, J. M., Mesnard, J. M., Vitale, N., and Beaumelle, B.** (2018) Cyclophilin A enables specific HIV-1 Tat palmitoylation and accumulation in uninfected cells. *Nat Commun* **9**, 2251
133. **Persing, D. H., Varmus, H. E., and Ganem, D.** (1987) The preS1 protein of hepatitis B virus is acylated at its amino terminus with myristic acid. *J Virol* **61**, 1672-1677
134. **Patrone, M., Coroadinha, A. S., Teixeira, A. P., and Alves, P. M.** (2015) Palmitoylation Strengthens Cholesterol-dependent Multimerization and Fusion Activity of Human Cytomegalovirus Glycoprotein B (gB). *J Biol Chem* **291**, 4711-4722
135. **Mach, M., Osinski, K., Kropff, B., Schloetzer-Schrehardt, U., Krzyzaniak, M., and Britt, W.** (2007) The carboxy-terminal domain of glycoprotein N of human cytomegalovirus is required for virion morphogenesis. *J Virol* **81**, 5212-5224

136. **Serwa, R. A., Abaitua, F., Krause, E., Tate, E. W., and O'Hare, P.** (2015) Systems Analysis of Protein Fatty Acylation in Herpes Simplex Virus-Infected Cells Using Chemical Proteomics. *Chem Biol* **22**, 1008-1017
137. **Gouttenoire, J., Pollan, A., Abrami, L., Oechslin, N., Mauron, J., Matter, M., Oppliger, J., Szkolnicka, D., Dao Thi, V. L., van der Goot, F. G., and Moradpour, D.** (2018) Palmitoylation mediates membrane association of hepatitis E virus ORF3 protein and is required for infectious particle secretion. *PLoS Pathog* **14**, e1007471
138. **Peng, T., Thinon, E., and Hang, H. C.** (2015) Proteomic analysis of fatty-acylated proteins. *Curr Opin Chem Biol* **30**, 77-86
139. **Bano, M. C., Jackson, C. S., and Magee, A. I.** (1998) Pseudo-enzymatic S-acylation of a myristoylated yes protein tyrosine kinase peptide in vitro may reflect non-enzymatic S-acylation in vivo. *Biochem J* **330** (Pt 2), 723-731
140. **Bizzozero, O. A., McGarry, J. F., and Lees, M. B.** (1987) Autoacylation of myelin proteolipid protein with acyl coenzyme A. *J Biol Chem* **262**, 13550-13557
141. **Duncan, J. A., and Gilman, A. G.** (1996) Autoacylation of G protein alpha subunits. *J Biol Chem* **271**, 23594-23600
142. **Veit, M.** (2000) Palmitoylation of the 25-kDa synaptosomal protein (SNAP-25) in vitro occurs in the absence of an enzyme, but is stimulated by binding to syntaxin. *Biochem J* **345** Pt 1, 145-151
143. **Veit, M., Sachs, K., Heckelmann, M., Maretzki, D., Hofmann, K. P., and Schmidt, M. F.** (1998) Palmitoylation of rhodopsin with S-protein acyltransferase: enzyme catalyzed reaction versus autocatalytic acylation. *Biochim Biophys Acta* **1394**, 90-98
144. **Chan, P., Han, X., Zheng, B., DeRan, M., Yu, J., Jarugumilli, G. K., Deng, H., Pan, D., Luo, X., and Wu, X.** (2016) Autopalmitoylation of TEAD proteins regulates transcriptional output of the Hippo pathway. *Nat Chem Biol* **12**, 282-289
145. **Kummel, D., Heinemann, U., and Veit, M.** (2006) Unique self-palmitoylation activity of the transport protein particle component Bet3: a mechanism required for protein stability. *Proc Natl Acad Sci U S A* **103**, 12701-12706
146. **Roth, A. F., Wan, J., Bailey, A. O., Sun, B., Kuchar, J. A., Green, W. N., Phinney, B. S., Yates, J. R., 3rd, and Davis, N. G.** (2006) Global analysis of protein palmitoylation in yeast. *Cell* **125**, 1003-1013
147. **Turnbull, A. P., Kummel, D., Prinz, B., Holz, C., Schultchen, J., Lang, C., Niesen, F. H., Hofmann, K. P., Delbruck, H., Behlke, J., Muller, E. C., Jarosch, E., Sommer, T., and Heinemann, U.** (2005) Structure of palmitoylated BET3: insights into TRAPP complex assembly and membrane localization. *The EMBO journal* **24**, 875-884
148. **Lobo, S., Greentree, W. K., Linder, M. E., and Deschenes, R. J.** (2002) Identification of a Ras palmitoyltransferase in *Saccharomyces cerevisiae*. *J Biol Chem* **277**, 41268-41273
149. **Roth, A. F., Feng, Y., Chen, L., and Davis, N. G.** (2002) The yeast DHHC cysteine-rich domain protein Akr1p is a palmitoyl transferase. *J Cell Biol* **159**, 23-28
150. **Fukata, M., Fukata, Y., Adesnik, H., Nicoll, R. A., and Brecht, D. S.** (2004) Identification of PSD-95 palmitoylating enzymes. *Neuron* **44**, 987-996

151. Ohno, Y., Kihara, A., Sano, T., and Igarashi, Y. (2006) Intracellular localization and tissue-specific distribution of human and yeast DHHC cysteine-rich domain-containing proteins. *Biochim Biophys Acta* **1761**, 474-483
152. Jennings, B. C., and Linder, M. E. (2012) DHHC protein S-acyltransferases use similar ping-pong kinetic mechanisms but display different acyl-CoA specificities. *J Biol Chem* **287**, 7236-7245
153. Berger, M., and Schmidt, M. F. (1984) Identification of acyl donors and acceptor proteins for fatty acid acylation in BHK cells infected with Semliki Forest virus. *The EMBO journal* **3**, 713-719
154. Lemonidis, K., Sanchez-Perez, M. C., and Chamberlain, L. H. (2015) Identification of a Novel Sequence Motif Recognized by the Ankyrin Repeat Domain of zDHHC17/13 S-Acyltransferases. *J Biol Chem* **290**, 21939-21950
155. Fredericks, G. J., Hoffmann, F. W., Rose, A. H., Osterheld, H. J., Hess, F. M., Mercier, F., and Hoffmann, P. R. (2014) Stable expression and function of the inositol 1,4,5-triphosphate receptor requires palmitoylation by a DHHC6/selenoprotein K complex. *Proc Natl Acad Sci U S A* **111**, 16478-16483
156. Ebsen, H., Lettau, M., Kabelitz, D., and Janssen, O. (2014) Identification of SH3 domain proteins interacting with the cytoplasmic tail of the α disintegrin and metalloprotease 10 (ADAM10). *PLoS One* **9**, e102899
157. Thomas, G. M., Hayashi, T., Chiu, S. L., Chen, C. M., and Huganir, R. L. (2012) Palmitoylation by DHHC5/8 targets GRIP1 to dendritic endosomes to regulate AMPA-R trafficking. *Neuron* **73**, 482-496
158. Rana, M. S., Kumar, P., Lee, C. J., Verardi, R., Rajashankar, K. R., and Banerjee, A. (2018) Fatty acyl recognition and transfer by an integral membrane S-acyltransferase. *Science* **359**
159. Gottlieb, C. D., Zhang, S., and Linder, M. E. (2015) The Cysteine-rich Domain of the DHHC3 Palmitoyltransferase Is Palmitoylated and Contains Tightly Bound Zinc. *J Biol Chem* **290**, 29259-29269
160. Greaves, J., Munro, K. R., Davidson, S. C., Riviere, M., Wojno, J., Smith, T. K., Tomkinson, N. C., and Chamberlain, L. H. (2017) Molecular basis of fatty acid selectivity in the zDHHC family of S-acyltransferases revealed by click chemistry. *Proc Natl Acad Sci U S A* **114**, E1365-E1374
161. Neess, D., Bek, S., Engelsby, H., Gallego, S. F., and Faergeman, N. J. (2015) Long-chain acyl-CoA esters in metabolism and signaling: Role of acyl-CoA binding proteins. *Prog Lipid Res* **59**, 1-25
162. Brown, M. S., Radhakrishnan, A., and Goldstein, J. L. (2018) Retrospective on Cholesterol Homeostasis: The Central Role of Scap. *Annu Rev Biochem* **87**, 783-807
163. Yuan, S., Chu, H., Chan, J. F., Ye, Z. W., Wen, L., Yan, B., Lai, P. M., Tee, K. M., Huang, J., Chen, D., Li, C., Zhao, X., Yang, D., Chiu, M. C., Yip, C., Poon, V. K., Chan, C. C., Sze, K. H., Zhou, J., Chan, I. H., Kok, K. H., To, K. K., Kao, R. Y., Lau, J. Y., Jin, D. Y., Perlman, S., and Yuen, K. Y. (2019) SREBP-dependent lipidomic reprogramming as a broad-spectrum antiviral target. *Nat Commun* **10**, 120

164. **Ohol, Y. M., Wang, Z., Kemble, G., and Duke, G.** (2015) Direct Inhibition of Cellular Fatty Acid Synthase Impairs Replication of Respiratory Syncytial Virus and Other Respiratory Viruses. *PLoS One* **10**, e0144648
165. **Yang, W., Hood, B. L., Chadwick, S. L., Liu, S., Watkins, S. C., Luo, G., Conrads, T. P., and Wang, T.** (2008) Fatty acid synthase is up-regulated during hepatitis C virus infection and regulates hepatitis C virus entry and production. *Hepatology* **48**, 1396-1403
166. **Kulkarni, M. M., Ratcliff, A. N., Bhat, M., Alwarawrah, Y., Hughes, P., Arcos, J., Loiselle, D., Torrelles, J. B., Funderburg, N. T., Haystead, T. A., and Kwiek, J. J.** (2017) Cellular fatty acid synthase is required for late stages of HIV-1 replication. *Retrovirology* **14**, 45
167. **Duncan, J. A., and Gilman, A. G.** (1998) A cytoplasmic acyl-protein thioesterase that removes palmitate from G protein alpha subunits and p21(RAS). *J Biol Chem* **273**, 15830-15837
168. **Yeh, D. C., Duncan, J. A., Yamashita, S., and Michel, T.** (1999) Depalmitoylation of endothelial nitric-oxide synthase by acyl-protein thioesterase 1 is potentiated by Ca(2+)-calmodulin. *J Biol Chem* **274**, 33148-33154
169. **Tian, L., McClafferty, H., Knaus, H. G., Ruth, P., and Shipston, M. J.** (2012) Distinct acyl protein transferases and thioesterases control surface expression of calcium-activated potassium channels. *J Biol Chem* **287**, 14718-14725
170. **Rusch, M., Zimmermann, T. J., Burger, M., Dekker, F. J., Gormer, K., Triola, G., Brockmeyer, A., Janning, P., Bottcher, T., Sieber, S. A., Vetter, I. R., Hedberg, C., and Waldmann, H.** (2011) Identification of acyl protein thioesterases 1 and 2 as the cellular targets of the Ras-signaling modulators palmostatin B and M. *Angew Chem Int Ed Engl* **50**, 9838-9842
171. **Tomatis, V. M., Trenchi, A., Gomez, G. A., and Daniotti, J. L.** (2010) Acyl-protein thioesterase 2 catalyzes the deacylation of peripheral membrane-associated GAP-43. *PLoS One* **5**, e15045
172. **Kong, E., Peng, S., Chandra, G., Sarkar, C., Zhang, Z., Bagh, M. B., and Mukherjee, A. B.** (2013) Dynamic palmitoylation links cytosol-membrane shuttling of acyl-protein thioesterase-1 and acyl-protein thioesterase-2 with that of proto-oncogene H-ras product and growth-associated protein-43. *J Biol Chem* **288**, 9112-9125
173. **Vartak, N., Papke, B., Grecco, H. E., Rossmannek, L., Waldmann, H., Hedberg, C., and Bastiaens, P. I.** (2014) The autodepalmitoylating activity of APT maintains the spatial organization of palmitoylated membrane proteins. *Biophys J* **106**, 93-105
174. **Abrami, L., Dallavilla, T., Sandoz, P. A., Demir, M., Kunz, B., Savoglidis, G., Hatzimanikatis, V., and van der Goot, F. G.** (2017) Identification and dynamics of the human ZDHHC16-ZDHHC6 palmitoylation cascade. *Elife* **6**
175. **O'Brien, P. J., and Zatz, M.** (1984) Acylation of bovine rhodopsin by [³H]palmitic acid. *J Biol Chem* **259**, 5054-5057
176. **Drisdel, R. C., and Green, W. N.** (2004) Labeling and quantifying sites of protein palmitoylation. *Biotechniques* **36**, 276-285

REFERENCES

177. **Forrester, M. T., Hess, D. T., Thompson, J. W., Hultman, R., Moseley, M. A., Stamler, J. S., and Casey, P. J.** (2011) Site-specific analysis of protein S-acylation by resin-assisted capture. *J Lipid Res* **52**, 393-398
178. **Percher, A., Ramakrishnan, S., Thinon, E., Yuan, X., Yount, J. S., and Hang, H. C.** (2016) Mass-tag labeling reveals site-specific and endogenous levels of protein S-fatty acylation. *Proc Natl Acad Sci U S A* **113**, 4302-4307
179. **Hang, H. C., Geutjes, E. J., Grotenbreg, G., Pollington, A. M., Bijlmakers, M. J., and Ploegh, H. L.** (2007) Chemical probes for the rapid detection of Fatty-acylated proteins in Mammalian cells. *J Am Chem Soc* **129**, 2744-2745
180. **Thinon, E., and Hang, H. C.** (2015) Chemical reporters for exploring protein acylation. *Biochem Soc Trans* **43**, 253-261
181. **Martin, B. R.** (2013) Nonradioactive analysis of dynamic protein palmitoylation. *Curr Protoc Protein Sci* **73**, Unit 14 15
182. **Martin, B. R., and Cravatt, B. F.** (2009) Large-scale profiling of protein palmitoylation in mammalian cells. *Nat Methods* **6**, 135-138
183. **Martin, B. R., Wang, C., Adibekian, A., Tully, S. E., and Cravatt, B. F.** (2011) Global profiling of dynamic protein palmitoylation. *Nat Methods* **9**, 84-89
184. **Fukata, Y., Iwanaga, T., and Fukata, M.** (2006) Systematic screening for palmitoyl transferase activity of the DHHC protein family in mammalian cells. *Methods* **40**, 177-182
185. **Lakkaraju, A. K., Abrami, L., Lemmin, T., Blaskovic, S., Kunz, B., Kihara, A., Dal Peraro, M., and van der Goot, F. G.** (2012) Palmitoylated calnexin is a key component of the ribosome-translocon complex. *The EMBO journal* **31**, 1823-1835
186. **Tian, L., McClafferty, H., Jeffries, O., and Shipston, M. J.** (2010) Multiple palmitoyltransferases are required for palmitoylation-dependent regulation of large conductance calcium- and voltage-activated potassium channels. *J Biol Chem* **285**, 23954-23962
187. **Tsutsumi, R., Fukata, Y., Noritake, J., Iwanaga, T., Perez, F., and Fukata, M.** (2009) Identification of G protein alpha subunit-palmitoylating enzyme. *Mol Cell Biol* **29**, 435-447
188. **Zhang, J., Planey, S. L., Ceballos, C., Stevens, S. M., Jr., Keay, S. K., and Zacharias, D. A.** (2008) Identification of CKAP4/p63 as a major substrate of the palmitoyl acyltransferase DHHC2, a putative tumor suppressor, using a novel proteomics method. *Mol Cell Proteomics* **7**, 1378-1388
189. **Marin, E. P., Derakhshan, B., Lam, T. T., Davalos, A., and Sessa, W. C.** (2012) Endothelial cell palmitoylproteomic identifies novel lipid-modified targets and potential substrates for protein acyl transferases. *Circ Res* **110**, 1336-1344
190. **Cohen, S. N., Chang, A. C., and Hsu, L.** (1972) Nonchromosomal antibiotic resistance in bacteria: genetic transformation of Escherichia coli by R-factor DNA. *Proc Natl Acad Sci U S A* **69**, 2110-2114
191. **Horvath, P., and Barrangou, R.** (2010) CRISPR/Cas, the immune system of bacteria and archaea. *Science* **327**, 167-170

192. **Jinek, M., Chylinski, K., Fonfara, I., Hauer, M., Doudna, J. A., and Charpentier, E.** (2012) A programmable dual-RNA-guided DNA endonuclease in adaptive bacterial immunity. *Science* **337**, 816-821
193. **Wyvekens, N., Tsai, S. Q., and Joung, J. K.** (2015) Genome Editing in Human Cells Using CRISPR/Cas Nucleases. *Curr Protoc Mol Biol* **112**, 31 33 31-18
194. **He, X., Tan, C., Wang, F., Wang, Y., Zhou, R., Cui, D., You, W., Zhao, H., Ren, J., and Feng, B.** (2016) Knock-in of large reporter genes in human cells via CRISPR/Cas9-induced homology-dependent and independent DNA repair. *Nucleic Acids Res* **44**, e85
195. **Mali, P., Yang, L., Esvelt, K. M., Aach, J., Guell, M., DiCarlo, J. E., Norville, J. E., and Church, G. M.** (2013) RNA-guided human genome engineering via Cas9. *Science* **339**, 823-826
196. **Livak, K. J., and Schmittgen, T. D.** (2001) Analysis of relative gene expression data using real-time quantitative PCR and the 2^{(-Delta Delta C(T))} Method. *Methods* **25**, 402-408
197. **Hoffmann, E., Neumann, G., Kawaoka, Y., Hobom, G., and Webster, R. G.** (2000) A DNA transfection system for generation of influenza A virus from eight plasmids. *Proc Natl Acad Sci U S A* **97**, 6108-6113
198. **Matrosovich, M., Matrosovich, T., Garten, W., and Klenk, H. D.** (2006) New low-viscosity overlay medium for viral plaque assays. *Virology* **3**, 63
199. **Werno, M. W., and Chamberlain, L. H.** (2015) S-acylation of the Insulin-Responsive Aminopeptidase (IRAP): Quantitative analysis and Identification of Modified Cysteines. *Sci Rep* **5**, 12413
200. **Edmonds, M. J., Geary, B., Doherty, M. K., and Morgan, A.** (2017) Analysis of the brain palmitoyl-proteome using both acyl-biotin exchange and acyl-resin-assisted capture methods. *Sci Rep* **7**, 3299
201. **Li, Y., Martin, B. R., Cravatt, B. F., and Hofmann, S. L.** (2012) DHHC5 protein palmitoylates flotillin-2 and is rapidly degraded on induction of neuronal differentiation in cultured cells. *J Biol Chem* **287**, 523-530
202. **Lerner, R. A., and Hodge, L. D.** (1969) Nonpermissive infections of mammalian cells: synthesis of influenza virus genome in HeLa cells. *Proc Natl Acad Sci U S A* **64**, 544-551
203. **McClafferty, H., and Shipston, M. J.** (2019) siRNA Knockdown of Mammalian zDHHCs and Validation of mRNA Expression by RT-qPCR. *Methods Mol Biol* **2009**, 151-168
204. **Daniotti, J. L., Pedro, M. P., and Valdez Taubas, J.** (2017) The role of S-acylation in protein trafficking. *Traffic* **18**, 699-710
205. **Benton, D. J., Nans, A., Calder, L. J., Turner, J., Neu, U., Lin, Y. P., Ketelaars, E., Kallewaard, N. L., Corti, D., Lanzavecchia, A., Gambin, S. J., Rosenthal, P. B., and Skehel, J. J.** (2018) Influenza hemagglutinin membrane anchor. *Proc Natl Acad Sci U S A* **115**, 10112-10117
206. **Sharma, M., Yi, M., Dong, H., Qin, H., Peterson, E., Busath, D. D., Zhou, H. X., and Cross, T. A.** (2010) Insight into the mechanism of the influenza A proton channel from a structure in a lipid bilayer. *Science* **330**, 509-512

207. **Veit, M., and Schmidt, M. F.** (1993) Timing of palmitoylation of influenza virus hemagglutinin. *FEBS Lett* **336**, 243-247
208. **Runkle, K. B., Kharbanda, A., Stypulkowski, E., Cao, X. J., Wang, W., Garcia, B. A., and Witze, E. S.** (2016) Inhibition of DHHC2-Mediated EGFR Palmitoylation Creates a Dependence on EGFR Signaling. *Mol Cell* **62**, 385-396
209. **Greaves, J., Carmichael, J. A., and Chamberlain, L. H.** (2011) The palmitoyl transferase DHHC2 targets a dynamic membrane cycling pathway: regulation by a C-terminal domain. *Mol Biol Cell* **22**, 1887-1895
210. **Lazarovits, J., and Roth, M.** (1988) A single amino acid change in the cytoplasmic domain allows the influenza virus hemagglutinin to be endocytosed through coated pits. *Cell* **53**, 743-752
211. **Korycka, J., Lach, A., Heger, E., Boguslawska, D. M., Wolny, M., Toporkiewicz, M., Augoff, K., Korzeniewski, J., and Sikorski, A. F.** (2012) Human DHHC proteins: a spotlight on the hidden player of palmitoylation. *Eur J Cell Biol* **91**, 107-117
212. **Kim, Y., Yang, H., Min, J. K., Park, Y. J., Jeong, S. H., Jang, S. W., and Shim, S.** (2018) CCN3 secretion is regulated by palmitoylation via ZDHHC22. *Biochem Biophys Res Commun* **495**, 2573-2578
213. **Heinz, S., Texari, L., Hayes, M. G. B., Urbanowski, M., Chang, M. W., Givarkes, N., Rialdi, A., White, K. M., Albrecht, R. A., Pache, L., Marazzi, I., Garcia-Sastre, A., Shaw, M. L., and Benner, C.** (2018) Transcription Elongation Can Affect Genome 3D Structure. *Cell* **174**, 1522-1536 e1522
214. **Roberts, B. J., Johnson, K. E., McGuinn, K. P., Saowapa, J., Svoboda, R. A., Mahoney, M. G., Johnson, K. R., and Wahl, J. K., 3rd.** (2014) Palmitoylation of plakophilin is required for desmosome assembly. *J Cell Sci* **127**, 3782-3793
215. **Wang, L., Fu, B., Li, W., Patil, G., Liu, L., Dorf, M. E., and Li, S.** (2017) Comparative influenza protein interactomes identify the role of plakophilin 2 in virus restriction. *Nat Commun* **8**, 13876
216. **Ohno, Y., Kashio, A., Ogata, R., Ishitomi, A., Yamazaki, Y., and Kihara, A.** (2012) Analysis of substrate specificity of human DHHC protein acyltransferases using a yeast expression system. *Mol Biol Cell* **23**, 4543-4551
217. **Yoon, S. W., Webby, R. J., and Webster, R. G.** (2014) Evolution and ecology of influenza A viruses. *Curr Top Microbiol Immunol* **385**, 359-375
218. **Hutchinson, E. C., Charles, P. D., Hester, S. S., Thomas, B., Trudgian, D., Martinez-Alonso, M., and Fodor, E.** (2014) Conserved and host-specific features of influenza virion architecture. *Nat Commun* **5**, 4816
219. **Collins, M. O., Woodley, K. T., and Choudhary, J. S.** (2017) Global, site-specific analysis of neuronal protein S-acylation. *Sci Rep* **7**, 4683
220. **Yang, W., Di Vizio, D., Kirchner, M., Steen, H., and Freeman, M. R.** (2010) Proteome scale characterization of human S-acylated proteins in lipid raft-enriched and non-raft membranes. *Mol Cell Proteomics* **9**, 54-70

-
221. **Requero, M. A., Gonzalez, M., Goni, F. M., Alonso, A., and Fidelio, G.** (1995) Differential penetration of fatty acyl-coenzyme A and fatty acylcarnitines into phospholipid monolayers. *FEBS Lett* **357**, 75-78
222. **Peitzsch, R. M., and McLaughlin, S.** (1993) Binding of acylated peptides and fatty acids to phospholipid vesicles: pertinence to myristoylated proteins. *Biochemistry* **32**, 10436-10443
223. **Reverey, H., Veit, M., Ponimaskin, E., and Schmidt, M. F.** (1996) Differential fatty acid selection during biosynthetic S-acylation of a transmembrane protein (HEF) and other proteins in insect cells (Sf9) and in mammalian cells (CV1). *J Biol Chem* **271**, 23607-23610
224. **Rodenburg, R. N. P., Snijder, J., van de Waterbeemd, M., Schouten, A., Granneman, J., Heck, A. J. R., and Gros, P.** (2017) Stochastic palmitoylation of accessible cysteines in membrane proteins revealed by native mass spectrometry. *Nat Commun* **8**, 1280
225. **Mineev, K. S., Lyukmanova, E. N., Krabben, L., Serebryakova, M. V., Shulepko, M. A., Arseniev, A. S., Kordyukova, L. V., and Veit, M.** (2013) Structural investigation of influenza virus hemagglutinin membrane-anchoring peptide. *Protein Eng Des Sel* **26**, 547-552
226. **Sharma, C., Yang, X. H., and Hemler, M. E.** (2008) DHHC2 affects palmitoylation, stability, and functions of tetraspanins CD9 and CD151. *Mol Biol Cell* **19**, 3415-3425
227. **McMichael, T. M., Zhang, L., Chemudupati, M., Hach, J. C., Kenney, A. D., Hang, H. C., and Yount, J. S.** (2017) The palmitoyltransferase ZDHHC20 enhances interferon-induced transmembrane protein 3 (IFITM3) palmitoylation and antiviral activity. *J Biol Chem* **292**, 21517-21526
228. **Chamberlain, L. H., and Shipston, M. J.** (2015) The physiology of protein S-acylation. *Physiol Rev* **95**, 341-376.

9. Publications

Articles

- 1) **Gadalla MR**, Abrami L, van der Goot FG, Veit M. Hemagglutinin of Influenza A, but not of Influenza B and C viruses is acylated by ZDHHC2, 8, 15 and 20. *Biochem J* 17 January 2020; 477 (1): 285–303. doi: <https://doi.org/10.1042>.
- 2) **Gadalla MR**, Veit M. Towards the identification of ZDHHC enzymes required for palmitoylation of viral proteins as a potential drug target. *Expert opinion on drug discovery*, 15:2, 159-177, DOI: 10.1080/17460441.2020.1696306
- 3) **Gadalla MR**, El-Deeb AH, Emara MM, Hussein HA. Insect cell surface expression of Hemagglutinin (HA) of Egyptian H5N1 avian influenza virus under transcriptional control of whispovirus immediate early-1 Promoter. *J Microbiol Biotechnol.* **2014 Aug 11**. PubMed PMID: 25112319.
- 4) HA Hussein, BM Ahmed, SM Aly, AH El-Deeb, AA El-Sanousi, MA Rohaim, AA Arafa, **MR Gadalla**. Protective efficacy of a prime-boost protocol using H5-DNA plasmid as prime and inactivated H5N2 vaccine as the booster against the Egyptian avian influenza challenge virus. *Acta virologica* **60: 307 – 315, 2016**.

Posters

“NS1 mediated upregulation of ZDHHC22 acyltransferase in Influenza virus infected cells”. **Mohamed Rasheed Gadalla** Eliot Morrison, Xuejiao Han, Larisa Kordyukova, Christian Freund, Thorsten Wolff and Michael Veit. *29th Annual meeting of the German society for Virology* (GFV), 20-23 March 2019, Düsseldorf, Germany (Poster).

“Identification of ZDHHC proteins catalyzing acylation of HA, a modification essential for Influenza virus replication” **Mohamed Rasheed Gadalla** Laurence Abrami, F Gisou van der Goot and Michael Veit. *Acylation of intracellular and secreted proteins: mechanisms and functional outcomes*, 10-12 September 2018, Brighton, United Kingdom (Poster).

“Identification of ZDHHC proteins catalyzing acylation of HA, a modification essential for Influenza virus replication” **Mohamed Rasheed Gadalla**, Laurence Abrami, F Gisou van der Goot and Michael Veit. *3rd International Symposium “Membranes and Modules”*, 5-8 September 2018, Berlin, Germany (Poster).

10. Acknowledgements

First and Foremost praise is to ALLAH, the Almighty, the greatest of all, on whom ultimately we depend for sustenance and guidance. I would like to thank Almighty Allah for giving me opportunity, determination and strength to do my PhD.

I could not find words to thank my supervisor "*Doktorvater*", PD. Dr. Michael Veit for the patient supervision, encouragement and advice he has provided throughout my time as his doctoral student. He is not only a good scientist but also a great human being, who always think for good future of his students. He always motivates, gives opportunities and freedom to me to follow my own ideas. I consider myself extremely lucky to have a supervisor who cared so much about my work, and who responded to my questions and queries so promptly. Without her guidance and constant feedback, this PhD would not have been achievable.

I would like to thank Prof. Dr. Klaus Osterrieder and Prof. Dr. Benedikt Kaufer for their valuable discussions, suggestions and support during the course of my PhD seminars.

My deep appreciation goes out to all postdocs at the Institute of Virology, Freie Universität Berlin: Ahmed Kheimar, Walid Azab, Darren Wight, Dusan Kunec, Jakob Trimpert, Ludwig Krabben, Timo Schippers, Kathrin Eschke, Luca bertzbach, Tobias Bergmann, Minze Zhang, Chris Höfer, Amr Aswad, Susanne Kaufer and Cosima Zimmermann. Thanks to all of my PhD colleagues in the institute: Atika Hadiati , Bodan Hu , Xuejiao Han , Nicole Groenke, Mohamed Kamel, Ibrahim Haggag , Na Xing , Pratik Khedkar, Tereza Faflikova , Pavulraj Selvaraj , Renato Previdelli, Anirban Sanyal, Oleksandr Kolyvushko, Georg Beythien, Andele Conradie , Giulia Aimola, Viviane Kremlin , Xiaorong Meng , Yu You, Liuba Cherkashchenko, Maksat Akhmedzhanov and Xu Zhang for their continuous help and support in my PhD project. My sincere thanks to our technicians in the institute, Ann Reum , Annett Neubert , Angelika Thomele , Michaela Zeitlow and Elke Dyrks for their great assist during the work and for making lab life easier.

I want to express my deepest gratitude and appreciation to Prof. Dr. Gisou van der Goot , Dr. Laurence Abrami, Dr. Oksana Sergeeva and Dr. Mathieu Blanc at Global health Institute Ecole Polytechnique Fédérale de Lausanne, Switzerland for hosting me to learn the acylation techniques and CRISPR technologies; they are very kind, supportive and helpful all the time.

I would like to thank our collaborators: Prof. Dr. Christian Freund, Dr. Eliot Morrison, Dr. Florian Krammer and Dr. Thorsten Wolff for doing the MS measurements and providing me with valuable antibodies and plasmids.

ACKNOWLEDGEMENT

I want to thank Prof. Dr. Klaus Osterrieder and Prof. Dr. Hafez Mohamed Hafez for evaluating and reviewing my thesis.

My sincere thanks and appreciation goes to Prof. Dr. Hussein Aly Hussein who first guided me and learned me alot through my first steps in Virology and during my master studies. I never forgot his advices in life and science, he was always encouraging and supportive during hard times of PhD and always ready to help.

Special Thanks goes for DAAD and EMBO organizations, for not only providing the funding, which allowed me to undertake this research, but also for giving me the opportunity to attend conferences and meet so many interesting people. Without their support and funding, this project could not have reached its goal.

Finally, I would like to express my deep love and appreciation to my parents, my beloved wife Asmaa, my Beautiful kids Ziad and Layan , my brother Ahmed , my sisters Heba and Dina and all of my family for always believing in me and encouraging me to follow my dreams. They all kept me going; I would not have this work done without their input.

11. Selbständigkeitserklärung

Hiermit bestätige ich, dass ich die vorliegende Arbeit selbstständig angefertigt habe. Ich versichere, dass ich ausschließlich die angegebenen Quellen und Hilfen in Anspruch genommen habe.

Berlin, den 25.02.2020

Mohamed Rasheed Gadalla



9 783967 290400
mbvberlin | mensch und buch verlag

49,90 Euro | ISBN: 978-3-96729-040-0